

University of Stuttgart  
Germany



Department of Hydraulic Engineering and Water Resources Management  
Institute for Modelling Hydraulic and Environmental Systems

# Fuzzy map comparison techniques for the evaluation of hydro-morphodynamic numerical models

Master's Thesis

M.Sc. Water Resources Engineering and Management (WAREM)

Beatriz Medeiros Fernandes Negreiros

Matriculation Number: 3379194

26th October, 2020

**Examiner:** Prof. Dr. Ing. Silke Wiprecht

**Supervisors:** Dr. Sc. Sebastian Schwindt  
Stefan Haun, PhD

# **Erklärung/ Declaration**

Ich erkläre hiermit, dass ich die vorliegende Masterarbeit selbstständig, ohne unerlaubte Assistenz und nur mit den zitierten Quellen erstellt habe. Darüber hinaus bin ich damit einverstanden, dass diese Studie und ihre Ergebnisse dem Institut für Wasser- und Umweltmodellierung an der Universität Stuttgart für wissenschaftliche Zwecke zu Verfügung stehen.

I hereby declare to have produced this Master's Thesis independently, without illicit assistance and using solely the sources cited. Additionally, I agree to make this study available for scientific purposes at the Institute for Modeling Hydraulic and Environmental Systems (IWS), University of Stuttgart.

Beatriz M. F. Negreiros  
Stuttgart, 26th October, 2020

# Acknowledgments

Accomplishment and recognition are two things that can not exist without each other. Therefore, I begin by thanking Prof. Silke Wiprecht and PhD Stefan Haun for supporting my research choices and providing me with a workplace at the Institute of modeling Hydraulic and Environmental Systems. They are inspiring researchers with whom I felt the door was always open for advice. Moreover, the colleagues at the Department of Hydraulic Engineering and Water Resources Management were extremely helpful, providing me with data and engaging in discussions with me. I appreciate that greatly.

I had the honor to work directly with Dr. Sc. Sebastian Schwindt. I am very thankful for his guidance with several meetings, which were rich of ideas and active discussions. He encouraged me to make my decisions while making sure I was on the right path. Such a supervisor is rare to find.

I would also like to express my gratitude to WAREM's course manager, MSc. Anne Weiß, who has been accompanying me during the whole Master's with counseling, recommendations and support for applications. Her support pushed me forward to be my best researcher version.

I was funded by the German Federal Ministry of Education (BMBF) through the DAAD (German Academic Exchange Service), which conceived me the NaWaM (Sustainable Water Resources Management) scholarship.

To my parents, Porfirio and Verônica Negreiros, who always understood my urge for international challenges, a gigantic thank you. You were the foundation upon which I was built and from which I learned to face adversity.

Finally, I am deeply grateful to my spouse Ricardo Barros. He has assisted me not only with scientific ideas but also with tremendous personal support.

# Abstract

Among the numerous challenges in modeling fluvial hydro-morphodynamics, there is the question of how to (realistically) evaluate model efficiency. Approaches used in the past have focused on comparing river elevation cross-sections using statistical methods which neither account for data nor model uncertainties. Furthermore, the widespread visual inspection of simulated and observed data is susceptible to interpretation and labor-intensive. To overcome these issues, this study applies map comparison techniques based on fuzzy sets theory to evaluate the efficiency of hydro-morphodynamic numerical models. A test approach is developed for performing fuzzy kappa (suitable for categorical data) and fuzzy numerical (suitable for continuous data) map comparisons. Each technique produces a measure of agreement between simulated and observed datasets. The approach is tested in two case studies, which consist of physical models of shallow reservoirs and the lower Salzach River (Austria and Germany). A novel algorithm for the fuzzy numerical method is developed in Python 3. Pre-processing routines for the generation of the input rasters for both methods are coded, which include interpolation, rasterization and, for the fuzzy kappa method, categorization of the continuous data. The results indicate that the fuzzy numerical method is able to capture similarity between simulated and observed bed elevation change while accounting for uncertainty in location. That is possible because the fuzzy numerical method considers fuzziness of location in a transparent manner. The fuzzy kappa method shows limitations to evaluate the performance of the numerical models, because the obtained fuzzy kappa coefficients do not match with expert opinion. This study attributes the problem of the fuzzy kappa technique to the categorization of the continuous data, which introduces an additional source of fuzziness. The codes for fuzzy numerical map comparison, the pre-processing and visualization of the results are available as an open source repository. As a whole, the computational investigations and novel algorithms developed here offer an additional and more realistic approach to hydro-morphodynamic model assessment.

# Contents

<b>Abstract</b>	<b>iii</b>
<b>List of Figures</b>	<b>ix</b>
<b>List of Tables</b>	<b>xi</b>
<b>Nomenclature</b>	<b>xiii</b>
<b>1 Introduction</b>	<b>1</b>
1.1 Research question . . . . .	1
1.2 Research objectives . . . . .	2
1.3 Outline of the study . . . . .	3
<b>2 State-of-the-art</b>	<b>4</b>
2.1 Spatially explicit data types . . . . .	4
2.1.1 Categorical and continuous data . . . . .	4
2.1.2 Types of map data . . . . .	5
2.2 Modeling of fluvial hydro-morphodynamics . . . . .	6
2.2.1 Background and fluvial systems . . . . .	6
2.2.2 Geospatial boundary conditions . . . . .	8
2.2.3 Model calibration and validation . . . . .	8
2.2.4 Terrain change analysis . . . . .	10
2.2.5 Model evaluation techniques in a nutshell . . . . .	11
2.2.6 Challenges in hydro-morphodynamic model evaluation . . . . .	14
2.3 Fuzzy sets theory . . . . .	15
2.3.1 Fuzzy sets . . . . .	15
2.3.2 Applications in modeling hydro-environments . . . . .	18

## Contents

---

2.4 Comparison of simulated and observed map data . . . . .	19
2.4.1 Approaches to measure spatial similarity . . . . .	19
2.4.2 Fuzzy kappa map comparison . . . . .	23
2.4.3 Fuzzy numerical map comparison . . . . .	29
2.4.4 The Map Comparison Kit (MCK) . . . . .	30
<b>3 Methods</b>	<b>32</b>
3.1 Case studies . . . . .	32
3.1.1 Terrain change analysis of physical models of shallow reservoirs . . . . .	32
3.1.2 Terrain change analysis of the lower Salzach River . . . . .	33
3.2 Algorithm development . . . . .	36
3.2.1 Hypotheses . . . . .	36
3.2.2 Development of pre-processing tools . . . . .	37
3.2.3 Code for the fuzzy numerical method . . . . .	40
3.2.4 Application of the fuzzy kappa method using the Map Comparison Kit (MCK) . . . . .	42
3.3 Summary of the test approach . . . . .	42
3.3.1 Physical models of shallow reservoirs . . . . .	42
3.3.2 The lower Salzach River . . . . .	46
<b>4 Results</b>	<b>52</b>
4.1 Physical models of shallow reservoirs . . . . .	52
4.1.1 Sensitivity analysis of parameters involved . . . . .	52
4.1.2 Fuzzy numerical . . . . .	54
4.1.3 Fuzzy kappa . . . . .	57
4.2 Terrain change analyses of the lower Salzach River . . . . .	58
4.2.1 Optimization of the fuzzy numerical algorithm . . . . .	58
4.2.2 Sensitivity analysis of parameters involved . . . . .	59
4.2.3 Fuzzy numerical . . . . .	60
4.2.4 Fuzzy kappa . . . . .	62
<b>5 Discussion</b>	<b>66</b>
5.1 Limitations of the fuzzy kappa method . . . . .	66
5.2 Algorithm efficiency and the Map Comparison Kit (MCK) . . . . .	67
5.2.1 Computation time . . . . .	67

5.2.2	Limitations of the Map Comparison Kit (MCK) . . . . .	68
5.3	Uncertainty in datasets: from laboratory to nature . . . . .	68
5.3.1	Uncertainty in the grain size distribution . . . . .	68
5.3.2	Uncertainty in the observed water levels . . . . .	69
5.3.3	Uncertainty in the bed elevation data . . . . .	69
5.3.4	Fuzzy map comparison and the consideration of uncertainty . . . . .	70
5.4	Reasons for using fuzzy map comparison . . . . .	70
<b>6</b>	<b>Conclusions</b>	<b>74</b>
<b>7</b>	<b>Recommendations and outlook</b>	<b>76</b>
7.1	Application in hydro-morphodynamic modeling . . . . .	76
7.2	Future Research . . . . .	76
<b>References</b>		<b>78</b>
<b>Appendices</b>		<b>88</b>
<b>A</b>	<b>Complete rasters of the lower Salzach River</b>	<b>89</b>
<b>B</b>	<b>Mathematical definitions of membership functions</b>	<b>100</b>

# List of Figures

2.1	Structure of a fuzzy set (Source of logic: Zadeh, 1965). . . . .	16
2.2	Shapes of membership functions. . . . .	17
2.3	Exponential distance decay function with a halving distance of 2 cells. The neighborhood is defined as 4 cells and the central cell is located at node (i=10, j=14). . . . .	25
2.4	Neighborhood of a (central) cell in map A (map of model results) and its respective location in map B (map of observations). . . . .	26
3.1	Geometry of the physical models. Flow is running from the left to the right. . .	33
3.2	Experimental setup (Source: Kantoush, 2008). . . . .	34
3.3	Study area of the lower Salzach River (Source: Beckers et al., 2020). . . . .	35
3.4	Examples of rasters without interpolation. . . . .	38
3.5	Data preparation process for fuzzy comparison. . . . .	38
3.6	Algorithm for generating $S_{fuzzy}$ and $K_{fuzzy}$ values of reference using random rasters. . . . .	40
3.7	Algorithm for performing fuzzy numerical map comparison. . . . .	41
3.8	Algorithm for fuzzy kappa map comparison. . . . .	43
3.9	Rasterized maps of measured and simulated $\Delta z$ for the diamond-shaped model (Resolution of 0.1 m). . . . .	44
3.10	Rasterized maps of measured and simulated $\Delta z$ for the hexagon-shaped model (Resolution of 0.1 m). . . . .	44
3.11	Categorized maps of measured and simulated $\Delta z$ for the diamond-shaped model using Jenks natural breaks. The definition of the categories are shown in Table 3.3	45
3.12	Categorized maps of measured and simulated $\Delta z$ for the hexagon-shaped model using Jenks natural breaks. The definition of the categories are shown in Table 3.3	45

3.13 Observed bed elevation change in the lower Salzach River for the validation period 2010-2013 (Cell size = 5m). . . . .	48
3.14 Bed elevation change in the lower Salzach River for the validation period 2010-2013 from the manually calibrated <i>HYDRO_FT-2D</i> model (Cell size = 5m) . . . . .	49
3.15 Bed elevation change in the lower Salzach River for the validation period 2010-2013 from the stochastically calibrated <i>HYDRO_FT-2D</i> model (Cell size = 5m). . . . .	49
3.16 Bed elevation change in the lower Salzach River for the validation period 2010-2013 from the aPC surrogate model (Cell size = 5m). . . . .	50
3.17 Categorized maps of (a) observed and (b, c, d) simulated $\Delta z$ for the lower Salzach River using Jenks natural breaks. (b) manually calibrated <i>HYDRO_FT-2D</i> model; (c) stochastically calibrated <i>HYDRO_FT-2D</i> model; (d) aPC surrogate model (Cell size = 5m). The definition of the categories are shown in Table 3.6. . . . .	50
4.1 Maps of comparison between observed and simulated $\Delta z$ (Resolution of 0.1m, method: <b>Fuzzy numerical</b> ). . . . .	56
4.2 Performance analysis of the numerical models of shallow reservoirs (Method: <b>Fuzzy numerical</b> ). . . . .	56
4.3 Maps of comparison between observed and simulated $\Delta z$ . Neighborhood = 4 cells and halving distance = 2 cells (Resolution of 0.1m, method: <b>Fuzzy kappa</b> ). . . . .	58
4.4 Effect of increased fuzziness in location on the evaluation of the aPC surrogate model (versus measurements) for a neighborhood of 8 cells (hd= halving distance). . . . .	60
4.5 Fuzzy map comparison of the models of the lower Salzach River for the validation period 2010-2013 compared to observed $\Delta z$ . (a) manually calibrated <i>HYDRO_FT-2D</i> model; (b) stochastically calibrated <i>HYDRO_FT-2D</i> model; (c) aPC surrogate model (Resolution of 5m, method: <b>Fuzzy numerical</b> ). . . . .	62
4.6 Performance analysis of the models for the validation period (2010-2013). . . . .	63
A.1 Raster of observed $\Delta z$ in the lower Salzach River for the validation period 2010-2013 (Resolution of 5m). . . . .	90
A.2 Raster of simulated $\Delta z$ in the lower Salzach River for the validation period 2010-2013 from the manually calibrated <i>HYDRO_FT-2D</i> model (Resolution of 5m). . . . .	91
A.3 Raster of simulated $\Delta z$ in the lower Salzach River for the validation period 2010-2013 from the stochastically calibrated <i>HYDRO_FT-2D</i> model (Resolution of 5m). . . . .	92

## List of Figures

---

A.4 Raster of simulated $\Delta z$ in the lower Salzach River for the validation period 2010-2013 from the aPC surrogate model (Resolution of 5m). . . . .	93
A.5 Fuzzy evaluation of the manually calibrated <i>HYDRO_FT-2D</i> model of the lower Salzach River for the validation period 2010-2013 compared to observed $\Delta z$ (Resolution of 5m, method: <b>Fuzzy numerical</b> ). . . . .	94
A.6 Fuzzy evaluation of the stochastically calibrated <i>HYDRO_FT-2D</i> model of the lower Salzach River for the validation period 2010-2013 compared to observed $\Delta z$ (Resolution of 5m, method: <b>Fuzzy numerical</b> ). . . . .	95
A.7 Fuzzy evaluation of the aPC surrogate model of the lower Salzach River for the validation period 2010-2013 compared to observed $\Delta z$ (Resolution of 5m, method: <b>Fuzzy numerical</b> ). . . . .	96
A.8 Fuzzy evaluation of the manually calibrated <i>HYDRO_FT-2D</i> model of the lower Salzach River for the validation period 2010-2013 compared to observed $\Delta z$ (Resolution of 5m, method: <b>Fuzzy kappa</b> ). . . . .	97
A.9 Fuzzy evaluation of the stochastically calibrated <i>HYDRO_FT-2D</i> model of the lower Salzach River for the validation period 2010-2013 compared to observed $\Delta z$ (Resolution of 5m, method: <b>Fuzzy kappa</b> ). . . . .	98
A.10 Fuzzy evaluation of the aPC surrogate model of the lower Salzach River for the validation period 2010-2013 compared to observed $\Delta z$ (Resolution of 5m, method: <b>Fuzzy kappa</b> ). . . . .	99

# List of Tables

2.1	Types of maps and their frequent application. . . . .	6
2.2	Model bias, accuracy, and skill (Source: Sutherland, Peet, & Soulsby, 2004). . .	12
2.3	Strength of agreement associated with kappa statistics (Landis & Koch, 1977). .	21
2.4	Example of similarity matrix for a pair of flood risk maps. $C^A$ and $C^B$ are the categories of map A and B, respectively. In this case the similarity between categories is only aimed at the very high and high flood risk classes. . . . .	24
3.1	Features of the experimental setup (Source: Kantoush, 2008). . . . .	33
3.2	Spacing (in m) of the measured and simulated points on both models. . . . .	43
3.3	Definition of the categories for the diamond- and hexagon-shaped models using the natural breaks algorithm. . . . .	46
3.4	Similarity matrix of the categories of the physical models of shallow reservoirs.	46
3.5	Spacing (in m) of the dataset from the lower Salzach River for both from the models and from the measurements (Source: Beckers et al., 2020). . . . .	47
3.6	Definition of categories for the lower Salzach River using the natural breaks algorithm. . . . .	51
3.7	Similarity matrix of the categories from the case study of the lower Salzach River.	51
4.1	Global fuzzy similarities[-] from the sensitivity analysis of the neighborhood and halving distance in the evaluation of the diamond-shaped model (Resolution of 0.1, method: <b>Fuzzy numerical</b> ). . . . .	53
4.2	Fuzzy Kappa coefficients[-] from the sensitivity analysis of the neighborhood and halving distance in the evaluation of the diamond-shaped model (Resolution of 0.1m, method: <b>Fuzzy kappa</b> ). . . . .	53
4.3	Global fuzzy similarities[-] from the sensitivity analysis of the cell size in the evaluation of both shallow reservoir models (Method: <b>Fuzzy numerical</b> ). . . . .	54

## List of Tables

---

4.4	Global Fuzzy Similarity versus coefficient of determination. . . . .	55
4.5	Fuzzy kappa coefficients [-] of the numerical models of shallow reservoirs (Resolution of 0.1m). . . . .	57
4.6	Computation time [s] for fuzzy numerical map comparison after algorithm optimization. Note: number of cells refers to non-masked cells. . . . .	59
4.7	Global fuzzy similarities [-] from the sensitivity analysis of the neighborhood and halving distance in the comparison of the aPC surrogate model with observations (Resolution of 5 m). . . . .	59
4.8	Fuzzy Kappa coefficients [-] from the sensitivity analysis of the neighborhood and halving distance in the evaluation of the aPC surrogate model of the lower Salzach River for the validation period 2010-2013 (Resolution of 5m, method: <b>Fuzzy kappa</b> ). . . . .	60
4.9	Global fuzzy similarities[-] from the sensitivity analysis of the cell size in the evaluation of the models of the lower Salzach River (Method: <b>Fuzzy numerical</b> ). . . . .	61
4.10	Global fuzzy similarities [-] of the lower Salzach River models and baseline prediction (compared with measurements) for a spatial tolerance of 4 cells of halving distance and 8 cells of neighborhood (Resolution of 5m, method: <b>Fuzzy numerical</b> ). . . . .	61
4.11	Fuzzy Kappa coefficients of the lower Salzach River models and baseline prediction (compared with measurements) for a spatial tolerance of 4 cells of halving distance and 8 cells of neighborhood (Resolution of 5m). . . . .	64
4.12	Summary of the results (n = neighborhood, hd = halving distance). . . . .	65
5.1	Complexity differences between the case studies. . . . .	69

# Nomenclature

## Abbreviations

MCK	Map Comparison Kit
PVC	Polyvinyl chloride
RANS	Reynolds-averaged Navier-Stokes
SSIIM	Sediment Simulation In Intakes with Multiblock

## Symbols

$\Delta z$	Bed elevation change	[m]
$\kappa$	Kappa coefficient	[−]
$\mu$	Degree of membership	[−]
$\omega$	Distance decay function	[−]
$BSS$	Brier Skill Score	[−]
$d_{50}$	Particle diameter representing the 50% cumulative percentile value (50% of the particles in the sediment sample are finer than the $d_{50}$ )	[cm]
$d_{90}$	Particle diameter representing the 90% cumulative percentile value (90% of the particles in the sediment sample are finer than the $d_{90}$ )	[cm]
$hd$	Halving Distance	[cells]
$K_{fuzzy}$	Fuzzy Kappa Coefficient	[−]
$MAE$	Mean Absolute Error	<sup>i</sup> [var]

## Nomenclature

---

$MSE$	Mean Square Error	$[var]^2$
$n$	Neighborhood	$[cells]$
$NSE$	Nash-Sutcliffe Efficiency	$[-]$
$r$	Pearson's correlation	$[-]$
$R^2$	Coefficient of determination	$[-]$
$RMSE$	Root Mean Square Error	$[var]$
$S_i$	Two-way local fuzzy similarity	$[-]$
$s_i$	One-way local fuzzy similarity	$[-]$
$S_{fuzzy}$	Global Fuzzy Similarity	$[-]$
$V_{neigh}$	Fuzzy Neighborhood Vector	$[-]$

---

<sup>i</sup>[var]: Unit of the variable under analysis

# **Chapter 1**

## **Introduction**

### **1.1 Research question**

The physical processes behind sediment transport are complex and still unraveled. Scientists have made significant progress in gaining knowledge and simulating these processes during the last decades. However, the challenging task of modeling sediment transport involves answering several questions, from which many of them deal with spatially explicit data. This study focuses on one fundamental question: how can simulated terrain change be realistically compared with observations in a realistic manner?

The comparison of simulated and observed data, in particular terrain change, is the basis for evaluating the performance of hydro-morphodynamic models. In the last years, the availability of geospatial data has increased exponentially due to advances in measuring methods such as remote sensing. As it follows, topographic and bathymetric data are becoming more precise and with a finer resolution. Simulation results can therefore be compared to the observed terrain change in the whole extension of the study area as 2D geospatial data, instead of profile-wise, as it has been done in the past.

In this context, map comparison techniques are powerful tools for model performance evaluation. Yet, creating a perfect model is not the ultimate goal of a hydro-morphodynamic model, as creating such model is unrealistic and not necessary for most engineering and pragmatic purposes. Through the comparison of simulated and observed map data, the modeler is rather interested in identifying which zones were successfully reproduced or not, and to rate

the overall performance of the model. Therefore, comparing terrain change point by point expecting that a model would predict the exact observed bed elevation change, despite all model and measurement uncertainties, is unreasonable.

Now, the attention is turned to the field of map comparison. Hagen (2003) introduced a new map comparison technique that tolerates uncertainties in space and in value. Fuzzy sets theory and kappa statistics were used to create a method for comparing categorical raster maps while allowing a degree of uncertainty in the data. More recent developments used the concepts behind this method to create a fuzzy comparison method also for continuous valued raster data (Hagen, 2006).

Fuzzy map comparison techniques are a promising approach for evaluating results from hydro-morphodynamic models. They use fuzzy sets theory to handle uncertainty in a more explicit way than traditional methods (Pappenberger et al., 2007). Calibration and validation of hydro-morphodynamic models are tasks that demand more sophisticated approaches for handling data uncertainty and which could notably benefit from these techniques.

The present study is motivated by the interest of improving the tools available for model evaluation. The goal is to contribute to a more comprehensive comparison of simulation results against observation data by using fuzzy map comparison techniques. Advances in such fields can assist modelers in the important yet challenging task of modeling hydro-morphodynamics.

## 1.2 Research objectives

The goal of this study is to investigate the use of fuzzy map comparison for the evaluation of hydro-morphodynamic models. Two techniques were assessed: the fuzzy kappa and the fuzzy numerical map comparison. The following objectives are in the scope of the work.

1. Perform a literature review on the weaknesses and strengths of available methods for model evaluation.
2. Create a framework for applying the fuzzy kappa (Hagen, 2003) and the fuzzy numerical methods (Hagen, 2006) to evaluate the performance of hydro-morphodynamic models. The test approach will compare simulated and observed bed elevation change of two case studies, which are physical models of shallow reservoirs and the lower Salzach River (Austria and Germany).

### **1.3. Outline of the study**

---

3. Develop an open-source package for fuzzy map comparison that can be readily implemented in further studies.
4. Perform sensitivity analyzes of the comparison parameters for both fuzzy kappa and fuzzy numerical methods to assess the consistency of the methods.
5. Analyze the methods on their ability to serve as a tool for model performance evaluation.

## **1.3 Outline of the study**

This study begins with Chapter 1, which introduces the research question and objectives. Chapter 2 presents the state-of-the-art of geospatial data, numerical modeling, fuzzy logic and map comparison. Section 2.1 handles types of geospatial data and their common application. As to Section 2.2, the main features of modeling hydro-morphodynamics are reviewed with special attention to terrain change analysis and model evaluation. Section 2.3 delineates the theory underlying fuzzy logic and its importance in modeling applications. In Section 2.4, the concepts in fuzzy logic and geospatial data are subsequently combined to describe the fuzzy map comparison techniques of this study.

Chapter 3 presents the methods developed in the study. Section 3.1 introduces the case studies with which the fuzzy map comparison techniques are tested: physical models by (Kantoush, 2008) and the lower Salzach River by (Beckers, Noack, & Weprecht, 2016) and (Beckers et al., 2020). The development of the necessary algorithms, including hypotheses, pre-processing, and computation of the fuzzy map comparison methods are given in Section 3.2. Finally, the developed algorithms are tested in the case studies in Section 3.3.

Chapter 4 shows the results of the fuzzy comparisons and Chapter 5 discusses the ability of the methods in capturing similarities and tolerating spatial errors. In addition, the performance of the models is evaluated and the fuzzy comparison methods are analyzed.

The conclusions of the study are drawn in Chapter 6, which gives a final word concerning the capabilities of the methods for assessing hydro-morphodynamic models.

Chapter 7 gives recommendations on the use of the tools and codes developed in the study. In addition, the chapter highlights future research needs based on the demonstrated potential of fuzzy map comparison techniques in hydro-morphodynamic research.

# **Chapter 2**

## **State-of-the-art**

### **2.1 Spatially explicit data types**

#### **2.1.1 Categorical and continuous data**

When working with spatial variables it is necessary to distinguish the different types of spatial data. The term 'spatial data' refers to values that represent the location, size and shape of objects found in the physical world (Burkholder, 2008). The terms geospatial and spatial data are often used interchangeably, yet they differ in concern to georeferencing. Spatial data does not require a georeferencing system (i.e., a coordinate system that can be related to Earth's geographic locations) necessarily. Geospatial data, on the other hand, deals with objects and phenomena that have a geographic location and a georeferencing system (Stock & Guesgen, 2016). Both types of data store information about one or more attributes in each location. In the case of raster maps, for instance, locations are typically represented by cells (i.e., pixels).

The information stored in each location can be either discrete or continuous data. Discrete data are commonly called categorical or discontinuous and each cell is assigned to a category. For instance, common land-use categories are 'Agriculture', 'Urban area' or 'Forest'. Continuous data, on the other hand, consist of specific values that represents phenomena at each (x,y) coordinate. Each specific value is therefore an attribute of the (x,y) surface. Examples of attributes are bathymetry or concentration levels.

### 2.1.2 Types of map data

Maps are important to visualize spatially distributed objects. They are a representation of spatial data and can be georeferenced or not. Maps can be classified according to their purpose, content, origin and other criteria. Robinson et al. (1985) points out that the most efficient method to describe map data is the scaling system according to Stevens (1946). This classification system is based on four scales of measurement: nominal, ordinal, interval and ratio. The next paragraphs shortly describe these four scales (i.e., levels of precision), which are relevant for the further understanding of this study.

#### Nominal Scale

The nominal scale is the most fundamental type of measurement data (Visser & De Nijs, 2006). It consists of classes that do not have an explicit mathematical correlation with each other and are built on qualitative considerations. Example of maps in the nominal scale are land use and soil type maps (Table 2.1).

#### Ordinal Scale

The ordinal scale is similar to the nominal scale. The difference is that classes in the ordinal scale have a quantitative measure of a given attribute. By interpreting a map in this measurement scale one is able to state whether a class is higher or lower (in terms of attribute ranking) than the other. A common example is a flood risk map, which consist of classes of low, medium and high risk of flooding (Table 2.1).

#### Interval Scale

The interval scale contains more information than the nominal and ordinal scales. Their additional feature is the assignment of intervals (in a standardized unit) to each class, which in turn have the final goal of differentiating locations. Ordinal scales can also be interval scales once each class is portrayed as a variable range of a unit. For instance, temperature classes like 'hot', 'warm', 'cool' and 'cold' can be depicted as ranges in °C: 35 – 25, 25 – 20, 20 – 10, 10 – -10 , respectively (Table 2.1).

Table 2.1: Types of maps and their frequent application.

<b>Scale</b>	<b>Utilization</b>
Nominal	Land use and soil maps
Ordinal	Flood risk maps
Interval	Temperature maps or Canopy Elevation Models (CEM)
Ratio	Precipitation maps

### **Ratio Scale**

Both interval and ratio scales are built on continuous data (Visser & De Nijs, 2006). They are, from the point of view of making maps, equal in terms of representation of geographical data (Robinson et al., 1985). The ratio scale has nonetheless one new descriptive improvement. Aside from all features of interval scales, ratio scales are based on absolute zeros, such as the Kelvin temperature scale, elevation above a datum and water depth. Interval scales, on the other hand, have an arbitrary zero point. For instance, the °C Scale begins at –273 Kelvin. This component enables raters (i.e., those who lead the test and rate the results) to make direct discernment between observations as for instance ‘tree times higher’ or ‘twice as deep’. In contrast, such statements have to be made with care when dealing with interval scales, because one should not infer more than what is assured by the nature of the unit (Robinson et al., 1985).

## **2.2 Modeling of fluvial hydro-morphodynamics**

### **2.2.1 Background and fluvial systems**

#### **Fluvial hydrodynamics and morphodynamics**

Rivers are complex systems where both water and sediment are subjected to many forces (i.e., gravity, viscosity, turbulence and momentum). While fluvial hydrodynamics focuses on the movement of water, fluvial morphodynamics studies the interaction between water flow and sediment to describe riverbed changes (Wright & Crosato, 2011). The study of fluvial hydro- and morphodynamics is of great relevance. For centuries it has been a constant challenge to manage river systems. Problems such as bridge collapses and formation of sand bars in navigable rivers derived from failed attempts of past generations of engineers to anticipate hydro-morphodynamic conditions (Mohammadi, 2017). Fluvial morphodynamics

## 2.2. Modeling of fluvial hydro-morphodynamics

---

are also connected ecosystem conditions, as riverbeds are habitat of benthic species and provide ground for fish to spawn (e.g., Hauer, Unfer, Schmutz, & Habersack, 2007; Parsapour-Moghaddam, Brennan, Rennie, Elvidge, & Cooke, 2019) . Furthermore, sedimentation processes in reservoirs have gained special attention in the last decade, as they cause head loss and consequentially storage capacity and hydropower generation losses (Annandale, 2006).

It is crucial to estimate the amount and type of sediment transported in river systems so that fish habitat, reservoir operation, maintenance of efficient river navigation and flood protection can be ensured (Wieprecht, Tolossa, & Yang, 2013). In this context, hydro-morphodynamic modeling techniques developed and turned into an essential assessment tool for the safeguard of the infrastructural and ecosystem services.

### **Modeling fundamentals**

Hydro-morphodynamic models aim at predicting hydraulic conditions and sediment processes that result in changes in the riverbed. A hydro-morphodynamic model couples a hydrodynamic and a sediment transport model into an unified model. That is done because the physics of river flow and sediment transport influence one another. Thus, hydrodynamic variables are exchanged between hydro- and morphodynamic models. The following example illustrates the inter-dependency between hydraulic and sediment transport variables. In a fluvial system, bedforms (such as ripples and dunes) may (dis)appear, thus altering the bed roughness. Since the boundary conditions at the riverbed change, flow velocity also changes.

By computing the transport of bed material, hydro-morphodynamic models are able to simulate morphodynamic changes in the riverbed. Bed material load is the portion of the total sediment load that actively undergoes exchange between the bed and the water column. Bed material can be transported as bed load (i.e., flux of sediment through rolling and gliding of particles) or suspended load (i.e., flux of sediment in suspension, which is occasionally in contact with the bed) (Graf & Altinakar, 1998). In both modes of transport, the driving force for sediment movement is the action of gravity on the fluid component (Garcia, 2008). The bed-level variation induced by the sediment transport is calculated by the sediment continuity equation (Exner, 1925).

## 2.2.2 Geospatial boundary conditions

### Digital Terrain Models

One of the most important input data for hydro-morphodynamic models is the bathymetry (i.e., the topography of underwater terrain). Bathymetric data is necessary to build Digital Elevation Models (DEMs) of fluvial systems. Additionally, the comparison of simulated and observed DoDs (Digital Elevation Model of Differences) during calibration and validation processes also requires bathymetric data (see Sections 2.2.3 and 2.2.4).

The acquisition of elevation data can be carried out with boat-based or ground-based bathymetric surveys, acquired from remote sensing techniques, as for example LiDAR (Light Detection and Ranging), or with a combination of these (Carley et al., 2012). If different mapping methods are used, consistency among datasets must be herein assessed in order to ensure compatibility (Wyrick, Gonzalez, & Pasternack, 2013). Hydro-morphodynamic simulations are thereon performed over the modeled terrain.

### Roughness and grain size

Estimates of riverbed and terrain are a major issue when building hydro- morphodynamic models. Chang (1988) divides flow resistance in two components: grain roughness and form roughness. The first is related to the grain size and the second is attributed to bedforms. For the estimation of grain roughness through particle size, well-known formulas such as Strickler (1923) and Meyer-Peter and Müller (1948) are commonly applied.

Due to advances in remote sensing, it is nowadays possible to obtain grain size information from photographs, also called 'photo-sieving' methods (Pearson et al., 2017). These techniques make possible accurate and high resolution grain size estimation in large areas, while traditional areal sampling methods are too labor-intensive and destructive (Pearson et al., 2017).

## 2.2.3 Model calibration and validation

### Calibration

Calibration is an important step for the more effective use of a hydro-morphodynamic model (Chang, 1988). It aims at adjusting parameters in order to reflect as realistically as possible the

## 2.2. Modeling of fluvial hydro-morphodynamics

---

dynamics of the system, i.e., to obtain a satisfactory match between observed and simulated variables (Oreskes, Shrader-Frechette, & Belitz, 1994).

Calibration is done by changing the parameters which have most influence on the model output. In order to identify them, sensitivity analyzes are done by varying different parameters within physical meaningful ranges and measuring the response of the model (Winter, 2007). If changes in the value of a parameter significantly influence the model output, the parameter is relevant for the calibration and is considered sensitive. Items that usually require calibration are for example roughness coefficient, sediment transport equation and bank erodibility factor (Chang, 1988).

In morphodynamic models, the number of parameters is considerably high (Beckers et al., 2020; Shoarinezhad, Wiprecht, & Haun, 2020). Therefore, sensitivity analyzes are important as they reveal the key parameters to perform calibration (Winter, 2007). By reducing the number and narrowing the range of parameters, computation time can be significantly improved. In this sense, calibration can be seen as an optimization process, which consists of minimizing model discrepancy through the adaptation of parameter values or equations. Having considered that, the fewer variables an optimization problem has, the more straightforward is the solution.

Model calibration can be done manually or automatic. Manual calibration is achieved by manually adjusting parameters after checking each model run (i.e., trial-and-error or heuristic approach) and it relies on the expertise of the modeler. In this process, model performance can be evaluated with objective measures, i.e., mathematical performance criteria (see Section 2.2.5) or subjective visual comparison (Boyle, Gupta, & Sorooshian, 2000). Manual calibration of hydro-morphodynamic models can be a very time-consuming task, due to the large number of input parameters (McKibbin & Mahdi, 2010; Shoarinezhad & Haun, 2018; Beckers et al., 2020; Melo et al., 2020). In contrast, automatic calibration is able to reduce the manual effort in calibration processes and decrease the subjectivity of the user (Shoarinezhad et al., 2020). Automatic calibration consists of automatically adjusting model parameters within a specified search scheme using optimization algorithms (Dung, Merz, Bárdossy, Thang, & Apel, 2011). The performance evaluation and parameter adjustment is done according to explicit rules, which are implemented with numerical methods.

### Validation

Model validation is done followed by calibration. Validation consists of using the calibrated model to test if the parameters obtained from calibration represent the real system. The model is thus run in order to check if the simulated bed elevation change actually represents the observed. This is done in order to assess whether the model is a good predictor (i.e., it is acceptable for its intended use) or if it simply reproduces the observations from the calibration dataset. In contrast to model calibration, model validation does not have the goal of improving the quality of the model (Landry, Malouin, & Oral, 1983). Rather than that, validation aims mainly at establishing the legitimacy of the model (Oreskes et al., 1994).

The usual approach is to calibrate a model for a time period and afterwards validate it for another period. However, validation can also be achieved using different observation points (i.e., at other locations) within the same time period, (e.g., Mohammadi, 2017). A key principle that should be respected is that the validation tests must be carried out against independent datasets, meaning that the validation data should not have been used in the calibration step (Refsgaard & Henriksen, 2004).

Jørgensen and Bendoricchio (2001) point out that the validation method depends on the objective of the model. Different validation criteria (i.e., degree of acceptable agreement between model and reality) are selected also depending on the quality of the data. The criteria and the method of validation should be determined early in the modeling process by the modeler (Landry et al., 1983). Refsgaard and Henriksen (2004) emphasize that validation should test how well the model can perform the tasks for which it is intended. For instance, if a hydro-morphodynamic model is validated against terrain change and water level, it can not be assumed valid for the simulation of the grain size distribution of the riverbed layers.

#### 2.2.4 Terrain change analysis

Hydro-morphodynamic models often predict variables in the continuous domain. These variables may take an infinite number of possible values. In contrast, categorical data are more common in coastal modeling. For instance, changes in shoreline position can be classified into retreat, equilibrium and advance (Sutherland et al., 2004), and inundation zones can be divided into baseflow, bar and floodway zones (Wyrick et al., 2013).

A common approach for analyzing terrain change is comparing simulated and observed bed

---

## 2.2. Modeling of fluvial hydro-morphodynamics

---

elevations in different cross-sections (e.g., Olsen & Haun, 2010; Haun, Dorfmann, Harb, & Olsen, 2012; Ahn & Yen, 2015; Kunz, 2019; Kantoush, Bollaert, & Schleiss, 2008). When profiles are more consistently available and spatial data are enough to establish a grid of values, the comparison can take place in a form of visual map comparison. For that, the spatial points are normally interpolated to constitute figures that enable the comparison and consequently model performance evaluation. Examples of such approach are found in Villaret et al. (2013); Shoarinezhad et al. (2021); Beckers et al. (2020).

The application of remote sensing to assess spatial and temporal variations in river systems has been an emerging discipline in the last years (Marcus & Fonstad, 2010). Not only surface elevations can be efficiently acquired with LiDAR techniques (Legleiter, 2012), but also riverbed elevation, although in the latter the accuracy depends significantly on the water turbidity and depth. Bathymetric LiDARs (i.e., those with the ability to penetrate water) are being increasingly optimized to map in-channel elevation. Next-generation systems such as the EAARL (Experimental Advanced Airborne Research LiDAR) have shown potential for the mapping of streambeds (Tonina et al., 2019; Skinner, 2011). As a result, elevation data are growing into accessible and accurate geospatial data (e.g., raster data) that can be readily applied in terrain change analyzes. Thus, it is observed that new mapping techniques are gradually infiltrating the field of hydro-morphodynamic modeling.

Therefore, terrain change analyzes represent a fundamental feature in hydro-morphodynamic modeling. Whether for calibration, validation or verification purposes, bed elevation changes must be compared against the observed. Such analysis results in measures of model performance that can be evaluated by several methods. These are discussed in following in Section 2.2.5.

### 2.2.5 Model evaluation techniques in a nutshell

Model evaluation is imperative for both calibration and validation procedures. It involves comparing simulated against observed data using statistical and/or visual approaches. Visual techniques are usually the first step in model evaluation, as they provide the modeler a first overview over the performance of a model. In the field of watershed modeling, hydrographs and percent exceedance probability curves are especially helpful. In hydro-morphodynamic modeling it is good practice to plot 2D maps in color gradients and have them analyzed by experts. When measured data are more limited, measured and observed elevation pro-

files (longitudinal or cross-sectional) are plotted superimposed for visual analysis. However, these techniques are subjective to the interpretation of the modeler and thus difficult to be automated.

Statistical measures to assess hydro-morphodynamic models aim at quantifying model performance by means of functions and mathematical formulations. These measures are important for automatic calibration as they are readily implemented in optimization problems. Via statistical approaches one is able to quantify model bias, accuracy and skill (see more in Table 2.2). Moreover, statistical measures are taken by the scientific community as an official indicator of model validity. In the next paragraphs, some of these these measures commonly used in hydro-morphodynamic model evaluation are reviewed in a nutshell.

Table 2.2: Model bias, accuracy, and skill (Source: Sutherland et al., 2004).

Statistical measure	Definition
Bias	Measure that reveals if the model has a tendency towards under- or over-prediction.
Accuracy	Measure of how much the predicted values match the observed.
Skill	Measure of accuracy that is relative to the the accuracy of a baseline prediction.

### Mean absolute error (MAE), mean square error (MSE) and root mean square error (RMSE)

According to Sutherland et al. (2004), the MAE, MSE and RMSE are the most commonly-used measures of model accuracy. Among these three accuracy measures the often preferred are the root mean square error (RMSE) and mean absolute error (MAE), as they results in values of the same unit as the variable under analysis. It should be noticed that the presence of a few outliers have a much greater influence on RMSE than MAE, as the first squares the differences (Sutherland et al., 2004). Despite the sensitivity to outliers, the RMSE is very often applied in hydro-morphodynamic model evaluation because it is well-known and familiar. Several authors (Beckers et al., 2020; Kunz, 2019; Ahn & Yen, 2015) have applied the RMSE to compare observed with simulated elevation (or elevation change).

$$MAE(Y, X) = \langle |Y - X| \rangle \quad (2.1)$$

## 2.2. Modeling of fluvial hydro-morphodynamics

---

$$MSE(Y, X) = \langle (Y - X)^2 \rangle \quad (2.2)$$

$$RMSE(Y, X) = \sqrt{MSE(Y, X)} \quad (2.3)$$

Where  $\langle \rangle$  symbolizes the mean,  $Y$  is the set of predicted values and  $X$  is the set of observed values.

### Pearson's correlation ( $r$ ) and coefficient of determination ( $R^2$ )

Both the coefficient of determination ( $R^2$ ) and its square root, the Pearson's correlation ( $r$ ), are measures of collinearity between simulated and measured data (Moriasi et al., 2007). Values of  $R^2$  range from 0 to 1, while for the Pearson's correlation, values vary between -1 and 1. Legates and McCabe Jr (1999) point out that  $r$  and  $R^2$  are familiar to all scientists and for this reason they are extensively applied model evaluation. Yet, they are over-sensitive to outliers or extreme values and provide a biased view of model efficacy. Willmott (1981) suggested that  $r$  and  $R^2$  are inadequate to statistically evaluate geographic models and concluded that the  $RMSE$  is a superior index for comparing simulated and observed data.  $r$  is calculated as:

$$\sqrt{R^2} = r = \frac{\sum_{i=1}^n (y_i - \langle Y \rangle)(x_i - \langle X \rangle)}{\sqrt{\sum_{i=1}^n (y_i - \langle Y \rangle)^2} \sqrt{\sum_{i=1}^n (x_i - \langle X \rangle)^2}} \quad (2.4)$$

Where  $\langle \rangle$  symbolizes the mean,  $Y$  is the set of predicted values and  $X$  is the set of observed values.

### Brier Skill Score (BSS)

The Brier Skill Score (BSS) has been extensively applied to assess performance of morphodynamic models (e.g., Brady & Sutherland, 2001; Sutherland & Soulsby, 2003; Aguirre Iñiguez, Bui, Giehl, Reisenbüchler, & Rutschmann, 2019; Sánchez-Arcilla Conejo, Gracia García, & García León, 2014; Ferreira et al., 2017). The BSS is a measure to quantify the skill of a model prediction when compared to a baseline prediction. Sutherland et al. (2004) suggests using an initial condition, an average value or a random choice within the range of possible outcomes as baseline prediction for hydro-morphodynamic models. A perfect agreement between simulated and observed values results in a BSS equal to one, while values falling below zero

indicate that the model prediction is less accurate than the baseline prediction. The BSS is calculated as (Sutherland et al., 2004):

$$BSS = 1 - \frac{MSE(Y, X)}{MSE(B, X)} = 1 - \frac{\langle(Y - X)^2\rangle}{\langle(B - X)^2\rangle} \quad (2.5)$$

Where  $Y$  is the set of predicted values,  $B$  is the set of values from the baseline prediction and  $X$  is the set of observed values.

### 2.2.6 Challenges in hydro-morphodynamic model evaluation

Sediment transport modeling is a challenging task in the field of river and coastal engineering. The uncertainty related to model structure and parameters are not the only concern, but also inaccuracies in measured data. In the previous section, several statistics were presented in which all disregard measurement errors. However, all bathymetric surveys contain errors. Moreover, it is almost always the case that surface interpolation is done in order to compare measured and simulated data on exactly the same grid, and therefore, additional errors are introduced.

The consideration of measurement error should be done when evaluating hydro-morphodynamic models. Sutherland, Hall, and Chesher (2001) and Van Rijn et al. (2003) addressed this issue by adjusting the equation of the Brier Skill Score. The adjusted equations are of great value for the consideration of error measurement, but in order to apply them, the modeler should have prior knowledge on the measurement error. This can be in turn a complicated task. For instance, a frequently applied method is measuring initial and final bed elevations at a location that appeared to have no changes between the beginning and end of bathymetric surveys. This procedure itself is susceptible to errors, as the occurrence of such unchangeable areas might not happen or the initial and final bed level measurements might be equally biased, which masks the measurement error.

Besides uncertainty in data, parameters and model structure, the modeler has also the challenge of selecting the most appropriate evaluation technique to assess model performance. Here, it is important to consider the drawbacks of the aforementioned statistical evaluation methods. For instance, it must be noted that sediment transport processes are considerably dominated by stochastic processes, and thus, some level of uncertainty in predictions of bed change has to be expected. In this sense, the modeler may conclude that the *RMSE* represents

### 2.3. Fuzzy sets theory

---

a sensitive measure of model performance. A couple of disagreements between measured and observed values are likely to affect the *RMSE* and improperly indicate low efficiency. This effect may occur even though the model was able to adequately simulate patterns of erosion and deposition and their magnitudes in most locations. As presented in Section 2.2.5, the MAE could seem a better candidate to assess model accuracy.

Further problems may arise when evaluating models. Georeferencing error such as subtle shifts between the observed and simulated data may compromise the comparison and result in low model performance, even if the shift is negligible. Therefore, given the challenges exposed here, new methods for realistically demonstrating model performance should be researched and tested.

## 2.3 Fuzzy sets theory

### 2.3.1 Fuzzy sets

The theory of fuzzy sets started being developed in the beginning of the nineteenth century, but its official benchmark is considered to be the work presented by Zadeh (1965), in which the definition of fuzzy sets was presented for the first time. The rationale behind fuzzy logic is that objects do not need to assume crispy responses like true or false, or a unique class of belongingness. A crispy response has a sudden and well defined transition between membership and non-membership in a set (Zimmermann, 2011). However, it is not rare to observe in nature variables that present some kind of vagueness, and thus, they would be better represented by a set of membership values. The role of fuzzy logic is, therefore, to enable some level of ambiguity in the data with the possibility of conveying more information on it in return.

According to Zadeh (1988), fuzzy sets aims at representing linguistic variables, which can be seen as imprecise modes of reasoning, on the grounds that they play a crucial role in human rationality and their decision making process. The remarkable ability to infer or judge something based on imprecise information was a feature of human thinking which would be highly advantageous for computing purposes. Thereby the theory of fuzzy sets was born.

Instead of characterizing an object by a unique response (i.e., a crispy response), Zadeh (1965) proposed a group of rules that conceptualizes a fuzzy set. Such a set recognizes that objects have fuzzy status. The following example illustrates it (Figure 2.1): a physical property like

humidity can be remodeled as a fuzzy set by assigning a set of linguistic terms that describe that property, which in this example are 'Very Humid', 'Humid', 'Comfortable', 'Dry' and 'Very Dry'. Following this way of thinking, a relative humidity of 45% can be displayed as a set of grades, in which each of them represents the belongingness to the respective term. The grading rules which will perform this task are called membership functions  $\mu$  and they take values between 0 and 1. Finally, the relative humidity of 45% can be translated to a membership vector shown in Figure 2.1.

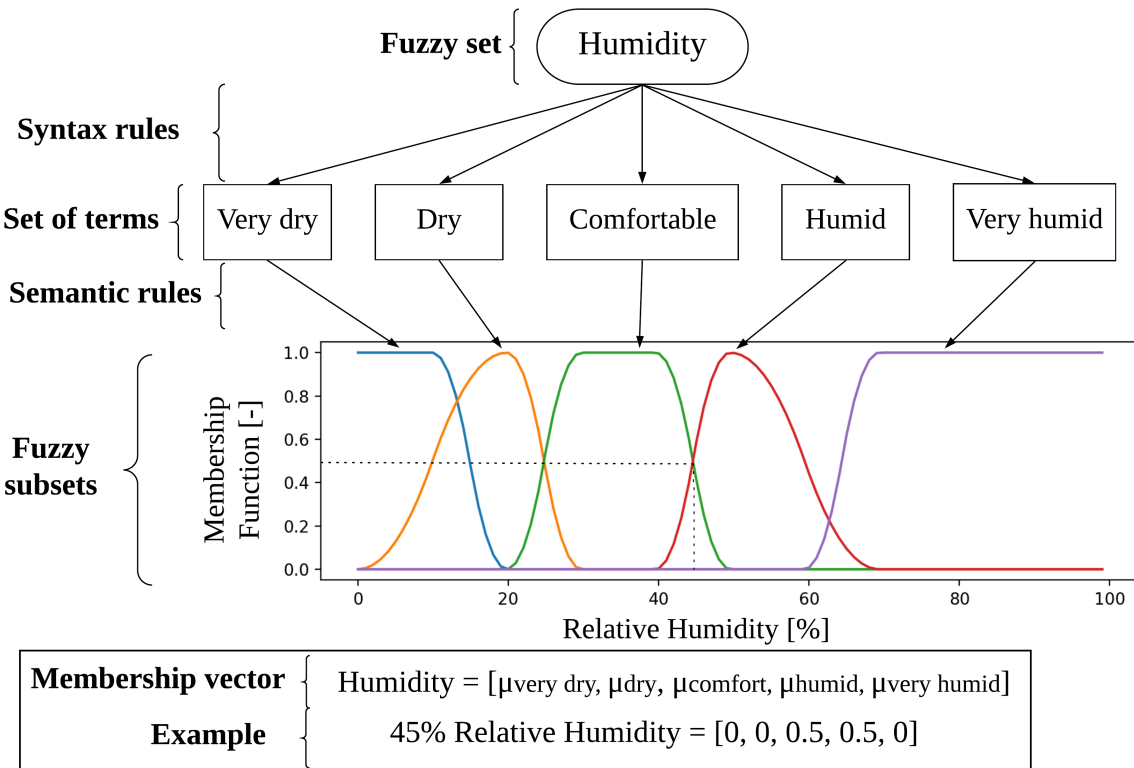


Figure 2.1: Structure of a fuzzy set (Source of logic: Zadeh, 1965).

### Classical sets versus fuzzy sets

The main difference between an ordinary set (defined in Equation 2.6) and a fuzzy set (Equation 2.7) is that, while the grades of membership for classical sets are based on Aristotelian two-valued logic (0 or 1), fuzzy sets can have different degrees of membership within this interval (Klir & Yuan, 1995). In the previous example, a relative humidity of 45% results in a membership of 0.5 for 'Comfortable' and 0.5 for 'Humid', and thus, belongs to two distinct

## 2.3. Fuzzy sets theory

---

classes. The number of membership functions can be yet higher than the five functions illustrated in Figure 2.1. That number depends directly on how accurate one wants to represent the data.

$$A = \{ x \mid x \in \chi \text{ and } x \text{ is } 0 \vee 1 \} \quad (2.6)$$

$$A_{fuzzy} = \{ (x, \mu_A(x)) \mid x \in \chi, \mu_A(x) \in [0, 1] \} \quad (2.7)$$

Where  $A$  and  $A_{fuzzy}$  are an ordinary and a fuzzy set respectively,  $x$  is a variable of the universe of discourse  $\chi$  and  $\mu_A$  is the membership function of  $A_{fuzzy}$ .

### Membership functions

Membership functions (MFs) describe to which degree an object is a member of a fuzzy subset. They vary in shape (Figure 2.2), scale, and boundaries. Their determination is considered to be the most crucial step to formulate a fuzzy set problem (Civanlar & Trussell, 1986).

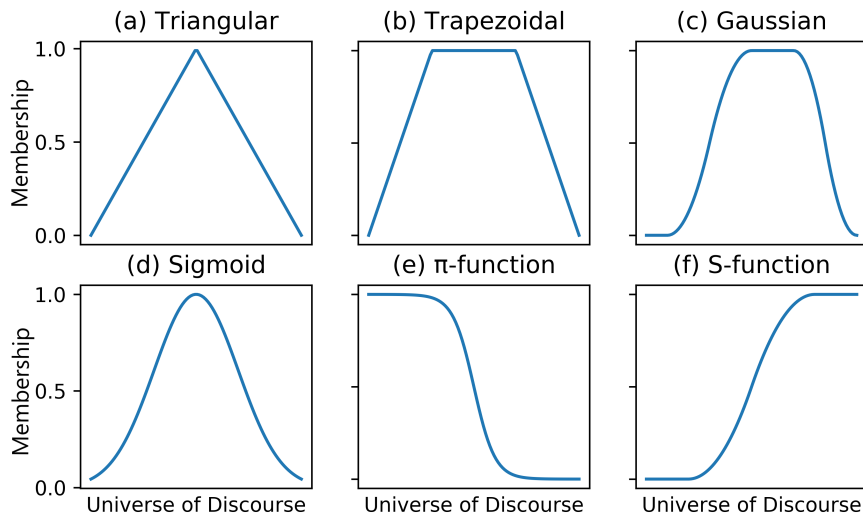


Figure 2.2: Shapes of membership functions.

Dombi (1990) emphasized that working without membership functions in fuzzy logic is analogous to employing probability theory without using probability distribution functions. Moreover, the application of appropriate membership functions (MFs) is crucial to satisfactorily describe fuzzy subsets.

### Fuzzy set operations

Fuzzy sets are a generalization of ordinary sets and follow the same definitions of union, intersection, complement and containment (Zadeh, 1965). These operations are shortly explained in following using the concept of membership  $f(x)$  of fuzzy sets.

Let A and B be fuzzy sets and X a space of points such as  $X = \{x\}$ . The fuzzy *complement* of A is:

$$f_{A'} = 1 - f_A. \quad (2.8)$$

The *containment* of A in B:

$$A \subset B \text{ iff } f_A \leq f_B. \quad (2.9)$$

The *union* C = A ∪ B:

$$f_C(x) = \max[f_A(x), f_B(x)], \quad x \in X \quad (2.10)$$

The *intersection* C = A ∩ B:

$$f_C(x) = \min[f_A(x), f_B(x)], \quad x \in X \quad (2.11)$$

### 2.3.2 Applications in modeling hydro-environments

Fuzzy sets theory has been extensively applied in hundreds of modeling studies. One of the advantages of fuzzy techniques is the capability of dealing with imprecise and/or uncertain data. Models of hydro-environments are built to reproduce or forecast phenomena of hydraulic and environmental systems. During the modeling process, uncertainties associated with input data and model structure are introduced. It is very useful, therefore, to be able to convey information on a model output considering some level of ambiguity of its results.

Significant advances in fuzzy techniques have been carried out in the last decades. This period consisted of rich advancements in computational power, which enabled the operation and processing of large fuzzy sets. Additionally, fuzzy sets were disseminated and applied over several disciplines, including water resources research. Noack, Ortlepp, and Wiprecht (2015) introduced a multivariate fuzzy-logical habitat modeling, in which habitat variables (e.g. particle size, water depth and flow velocity) were fuzzified to characterize the suitability of spawning ground for the brown trout. Wiprecht et al. (2013) used a data-driven neuro-fuzzy

## 2.4. Comparison of simulated and observed map data

---

modeling approach to estimate bed load and total bed material at the Rhine River. These and other studies (Noack, Schneider, & Wieprecht, 2013; Pappenberger et al., 2007; Wealands, Grayson, & Walker, 2005a) demonstrate innovative and powerful tools based on fuzzy-based techniques in many fields of water research.

## 2.4 Comparison of simulated and observed map data

The comparison of spatial data is essential to assess differences among data of any kind. It provides answers to questions on how spatially explicit data changed over years and it is a fundamental tool for several model validation techniques (Foody, 2007). Map comparison methods were mainly developed by remote sensing and GIS communities (White, 2006). They have also been applied in a vast number of research fields beyond this scope (Dou et al., 2007; Pawłowski & Godzik, 2001) and offer powerful tools in research fields, such as hydrology, flood protection, and sediment management. Visser and De Nijs (2006) name four main reasons for using map comparison. They are:

- evaluate maps produced by models under different circumstances;
- detect temporal changes depicted by maps;
- calibrate or validate models;
- perform uncertainty and sensitivity analysis by comparing model output to a reference map.

However, the task of comparing maps is not as simple as one might think. The reason is that humans and their pattern recognition capabilities to capture similarities can not be easily implemented in algorithms. At the same time, human observers are prone to interpretation errors, and do not serve as a standardized method.

### 2.4.1 Approaches to measure spatial similarity

#### Visual comparison

In some research fields, it is still common to assess map similarity through visual comparison. The reason is that despite its weaknesses, visual assessments performed by experts are believed to convey more knowledge on a given phenomenon than automated techniques. Nevertheless,

not only is this approach extremely subjective, but also is neither repeatable nor quantitative (Wealands, Grayson, & Walker, 2005b).

### Cell-by-cell comparison

In contrast to visual inspection, computational comparison techniques can be automated for model calibration and validation purposes. One of the first methods invented to computationally capture spatial patterns was the cell-by-cell comparison. At each cell, the value of a given attribute is compared between maps. Frequent measures of global similarity (or dissimilarity) for continuous-valued rasters are the root mean square error (*RMSE*) and coefficient of determination ( $R^2$ ), as presented in Section 2.2.5.

While efficient for calculating relations between variables, the *RMSE* and  $R^2$  are aspatial in that they treat datasets as stacked vectors and do not account for spatial distribution of the pairs of values (Haining, 1991). Furthermore, Wealands et al. (2005b) argue that local similarity methods are considerably more sensitive to discrepancies as they evaluate every location without capturing global spatial patterns. This problem is particularly critical when map comparison is used to evaluate a model simulation because firstly, the map output by a model might not be as accurate as the pixel scale (Power, Simms, & White, 2001) and second, the map of observations also involves uncertainties associated with measurement inaccuracies.

### Kappa statistics

In many cases there is the necessity to quantify agreement between categorical maps in terms of a single statistical value (e.g., *RMSE*,  $r$ ,  $R^2$ ). In 1960, the psychologist and statistician Jacob Cohen proposed such a coefficient to measure the agreement between nominal scales (Cohen, 1960) and named the method Cohen's Kappa. His work was later extended by Fleiss, Levin, and Paik (1981) and others (e.g., Thompson & Walter, 1988; Cohen, 1972).

Kappa statistics is a cell-by-cell approach for geospatial analysis, which produces a measure of agreement among map datasets. It considers the proportion of times that the datasets agree  $P(A)$  and corrects it with the probability of the data agreeing merely by chance  $P(E)$ . Thus,  $P(A) - P(E)$  represents the proportion of agreement related to the reproducibility of the results which, when divided by its maximum possible value  $1 - P(E)$ , results in the kappa coefficient shown in Equation 2.12 (Cohen, 1960).

One might ask what is the main advantage of kappa statistics in relation to other statistics. The

## 2.4. Comparison of simulated and observed map data

---

whole idea behind Cohen's work relies in the fact that certain variables can take a finite, instead of an infinite, number of possible outcomes. A finite number of outcomes are commonly described by categories, while an infinite number of outcomes belong to a continuous domain of values. When the number of possible outcomes is finite, the chance of an event (i.e., outcome) occurring merely by chance is higher than zero, according to probability theory. The following example illustrates that. In theory, the probability of two people randomly picking the same exact number from a dataset of real numbers simultaneously (e.g., values between 0 and 1) is zero. That does not happen when the data is separated in a defined and limited number of categories (such as integers from 1 to 10). Therefore, when dealing with categorical data, it makes sense to measure agreement that actually occurred by intention and disregard the agreement that is anyway expected from random choices.

$$\kappa = \frac{P(A) - P(E)}{1 - P(E)} \quad (2.12)$$

Kappa values range from 0 (the observed agreement equals the expected by chance) to 1 (perfect agreement). Values within this range are frequently labeled according to Landis and Koch (1977), as shown in Table 2.3.

Table 2.3: Strength of agreement associated with kappa statistics (Landis & Koch, 1977).

<b>Kappa Statistic</b>	<b>Strength of Agreement</b>
< 0.00	Poor
0.00 – 0.20	Slight
0.21 – 0.40	Fair
0.41 – 0.60	Moderate
0.61 – 0.80	Substantial
0.81 – 1.00	Almost Perfect

The kappa coefficient is the most widely accepted measure of inter-rater reliability (i.e., the degree of agreement among raters) when dealing with nominal data (Sun, 2011). However, there are limitations on its applicability. One of its prerequisites is that each observation should be assigned to a unique category, which is objectionable because an observation often shows traits of different categories. Kraemer (1980) argues that by assigning an observation to a one-and-only category, one is forced to give inconclusive and deficient responses.

Another weakness pointed out by Maclure and Willett (1987) is that kappa statistics focuses solely on exact matches and disregards approximate agreements between categories. If a rater

assigns a category to a given observation, which differs from the other rater's in comparison, kappa treats it as total disagreement, regardless of any similarity the two categories may have. In addition, situations exist, in which disagreements are more dramatic than others (Cohen, 1972). For dichotomous (i.e., binary) data this characteristic does not represent a shortcoming, as observations either agree or disagree completely. Yet, for nominal polytomous (i.e., multiple categories) data, kappa statistics can be ineffective.

The following example illustrates the rationale of the previous paragraph. Predictions whether a river is deep enough for a specific ship cargo in certain locations are two-folded: yes or no. In this case, no mid-state (i.e., category) is considered, and thus, kappa statistics can be straightforwardly applied. Now, types of river mesohabitats are considered. For instance, Hauer, Mandlburger, and Habersack (2009) proposed the categories 'riffle', 'fast run', 'run', 'pool', 'backwater' and 'shallow water'. It can be argued that the category 'riffle' is much more similar to 'fast run' than it is to 'pools', as 'riffles' and 'fast runs' are high-energy habitats, whereas 'pools' are slow (even still) zones (i.e., low-energy). Kappa statistics does not account for that and would treat all categories equally.

Despite its weaknesses, kappa statistics has the particular strength of judging agreement between datasets taking into consideration the probability of the data agreeing by chance. Therefore, it has important traits for comparing categorical spatial data and its theory gave birth to other methods, which are discussed in the following section.

### Spatial comparison based on fuzzy sets theory

Humans are capable of recognizing not only local, but also global similarities, as well as visual patterns, without deliberately trying (Hagen, 2003). In this context, fuzzy set capabilities discussed in Section 2.3.1 are therein helpful because it mimics human judgement to some extent and it can be more easily automated.

Imperfect and imprecise information are issues that have to be handled in all spatial data processing and computer vision applications. By using the framework of fuzzy sets, crispy spatial data can be fuzzified to account for different levels of uncertainty (Bloch, 2005). Power et al. (2001) demonstrated a successful fuzzy-based method to measure both map agreement and land use change. Pappenberger et al. (2007) analyzed predictions of flood inundation models using fuzzy map comparison. This study considers two promising methods based on fuzzy sets theory: (1) fuzzy kappa and (2) fuzzy numerical map comparison.

### 2.4.2 Fuzzy kappa map comparison

Fuzzy kappa map comparison combines concepts from fuzzy logic and kappa statistics to create a new method of measuring spatial similarity in categorical maps. It was initially introduced by Hagen (2003), and later developed to fill theoretical gaps (Hagen, Straatman, & Uljee, 2005) and to account for auto-correlation (Hagen, 2009). In contrast to boolean comparison, fuzzy kappa comparison handles pairs of maps using fuzzy sets theory. Instead of belonging to a single category, each cell has a degree of belongingness to each of the categories encountered in the map, which results in a membership vector. This vector is assigned to each cell and is called **interpretation vector** (Hagen et al., 2005).

To compute each interpretation vector, two types of fuzziness are considered: fuzziness of category and fuzziness of location. Here, the word fuzziness is understood as uncertainty or error.

#### Fuzziness of category

Categories always involve a degree of uncertainty, which stems from classification methods during data processing. Moreover, one might want to allow vagueness among categories because in many practical applications it is not imperative to sharply differentiate the categories. In contrast to kappa statistics, fuzzy kappa map comparison considers that some classes can be similar to one another, thereby fuzziness of category is introduced. Fuzziness of category can be understood as the representation of how similar one category is to the others. This alikeness among categories is expressed by a similarity matrix (for instance, in Table 2.4).

Equations 2.13 and 2.14 define the categories in maps A (map of model results) and B (map of observations), where  $i$  and  $j$  indicate the indices of the categories of maps A and B, respectively.  $r$  and  $s$  are the number of categories of the corresponding map.

$$C^A = \{C_i^A\} \mid i = \{1, 2, \dots, r\} \quad (2.13)$$

$$C^B = \{C_j^B\} \mid j = \{1, 2, \dots, s\} \quad (2.14)$$

Categories that are present in one map may not be the same as in the other, but for the sake of simplicity, when formulating the similarity matrix, all categories  $C$  present both in map A and

Table 2.4: Example of similarity matrix for a pair of flood risk maps.  $C^A$  and  $C^B$  are the categories of map A and B, respectively. In this case the similarity between categories is only aimed at the very high and high flood risk classes.

$C^A/C^B$	Very high	High	Medium	Low
Very high	1	0.3	0	0
High	0.3	1	0.1	0
Medium	0	0.1	1	0.1
Low	0	0	0.1	1

B must be considered (Equation 2.15).

$$C = \{C^A \cup C^B\} \quad (2.15)$$

The similarity matrix  $M$  is formulated in Equation 2.16. The membership  $\mu_{i,j}$  of a category  $i$  in category  $j$  ranges from 0 to 1 and when  $i = j$  the membership must equal 1, since it comes to the membership of the category in itself;  $C$  is the total number of categories resulting from Equation 2.15.

$$M = \begin{bmatrix} \mu_{1,1} & \cdots & \mu_{1,C} \\ \vdots & \ddots & \vdots \\ \mu_{C,1} & \cdots & \mu_{C,C} \end{bmatrix} \quad (2.16)$$

Where  $\mu_{i,j} \in [0, 1] \supset \mathbb{R}$  and  $\mu_{i,j} = 1$  if  $i = j$ .

It should be noticed that the decision on membership values does not necessarily follow clear and objective rules. The values can be assigned according to the type of the map, the aim of the comparison, and the number of categories (Hagen, 2003).

### Fuzziness of location

Another type of fuzziness is also considered in the fuzzy kappa method, which is called fuzziness of location. The idea behind introducing fuzziness in location relies on the concept that a cell of a map A (here considered as the map of model results) may be similar not only to its exact equivalent in map B (here considered the map of observations), but also to the neighbors of this same cell in map B. (Hagen et al., 2005) defines the neighborhood of a cell as

## 2.4. Comparison of simulated and observed map data

---

all cells within a given distance from that same cell plus the cell itself. The degree to which a neighbor cell contributes to the local similarity measure is expressed by a distance decay function. This function describes the degree of belongingness of neighbor cell to the fuzzy representation of the cell considered. Distance decay functions can be such as those shown in Figure 2.2. Visser and De Nijs(2006) explain that it is helpful to experiment with different functions and size. Thus, one can choose a decay function that is adequate to the uncertainty and nature of the spatial data. The default distance decay function of the fuzzy kappa method is an exponential decay defined by the halving distance  $d_{halv}$ . The halving distance consists of the distance, in cells, where the membership decays to its half. Equation 2.17 and Figure 2.3 describe the distance decay function with a halving distance of 2 cells.

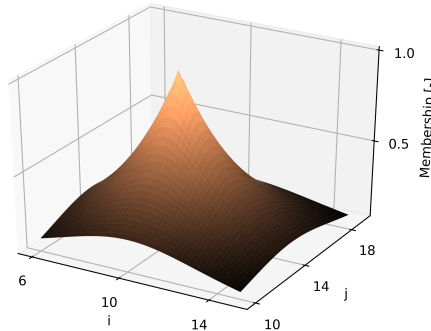


Figure 2.3: Exponential distance decay function with a halving distance of 2 cells. The neighborhood is defined as 4 cells and the central cell is located at node ( $i=10, j=14$ ).

$$\omega(d_{i,j}) = e^{\ln(1/2)*d/d_{halv}} = 2^{-d/2} \quad (2.17)$$

### The Fuzzy Neighborhood Vector

Considering both fuzziness of location and category, the Fuzzy Neighborhood Vector (Hagen, 2003) is calculated for each cell. The  $V_{neigh}$  results from the fuzzy union of all categorical and distance based memberships present in the neighboring cells. Thus, it expresses the different membership contributions of the neighboring cells to the fuzzy representation of the central cell. The highest contribution of each category determines the membership value of that

category. This step is done by Equations 2.18 and 2.19.

$$\mu_k = \max_{n=1}^N (\mu_{c_n, k} * \omega(d_n)) \quad (2.18)$$

$$V_{neigh} = \begin{pmatrix} \mu_1 \\ \mu_2 \\ \vdots \\ \mu_C \end{pmatrix} \quad (2.19)$$

Where  $k$  iterates through all categories  $C$ ;  $n$  iterates through all neighbors  $N$ ;  $c_n$  is the category found in neighbor  $n$ ;  $d_n$  is the distance from the center cell to the neighbor  $n$ ;  $\omega(d_n)$  is the distance decay function; and  $\mu$  is the membership of category  $k$  for the neighboring cell  $n$  in  $V_{neigh}$ .

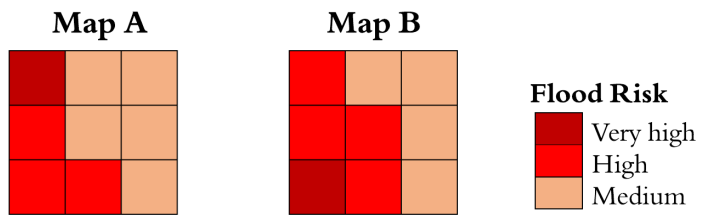


Figure 2.4: Neighborhood of a (central) cell in map A (map of model results) and its respective location in map B (map of observations).

In following, an example using the similarity matrix from Table 2.4 and two synthetic neighborhoods from flood risk maps are shown (Figure 2.4). The two neighborhoods present three levels (i.e., categories) of flood risk: 'Very High', 'High' and 'Medium' risk. In this example the exponential decay function is used with a halving distance of one cell. The  $V_{neigh}$  of the center cell of map A is calculated by Equation 2.20. For the corner cells where  $d_n$  is equal to  $\sqrt{2}$  cells, the distance based membership is  $2^{-\sqrt{2}/1} = 0.37$ . The following calculations demonstrate the

## 2.4. Comparison of simulated and observed map data

---

calculus of the  $V_{neigh}$ :

$$V_{neigh,A} = \begin{bmatrix} \mu_{Veryhigh} \\ \mu_{High} \\ \mu_{Medium} \end{bmatrix} = \begin{bmatrix} max\begin{pmatrix} 1.0 * 0.37 & 0 * 0.5 & 0 * 0.37 \\ 0.3 * 0.5 & 0 * 1.0 & 0 * 0.5 \\ 0.3 * 0.37 & 0.3 * 0.5 & 0 * 0.37 \end{pmatrix} \\ max\begin{pmatrix} 0.3 * 0.37 & 0.1 * 0.5 & 0.1 * 0.37 \\ 1.0 * 0.5 & 0.1 * 1.0 & 0.1 * 0.5 \\ 1.0 * 0.37 & 1.0 * 0.5 & 0.1 * 0.37 \end{pmatrix} \\ max\begin{pmatrix} 0 * 0.37 & 1.0 * 0.5 & 1.0 * 0.37 \\ 0.1 * 0.5 & 1.0 * 1.0 & 1.0 * 0.5 \\ 0.1 * 0.37 & 0.1 * 0.5 & 1.0 * 0.37 \end{pmatrix} \end{bmatrix} = \begin{bmatrix} 0.37 \\ 0.5 \\ 1.0 \end{bmatrix} \quad (2.20)$$

$$V_{neigh,B} = \begin{bmatrix} 0.37 \\ 1.0 \\ 0.5 \end{bmatrix} \quad (2.21)$$

### The interpretation vector

For every cell, two interpretation vectors are produced. For the calculation of the interpretation vectors, the concepts of a Fuzzy Neighborhood Vector and of a crisp vector are needed.  $V_{neigh}$  was presented in the previous section. A crisp vector, as the term indicates, considers only crisp states of belongingness. It expresses which category is or is not found at a cell. Thus, each vector entry may take 0 (if the category is not found there) or 1 (if the category is found) values. For instance, the  $V_{crisp,A}$  and  $V_{crisp,B}$  are given by Equation 2.27.

The first interpretation vector stems from the comparison of each cell in map A with the analogous cell and its neighbors in map B. The second interpretation vector is the inverse, where each cell in map B is compared with the analogous cell and its neighbors in map A.

Both comparisons can be seen as cell-by-cell comparisons. For instance, the first comparison uses the crisp vector of the cell in map A versus the  $V_{neigh}$  of the analogous cell in map B and the second comparison, the crisp vector of the cell in map B versus the  $V_{neigh}$  of map A.

Hagen(2003) explains that this two-way comparison is done in the interest of not overpowering possible similarities between the two neighborhoods, which would be the case if the two fuzzy cells were directly compared. The author investigated six situations that demonstrate the preference for this procedure over the direct comparison of the Fuzzy Neighborhood Vectors.

The two interpretation vectors,  $S(V_{neigh,A}, V_{crisp,B})$  and  $S(V_{neigh,B}, V_{crisp,A})$ , are calculated according to Equations 2.22 and 2.23. With them, the two-way similarity measure is calculated by Equation 2.24. The values establishes the fuzzy similarity at that cell.

$$S(V_{neigh,A}, V_{crisp,B}) = \max \left[ \min(V_{neigh,A}^{k=1}, V_{crisp,B}^{k=1}), \min(V_{neigh,A}^{k=2}, V_{crisp,B}^{k=2}), \dots, \min(V_{neigh,A}^{k=C}, V_{crisp,B}^{k=C}) \right] \quad (2.22)$$

$$S(V_{neigh,B}, V_{crisp,A}) = \max \left[ \min(V_{neigh,B}^{k=1}, V_{crisp,A}^{k=1}), \min(V_{neigh,B}^{k=2}, V_{crisp,A}^{k=2}), \dots, \min(V_{neigh,B}^{k=C}, V_{crisp,A}^{k=C}) \right] \quad (2.23)$$

$$S_{Two-way} = \min \left[ S(V_{neigh,A}, V_{crisp,B}), S(V_{neigh,B}, V_{crisp,A}) \right] \quad (2.24)$$

Where  $k$  iterates through all categories  $C$ . For example, the interpretation vectors for the flood risk maps are calculated in Equations 2.25 and 2.26.

$$S(V_{neigh,A}, V_{crisp,B}) = \max \left[ \min(0.37, 0), \min(0.5, 1.0), \min(1.0, 0) \right] = \max [0, 0.5, 0] = 0.5 \quad (2.25)$$

$$S(V_{neigh,B}, V_{crisp,A}) = \max \left[ \min(0.37, 0), \min(1.0, 0), \min(0.5, 1.0) \right] = \max [0, 0, 0.5] = 0.5 \quad (2.26)$$

$$V_{crisp,A} = \begin{bmatrix} 0 \\ 0 \\ 1 \end{bmatrix} \text{ and } V_{crisp,B} = \begin{bmatrix} 0 \\ 1 \\ 0 \end{bmatrix} \quad (2.27)$$

$$S_{Two-way} = \min[0.5, 0.5] = 0.5 \quad (2.28)$$

### The Fuzzy Kappa coefficient $K_{fuzzy}$

In addition to a fuzzy similarity measure for each cell, it is advantageous to express similarity in terms of an overall measure. Hagen (2003) argues that simply integrating over all local similarities, which corresponds to the average of all cells for regular grids, is not necessarily a meaningful measure. An extreme case to illustrate that is a pair of maps in which only 2 categories exist. The probability of a pair of cells of belonging to the same category is 50%. Therefore, it is expected that a number of cells match just because of chance. In order to account for this expected agreement, kappa statistics come herein into use.

In categorical maps, the average similarity is considerably influenced by the number of categories and the distribution of the data. To tackle this problem, Hagen (2003) came up with a measure similar to Cohen's kappa and called it Fuzzy Kappa coefficient  $K_{fuzzy}$ . In contrast to the similarity measures per cell, which can range from 0 to 1.0,  $K_{fuzzy}$  can take values from  $-\infty$  up to 1.0. The formula for  $K_{fuzzy}$  is identical to Equation 2.12 (Section 2.4.1) with exception of the calculation of the expected agreement, which involves a more sophisticated approach. The reader is referred to Hagen (2003) for a complete description of the modified kappa measure. Here, it is sufficient to understand that by means of the Fuzzy Kappa coefficient, one can quantify overall map similarity while accounting for expected agreement.

### 2.4.3 Fuzzy numerical map comparison

While the fuzzy kappa approach handles comparison of categorical maps, the fuzzy numerical approach follows the same rationale, but adapted for handling maps of numerical and continuous data (Hagen, 2006). Likewise, the fuzzy numerical approach performs a two way comparison. First, it measures the local similarity  $s_i^{A,B}$  considering the crisp cell in a map A (map of model results) and a fuzzy cell in the other map B (map of observations), and

afterwards the inverse. Here, a cell  $i$  in one map is compared to the analogous cell and its neighbors  $j$  in the other map. The resulting similarity measure (calculated by Equation 2.29) between neighbors  $j$  and  $i$  is penalized by the distance decay membership. Thus, spatial uncertainty is tolerated inside the neighborhood.

Equation 2.29 is the particular similarity function that is applied for each pair of values according to Hagen (2006). Different functions can be applied though, as the method can be implemented with other similarity measures.

$$f(a, b) = 1 - \frac{|a - b|}{\max(|a|, |b|)} \quad (2.29)$$

The one-way similarity between maps  $A$  and  $B$  at a given cell  $i$  is determined by Equation 2.30.

$$s_i^{A,B} = \max_{j=1}^N [f(A_i, B_j) * \omega(d_{i,j})] \quad (2.30)$$

Where index  $j$  iterates through all  $N$  neighbor cells of cell  $i$  and  $\omega(d_{i,j})$  is the exponential decay membership function. (Equation 2.17).

Then,  $S_i(A, B)$  combines the two one-way similarities into one single similarity value (Equation 2.31).

$$S_i = \min[s_i^{A,B}, s_i^{B,A}] \quad (2.31)$$

Finally, the Global Fuzzy Similarity  $S_{fuzzy}$  is expressed as the mean of  $S_i(A, B)$  in all  $n$  locations, shown in Equation 2.32.

$$S_{fuzzy} = \frac{1}{n} \sum_{i=1}^n S_i \quad (2.32)$$

#### 2.4.4 The Map Comparison Kit (MCK)

The Map Comparison Kit (MCK) (Visser & De Nijs, 2006) is an open source software package for map comparison. It was initially released in 2001 under the name 'Analyse tool' and it was developed by the Research Institute for Knowledge Systems (RIKS) and the Netherlands Environmental Assessment Agency ('MNP-RIVM' or NEAA, in English). Its initial version

## 2.4. Comparison of simulated and observed map data

---

provided five map comparison techniques depending on the scaling system (nominal, ordinal, interval or ratio) and comparison algorithms. Although it was originally designed for land-use and environmental applications within the NEAA, the software is applicable in several other types of map comparisons (Visser & De Nijs, 2006).

Since its release, significant extensions have been made. For example, methods for comparison of continuous valued raster data were implemented (Hagen, 2006). The fuzzy kappa and the fuzzy numerical method, which are in the scope of the present study, are also included in the MCK.

# **Chapter 3**

## **Methods**

### **3.1 Case studies**

#### **3.1.1 Terrain change analysis of physical models of shallow reservoirs**

##### **Setup of the physical models**

Kantoush (2008) conducted a series of experiments with physical models to investigate flow fields and sedimentation processes in shallow reservoirs at the EPFL (École Polytechnique Fédérale de Lausanne, Switzerland). The present study focuses on two configurations of these physical models with the geometries shown in Figure 3.1. The assembled basins had adjustable PVC walls that enabled different geometry shapes. The bottom of the basins consisted of hydraulically-smooth PVC flat plates and there was no mobile sediment deposits initially. During experiments, sediment was fed with the water inflow. The main experimental features are listed in Table 3.1. The results of the experiments (i.e., bed elevation change) are provided to the present study in form of text files.

##### **Setup of the numerical models**

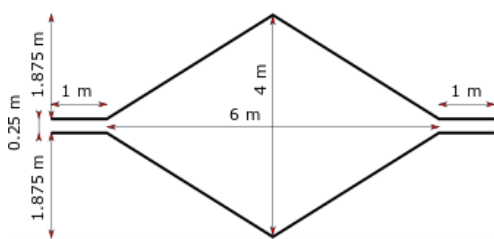
Both the diamond- and hexagon-shaped physical models were simulated by Shoarinezhad et al. (2021) using the software SSIIM 2 (Olsen, 2014). SSIIM 2 - acronym for Sediment Simulation In Intakes with Multiblock - is a software for 3D hydro-morphodynamic modeling that solves the Reynolds-averaged Navier-Stokes (RANS) equations and the continuity equation on an adaptive grid. Calibration was performed using the calibration tool PEST (Model-Independent

### 3.1. Case studies

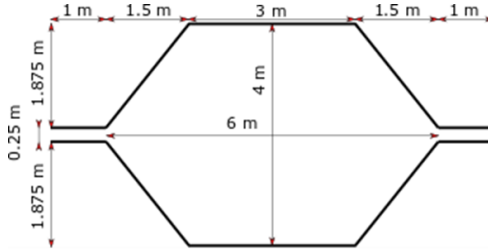
---

Table 3.1: Features of the experimental setup (Source: Kantoush, 2008).

Feature	Value
Discharge	7.0 l/s (constant)
Water depth	0.2 m
Sediment density	1,500 kg/m <sup>3</sup> (crushed walnut shells)
Bottom slope	0%
Inlet Froude number	0.1
Suspended sediment concentration	3.0 g/l



(a) Geometry of the diamond-shaped physical model.



(b) Geometry of the hexagon-shaped physical model.

Figure 3.1: Geometry of the physical models. Flow is running from the left to the right.

Parameter Estimation and Uncertainty). PEST (Doherty et al., 1994) is a software package for automatic calibration and sensitivity analysis. It aims at minimizing the sum of the square errors between simulated and measured data. The algorithm consists of an iterative process, which uses gradient descent methods to find a minimum of the objective function. The user defines which parameters, and also the parameter ranges, are relevant for the calibration (Shoarinezhad & Haun, 2018). The selected parameters are hence automatically adjusted at each iteration. The final results of the simulations are provided to this study in form of text files.

#### 3.1.2 Terrain change analysis of the lower Salzach River

##### Study area

The Salzach River (Austria and Germany) has its source in the Kitzbuehel Alps and drains to the Inn River, which is in turn a tributary of the Danube River. The Salzach River had originally active braided zones where rich morphological features such as alternating bars, river islands, and gravel banks existed (Foeckler, Diepolder, & Deichner, 1991). Because of anthropogenic measures, the dynamics of the natural flow and sediment continuity are today impaired.



(a) Experimental setup of the diamond-shaped physical model.  
 (b) Experimental setup of the hexagon-shaped physical model.

Figure 3.2: Experimental setup (Source: Kantoush, 2008).

The river section between km 59.3 and km 52.4 is considered in this study (Figure 3.3). This section suffered considerable riverbed deepening after flood events in 2002 and 2013, when the discharge of a 100-year flood ( $3100m^3/s$ ) was exceeded (Beckers et al., 2020). The sediment transport behavior of the lower Salzach River is significantly influenced by the bed load of its largest tributary, the Saalach River (Beckers, Noack, & Wiprecht, 2018). The Saalach/Salzach confluence is located at the river chainage 59.3 km (see Figure 3.3).

### Setup of the numerical models

A comprehensive set of modeling studies on the lower Salzach River is performed by Beckers et al. (2016, 2018, 2020) in order to aid future sediment management plans. To do so, the 2D morphodynamic modeling software *HYDRO\_FT-2D* was used. *HYDRO\_FT-2D* calculates bed evolution by solving Exner's equation (Exner, 1925) with a finite volume spatial discretization and explicit Runge-Kutta time discretization. A short summary of the models of the lower Salzach is given in following:

- **Manually calibrated *HYDRO\_FT-2D* model:** Beckers et al. (2016) applied the software module *HYDRO\_FT-2D* coupled with the hydraulic module *HYDRO\_AS-2D*. The model was calibrated and validated for the periods between 2002 - 2010 and 2010 - 2013, respectively. Manual calibration was done by means of an extensive set of model runs while testing more than 200 combinations of parameters, which corresponds to approximately 1828 hours of computation time (Beckers et al., 2020). The calibration consisted of comparing simulated against observed bed level changes, as well as the total sediment balance (erosion and deposition volumes), of several river cross sections.
- **Stochastically calibrated *HYDRO\_FT-2D* model:** Beckers et al. (2020) used a surrogate

### 3.1. Case studies

---

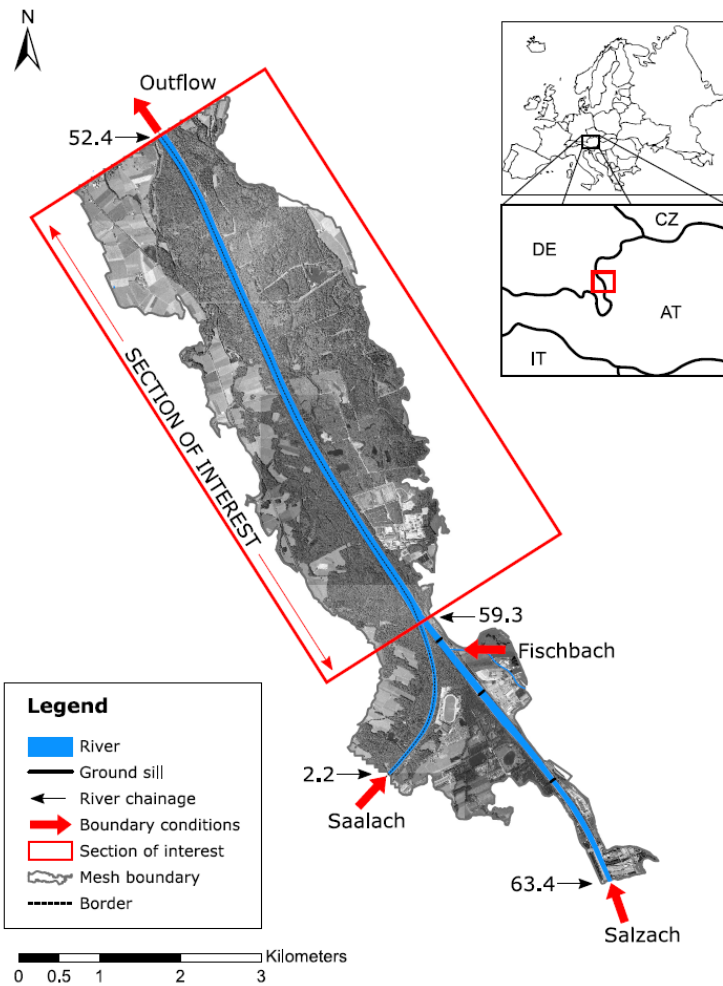


Figure 3.3: Study area of the lower Salzach River (Source: Beckers et al., 2020).

model to perform Bayesian calibration of the numerical morphodynamic model of the lower Salzach River. The surrogate model works as a calibration tool that is built with a reduced number of parameters. It aims at approximating model complexity via the arbitrary polynomial chaos expansion technique (aPC) developed by Oladyshkin and Nowak (2012). The resulting stochastically calibrated model performs better than the manually calibrated model and was obtained in much less time. The methods of the surrogate modeling approach are not discussed here, as they are of minor relevance for the objective of this study.

## 3.2 Algorithm development

### 3.2.1 Hypotheses

One way to overcome the challenge of comparing uncertain spatial data that was forced to take discrete values is by applying fuzzy mapping techniques. To this day, there has been no study of fuzzy based map comparison to evaluate hydro-morphodynamic model performance. Therefore, the present study applies the fuzzy numerical and fuzzy kappa methods to assess the performance of the presented hydro-morphodynamic models (Section 3.1). In order to do so, the following hypotheses are used:

#### Application of the fuzzy numerical method

- Because the fuzzy numerical method was designed to compare continuous raster data, the method is a promising approach for comparing simulated with observed bed level changes. The Global Fuzzy Similarity  $S_{fuzzy}$  can convey relevant statistical information about the efficiency of numerical morphodynamic models.

#### Application of the fuzzy kappa method

As explained in the previous section, the fuzzy kappa method compares categorical spatial data. Therefore, the present study uses the following hypotheses:

- Bed elevation change can be categorized in classes of erosion and deposition (at the ordinal scale). The concept behind categorizing data lies in the assumption that categories provide a representative simplification of the model output. In many cases, the predictions of morphodynamic models can be well represented by classes (such as intervals of erosion and deposition patterns), rather than specific values. Specific values are rarely used in practical applications<sup>i</sup>.
- If the classification is well performed, erosion and deposition spatial patterns can be successfully captured and data uncertainty can be considered within each class interval.
- The category breaks (limits of the class intervals) are optimized for each dataset, thus they can vary for each map. Here, the categories of the observed map are treated as

---

<sup>i</sup>In reservoir maintenance, for instance, it is very common for operators to make decisions based on spatial sedimentation trends. The difference between, for example, 1.5 or 1.4 meters of sedimentation depth can be negligible.

### 3.2. Algorithm development

---

the real responses that a model should simulate. Therefore, the determination of the category breaks should be done using the map of observations.

#### 3.2.2 Development of pre-processing tools

For the application of both fuzzy map comparison techniques, the spatial data has to be in raster format. However, the output data from hydro-morphodynamic models and measurements are typically obtained in text format. This study prepared Python codes to read and pre-process both simulated and observed bed elevation change  $\Delta z$ .

##### **Interpolation**

In order to put spatial data into regular and quadratic gridded data, a code for normalizing the data is programmed. Here, the term normalization is understood as the generation of new set of points based on available data (possibly unequally distributed and scattered) via interpolation techniques. These interpolated points are important to fill the values of otherwise empty cells (see Figure 3.4a).

In addition, this step also offers the possibility of generating finer maps and it enables comparison with other maps of the same cell size. Figure 3.4a shows the raster of the simulated bed elevation change for the hexagon-shaped model when no interpolation is performed and a resolution of 0.1 m was used. Since the points in the x direction were spaced with equidistance of 0.2 m, the rasterization results in a disjointed map. As to using the spacing of 0.2 m it results in Figure 3.4b, which is a coarser map that may oversee the variability of the spatial data.

The algorithms are developed upon existing interpolation-to-uniform-grid methods and take two input parameters: (1) cell size and (2) interpolation method. In order to assess the effect of the cell size in fuzzy numerical map comparison, sensitivity analyzes are performed in Sections 4.1.1 and 4.2.2.

##### **Rasterization**

The rasterization process consists of converting spatial data such as shapefile points or other geospatial data to georeferenced images called rasters. In the previous step, the spatial points were normalized and interpolated to ensure that the maps are comparable and overlay-able. Now, in the rasterization step, the interpolated data are converted to rasters with equally

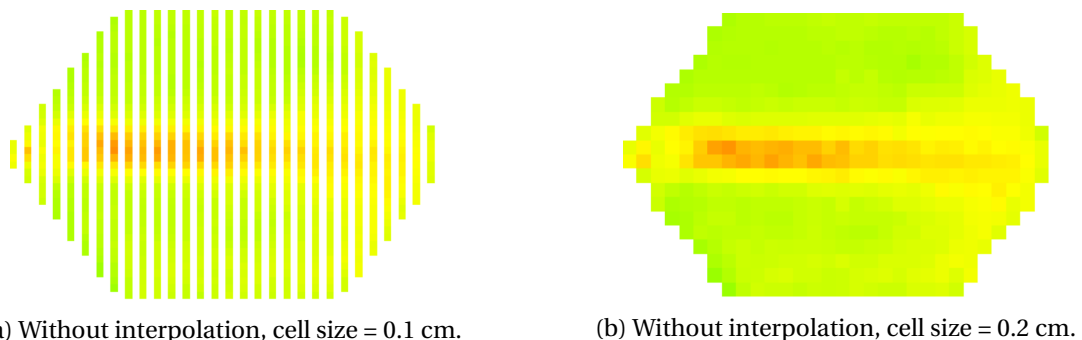


Figure 3.4: Examples of rasters without interpolation.

sized pixels (quadratic and equally spaced cells), which are the input for the fuzzy numerical method.

The rasterization (i.e., conversion of a text file into a GeoTIFF file) is not entirely necessary, as the normalized spatial points (in form of matrices) already represent the value of each cell to be compared. However, with the rasters of simulated and observed values the theoretical background of fuzzy map comparison explained in Section 2.4.3 is maintained.

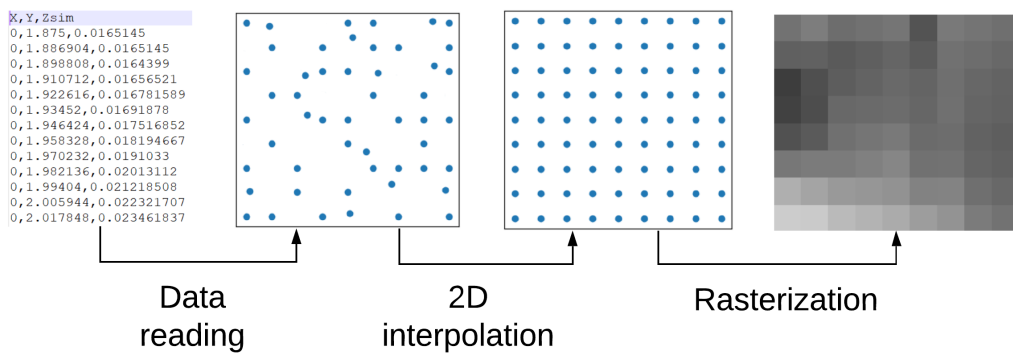


Figure 3.5: Data preparation process for fuzzy comparison.

### Categorization of the continuous spatial data

When performing fuzzy kappa map comparison, the rasters to be compared should be categorical. Hence, continuous rasters such as in this study should be categorized in classes for enabling the fuzzy comparison.

The categorization of a variable in the continuous domain can be done following several approaches. Map classification methods such as equal intervals, quantiles, and natural breaks

### 3.2. Algorithm development

---

are commonly used. It is worth experimenting with different classification methods in order to find the most adequate for the given dataset. In this study, two concerns arise while classifying data. First, the number of classes and their intervals should be representative enough to characterize the data and minimize the loss of information. Second, the data should not be excessively categorized in only a few classes, as that would produce a very simplified map.

To overcome these issues, the classification method named natural breaks (Jenks & Caspall, 1971) is selected and implemented in the algorithm of this study. This method has shown to be an adequate approach for classifying several types of data (Toshiro, 2002) and in this study it sufficiently captures the spatial trends of the pairs of maps. The method, also called Jenks optimization method, aims at minimizing the average deviation of each category from the class mean. It also maximizes differences between categories by maximizing deviations of each category from the means of the other classes. The algorithm requires solely the number of classes into which the data should be classified and the dataset itself.

#### **Generation of a random raster to create a baseline prediction**

A model performance statistic should measure skill rather than accuracy (Sutherland et al., 2004). The skill of a model (see Section 2.2.5) is assessed considering the performance relative to a baseline prediction. With this purpose, a raster of values following a uniform random distribution is generated for each numerical model. The range of the randomly generated values is between the minimum and maximum  $\Delta z$  of the dataset of observations. The randomly generated map is compared with the respective map of observations using the fuzzy numerical algorithm, which results in a  $S_{fuzzy,baseline}$  value (Figure 3.6). When compared with a  $S_{fuzzy,baseline}$  value,  $S_{fuzzy}$  offers an insight into the skill of a hydro-morphodynamic numerical model.

Furthermore, a random categorical raster is generated for each numerical model. This is done by classifying the continuous randomly generated raster using the respective class intervals obtained using the natural breaks algorithm. The categorical raster is compared with the respective (categorical) raster of observations using fuzzy kappa map comparison to produce a  $K_{fuzzy}$  value of reference (Figure 3.6). Both random categorical and continuous rasters are produced for the diamond-shaped model, hexagon-shaped model and the lower Salzach River.

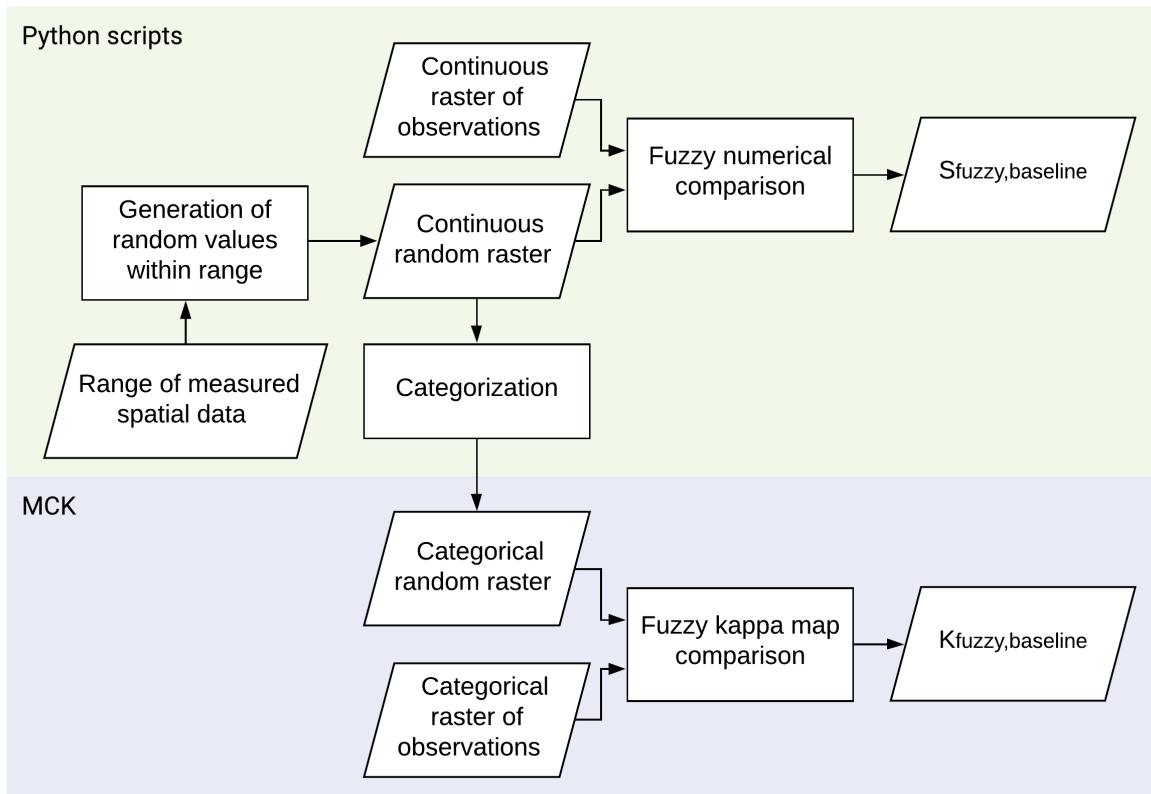


Figure 3.6: Algorithm for generating  $S_{fuzzy}$  and  $K_{fuzzy}$  values of reference using random rasters.

### 3.2.3 Code for the fuzzy numerical method

#### Outline of the steps

This section outlines the methodology used to perform fuzzy numerical map comparison. An overview of the steps can be seen in Figure 3.7.

After the measured and simulated data are converted to overlay-able points and rasterized to produce uniformly spaced cells, the next step is the selection of the neighborhood and halving distance (see Section 2.4.2). Here, the modeler has to decide how much fuzziness (i.e., uncertainty and error) should be considered and tolerated. Finally, the fuzzy numerical method can be applied and the results used to analyze model performance.

### 3.2. Algorithm development

---

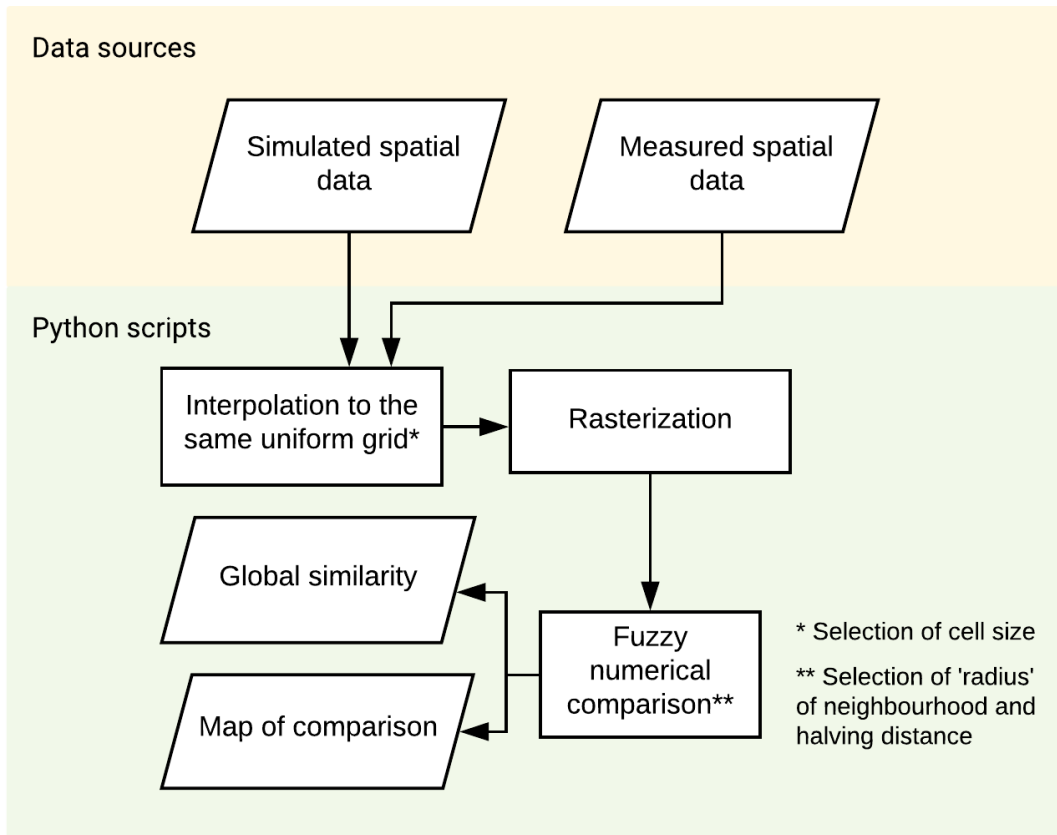


Figure 3.7: Algorithm for performing fuzzy numerical map comparison.

### Code development and verification

The code for the fuzzy numerical method is, to the author's best knowledge, not open source, although it is comprised in the Map Comparison Kit (MCK) through its graphical user interface. Therefore, with the purpose of performing fuzzy numerical map comparison decoupled from the MCK, this study focuses on coding the method and making it available as open source code. The method is programmed in Python 3 (Python Software Foundation) and made available by Negreiros (2020).

A Python package consists of a group of modules (i.e., Python scripts). Modules are built to group similar routines and variables. With Python modules, codes can scale from simple scripts to more elaborate applications (Oliphant, 2007). The present study constitutes a new package. One of the modules of this package was equipped with routines for reading model output data (typically text files), interpolating it to a regular grid, and finally rasterizing it. Different functionalities such as the cell size and the interpolation method can be selected by

the user. Another module was developed for fuzzy numerical map comparison. The output of the latter includes the Global Fuzzy Similarity and the map of comparison in raster (GeoTIFF) format. The results were vetted (i.e., verified) against the MCK package for the case study of the physical models of the shallow reservoirs. Finally, a third Python module was developed to plot and analyze rasters and the results of the fuzzy comparison. The reader is referred to (Negreiros, 2020) for more details of the code usage.

#### 3.2.4 Application of the fuzzy kappa method using the Map Comparison Kit (MCK)

Similarly to the steps elucidated for fuzzy numerical map comparison, spatial data have to be correctly prepared to perform fuzzy kappa map comparison. Initially, the data should be interpolated to the same grid, followed by the rasterization, and the conversion to categorized maps. Figure 3.8 delineates the algorithm created in this study to leverage fuzzy kappa map comparison.

The interpolation of the data to the same grid, rasterization and categorization steps are comprised in the pre-processing module, which is coded in the present study. Here, the comparison method is not programmed in a Python script, as it was done for the fuzzy numerical method, but it was performed with the MCK software package. The codes for fuzzy kappa map comparison are available in C++ programming language (Hagen, 2018).

## 3.3 Summary of the test approach

### 3.3.1 Physical models of shallow reservoirs

#### Interpolation and rasterization

The spacing (in the x and y direction) of the simulated and observed  $\Delta z$  points is approximately constant in the diamond-shaped reservoir, though the points are not always aligned at the same axis. Thus, an inconsistent assignment of point values to pixel values may occur. Furthermore, simulated values for the hexagon-shaped reservoir are only obtained every 0.2m, while observed values have a spacing of 0.1m (Kantoush, 2008). To overcome these two issues, a linear interpolation is performed in the present study and the gridded (i.e., in form of an evenly spaced matrix) data is burnt in raster maps (Figures 3.9 and 3.10) using a cell size of

### 3.3. Summary of the test approach

---

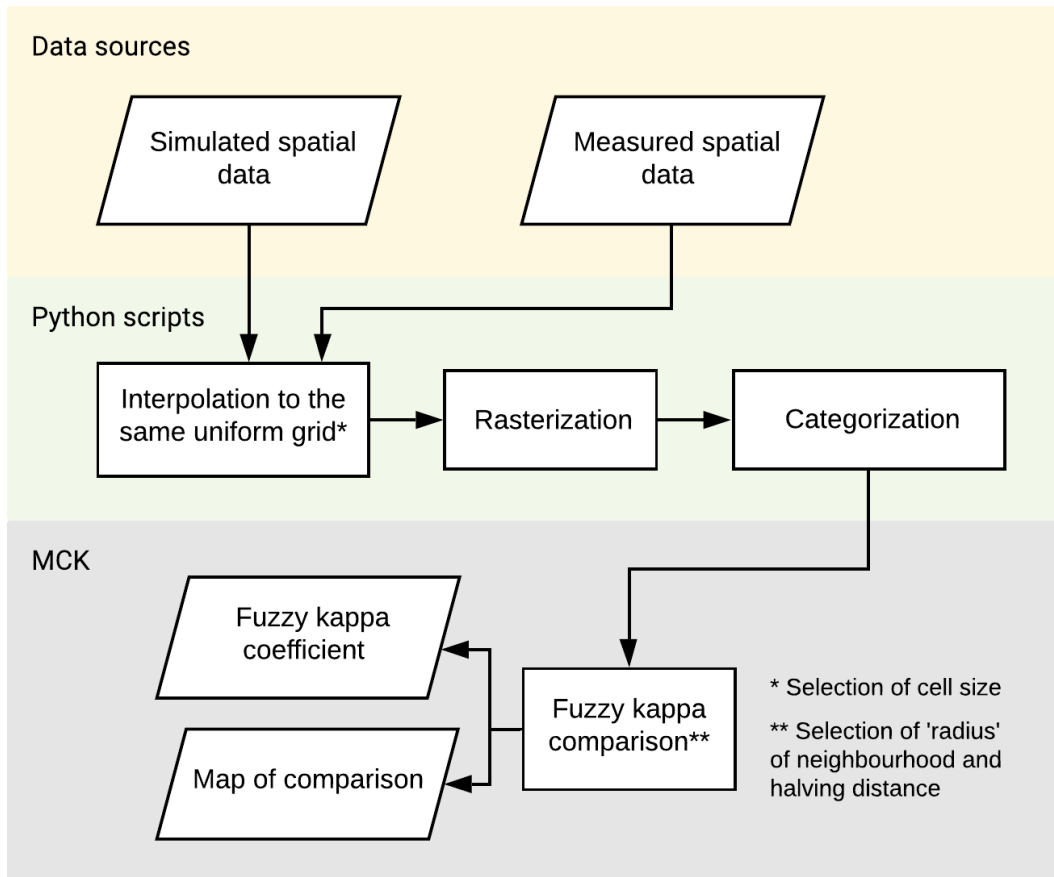
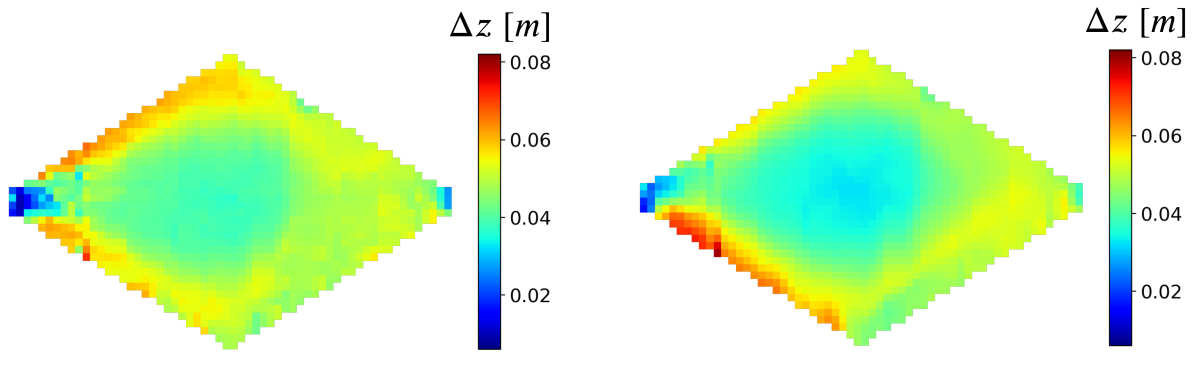


Figure 3.8: Algorithm for fuzzy kappa map comparison.

0.1m.

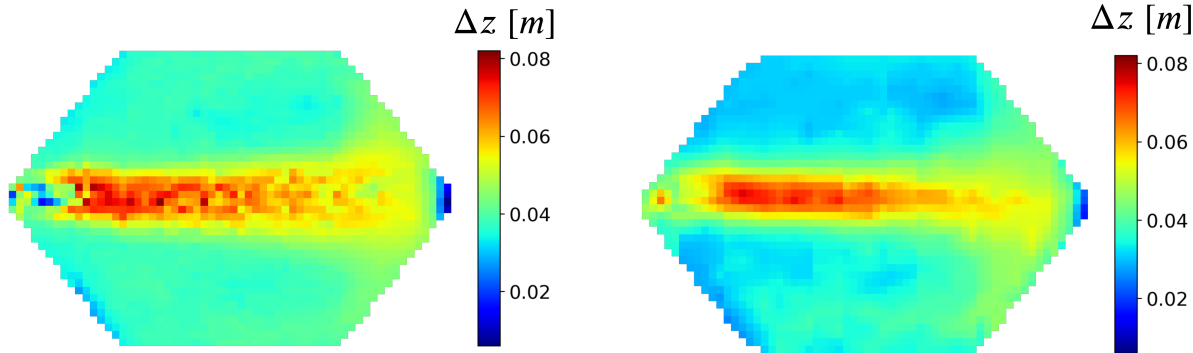
Table 3.2: Spacing (in m) of the measured and simulated points on both models.

Spacing	Diamond-shaped	Hexagon-shaped
Measurement	$\Delta X = 0.1, \Delta Y \approx 0.01$	$\Delta X = 0.1, \Delta Y \approx 0.01$
Simulation	$\Delta X = 0.1, \Delta Y \approx 0.01$	$\Delta X = 0.2, \Delta Y \approx 0.01$



(a) Observed  $\Delta z$  (Source of the raw data: Kantoush, 2008). (b) Simulated  $\Delta z$  (Source of the raw data: Shoarinezhad et al., 2021).

Figure 3.9: Rasterized maps of measured and simulated  $\Delta z$  for the diamond-shaped model (Resolution of 0.1 m).



(a) Observed  $\Delta z$  (Source of the raw data: Kantoush, 2008). (b) Simulated  $\Delta z$  (Source of the raw data: Shoarinezhad et al., 2021).

Figure 3.10: Rasterized maps of measured and simulated  $\Delta z$  for the hexagon-shaped model (Resolution of 0.1 m).

### Categorization of the continuous spatial data

The rasters from the previous step are also transformed to categorical maps to perform fuzzy kappa map comparison (Figures 3.11 and 3.12). Since only deposition processes happened in the experiments, 6 classes in the ordinal scale ranging from 'Very Low Deposition' to 'Elevated Deposition' are sufficient to characterize the sedimentation patterns. The intervals of the classes are shown in Table 3.3.

### 3.3. Summary of the test approach

---

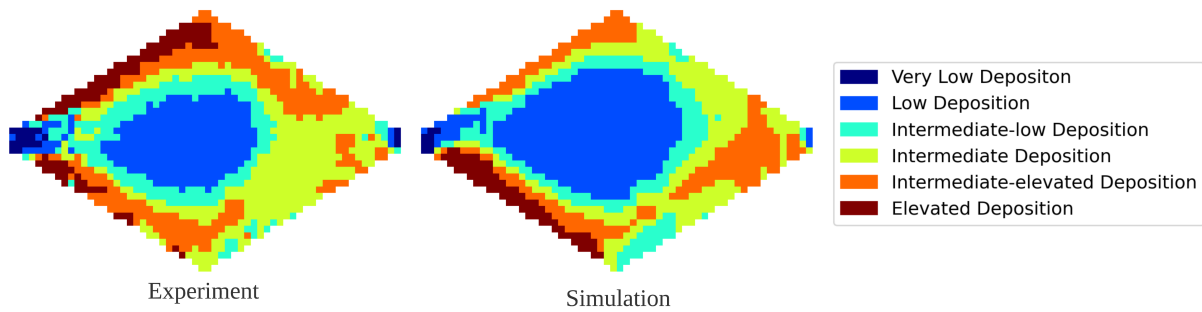


Figure 3.11: Categorized maps of measured and simulated  $\Delta z$  for the diamond-shaped model using Jenks natural breaks. The definition of the categories are shown in Table 3.3

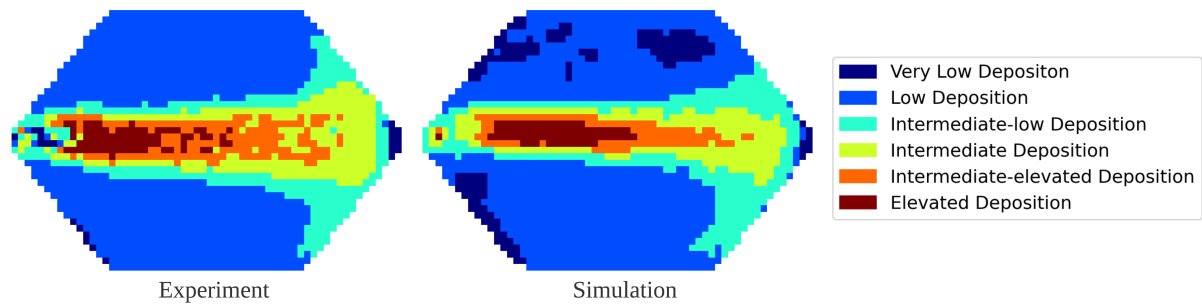


Figure 3.12: Categorized maps of measured and simulated  $\Delta z$  for the hexagon-shaped model using Jenks natural breaks. The definition of the categories are shown in Table 3.3

#### Fuzziness of location

According to Kantoush (2008), bed elevation change was measured with an echo sounder (Ultralab UWS), which was assembled on the movable frame and scanned the whole basin area with consistent spacing. Therefore, since positional accuracy was ensured, errors in location are low.

Spatial error is considered in the neighborhood and halving distance of the exponential distance decay function. To understand the effect of these in the analysis, a sensitivity analysis is performed and adequate values selected. The results are later described in Section 4.1.1.

#### Fuzziness of category

The fuzzy kappa map comparison method considers that categories may share similarities. That means, some categories may be similar to others to a certain degree, while some may be totally dissimilar. As follows, one can express these (dis)similarities with a similarity matrix.

Table 3.3: Definition of the categories for the diamond- and hexagon-shaped models using the natural breaks algorithm.

Category	Interval [m]	
	Diamond-shaped	Hexagon-shaped
(1) Very low Deposition	$\leq 0.028$	$\leq 0.031$
(2) Low Deposition	$]0.028, 0.042]$	$]0.031, 0.041]$
(3) Intermediate-low Deposition	$[0.042, 0.047]$	$]0.041, 0.049]$
(4) Intermediate Deposition	$]0.047, 0.051]$	$]0.049, 0.056]$
(5) Intermediate-elevated Deposition	$]0.051, 0.056]$	$]0.056, 0.065]$
(6) Elevated Deposition	$> 0.056$	$> 0.065$

The entries of the matrix are selected depending on the tolerance the modeler wishes to consider.

The raster maps are categorized using Jenks optimization (Section 3.2.2), which results in categories ranging from very low to elevated deposition. Since the data is in the ordinal scale, categories that are closer to each other naturally share more similarity, while more distant categories take lower categorical tolerance. The matrix shown in Table 3.4 shows the selected categorical fuzziness of 0.5 for classes immediately next to each other, 0.2 for classes less similar (for instance Very low and Intermediate Deposition) and 0 for all others.

Table 3.4: Similarity matrix of the categories of the physical models of shallow reservoirs.

Category	1	2	3	4	5	6
1	1.0	0.5	0.2	0.0	0.0	0.0
2	0.5	1.0	0.5	0.2	0.0	0.0
3	0.2	0.5	1.0	0.5	0.2	0.0
4	0.0	0.2	0.5	1.0	0.5	0.2
5	0.0	0.0	0.2	0.5	1.0	0.5
6	0.0	0.0	0.0	0.2	0.5	1.0

### 3.3.2 The lower Salzach River

#### Interpolation and rasterization

Modeling approaches to simulate river systems are closely related to geospatial interpolation. That is because firstly, enough measurements are not always available, and second, geospatial data (whether from the measurements or the model) have to be interpolated to the same points in order to be compared. In rivers with a considerable degree of sinuosity, the interpolation

### 3.3. Summary of the test approach

---

of river channel data is more challenging than for simpler geometries (Wu et al., 2019), as Cartesian coordinates (x,y) are no longer appropriate. Therefore, the mapping of the sinuous lower Salzach River requires a more sophisticated interpolation method.

Based on the available methods, the selected interpolation technique for the lower Salzach River consists of a continuously differentiable and approximately curvature-minimizing polynomial surface. This algorithm constructs an interpolant using Delaunay triangulation and computing a piecewise cubic Bezier polynomial on each triangle. The gradients are optimized to result in smooth surfaces. The reader is referred to Section 4.2.1 and Bell et al. (2020) for more details.

For this study, model output and measurement data was made available by Beckers et al. (2019). Despite the coarser spacing of the points in the s- (along the flow direction) and n-axis (perpendicular to the s-axis, as shown in Table 3.5), the interpolation and consequent rasterization using a cell size of 5 m shows adequate agreement with the plots in Beckers et al. (2020). That means, the generated maps represents the zones where erosion and deposition takes place.

Table 3.5: Spacing (in m) of the dataset from the lower Salzach River for both from the models and from the measurements (Source: Beckers et al., 2020).

Direction	Spacing [m]
s-axis	$\approx 36$
n-axis	$\approx 16$

After the interpolation, the spatial data is obtained in a regular grid, and therefore, ready to be rasterized. Figures 3.13 to 3.16 show a section of the rasterized model outputs for the validation period (2010-2013).

#### Categorization of the continuous geospatial data

The classification of the continuous rasters of the Salzach River is herein also performed in order to execute the fuzzy kappa method. For this purpose, the spatial data is categorized by the natural breaks algorithm described in Section 2.4.2 using 12 classes (Table 3.6).

#### Fuzziness of category and location

Table 3.7 shows the similarity matrix used for fuzzy kappa map comparison. The same rationale from the similarity matrix of the case study of the numerical and physical models of

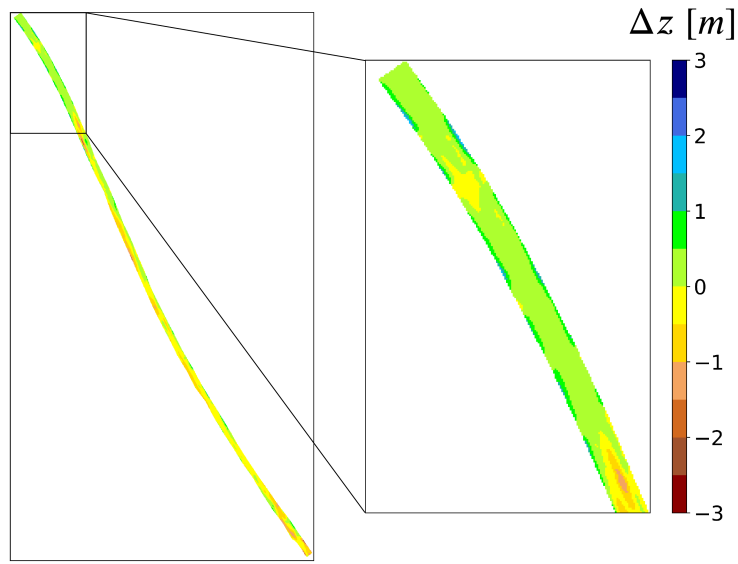


Figure 3.13: Observed bed elevation change in the lower Salzach River for the validation period 2010-2013 (Cell size = 5m).

shallow reservoirs (Table 3.4) is applied.

Fuzziness of location is considered as 8 cells of neighborhood and 4 cells of halving distance. Furthermore, a sensitivity analysis of these two parameters is done and the results are shown in Section 4.2.2.

### 3.3. Summary of the test approach

---

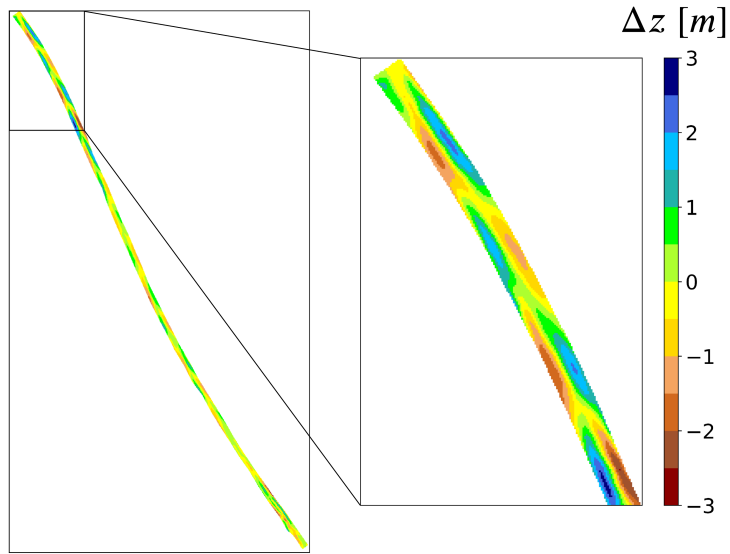


Figure 3.14: Bed elevation change in the lower Salzach River for the validation period 2010-2013 from the manually calibrated *HYDRO\_FT-2D* model (Cell size = 5m)

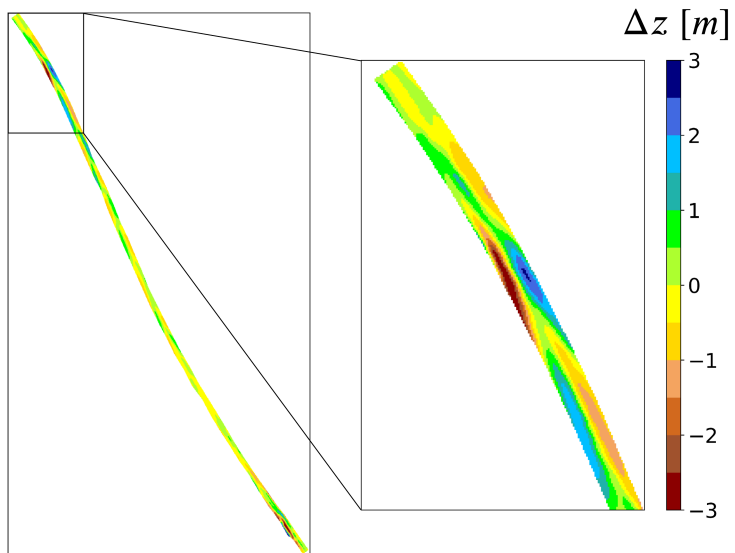


Figure 3.15: Bed elevation change in the lower Salzach River for the validation period 2010-2013 from the stochastically calibrated *HYDRO\_FT-2D* model (Cell size = 5m).

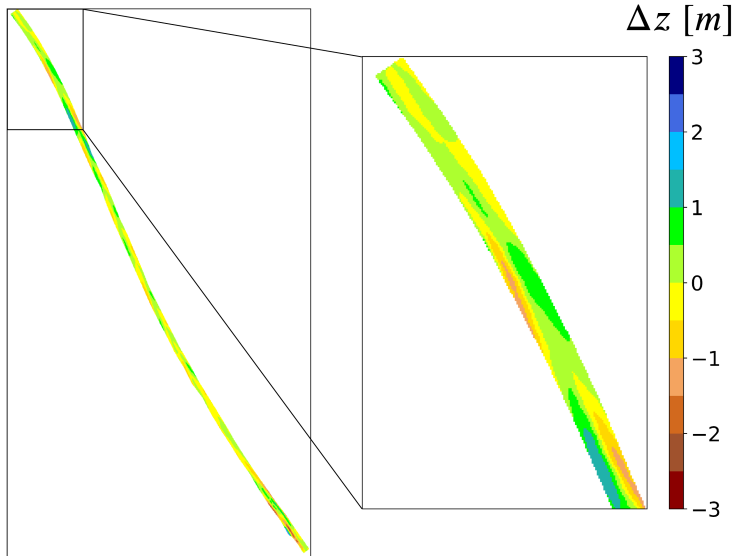


Figure 3.16: Bed elevation change in the lower Salzach River for the validation period 2010-2013 from the aPC surrogate model (Cell size = 5m).

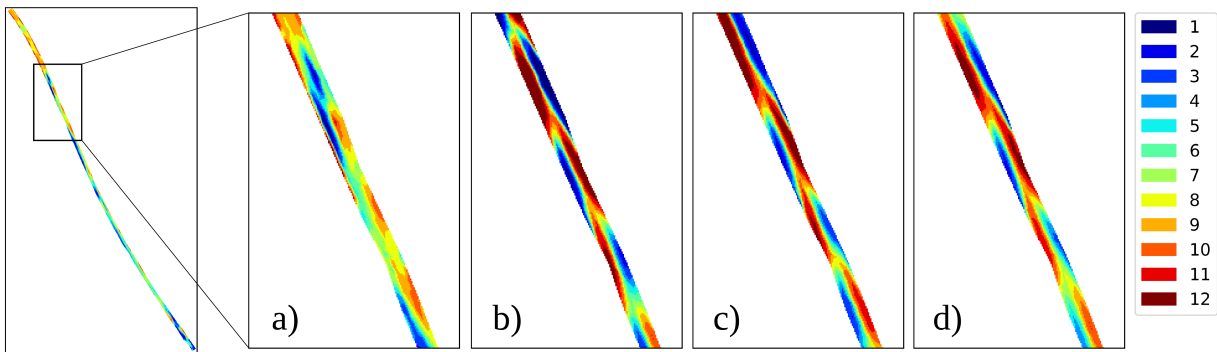


Figure 3.17: Categorized maps of (a) observed and (b, c, d) simulated  $\Delta z$  for the lower Salzach River using Jenks natural breaks. (b) manually calibrated *HYDRO\_FT-2D* model; (c) stochastically calibrated *HYDRO\_FT-2D* model; (d) aPC surrogate model (Cell size = 5m). The definition of the categories are shown in Table 3.6.

### 3.3. Summary of the test approach

---

Table 3.6: Definition of categories for the lower Salzach River using the natural breaks algorithm.

<b>Category</b>	<b>Interval [m]</b>
<b>(1) Elevated Erosion</b>	$\leq -1.23$
<b>(2) Intermediate-elevated Erosion</b>	$] -1.23, -0.85]$
<b>(3) Intermediate Erosion</b>	$] -0.85, -0.62]$
<b>(4) Intermediate-low Erosion</b>	$] -0.62, -0.44]$
<b>(5) Low Erosion</b>	$] -0.44, -0.28]$
<b>(6) Very low Erosion</b>	$] -0.28, -0.12]$
<b>(7) Small changes</b>	$] -0.12, 0.032]$
<b>(8) Low Deposition</b>	$] 0.032, 0.19]$
<b>(9) Intermediate-low Deposition</b>	$] 0.19, 0.37]$
<b>(10) Intermediate Deposition</b>	$] 0.37, 0.62]$
<b>(11) Intermediate-elevated Deposition</b>	$] 0.62, 1.00]$
<b>(12) Elevated Deposition</b>	$> 1.00$

Table 3.7: Similarity matrix of the categories from the case study of the lower Salzach River.

<b>Category</b>	<b>1</b>	<b>2</b>	<b>3</b>	<b>4</b>	<b>5</b>	<b>6</b>	<b>7</b>	<b>8</b>	<b>9</b>	<b>10</b>	<b>11</b>	<b>12</b>
<b>1</b>	1.0	0.5	0.2	0.0	0.0	0.0	0.0	0.0	0.0	0.0	0.0	0.0
<b>2</b>	0.5	1.0	0.5	0.2	0.0	0.0	0.0	0.0	0.0	0.0	0.0	0.0
<b>3</b>	0.2	0.5	1.0	0.5	0.2	0.0	0.0	0.0	0.0	0.0	0.0	0.0
<b>4</b>	0.0	0.2	0.5	1.0	0.5	0.2	0.0	0.0	0.0	0.0	0.0	0.0
<b>5</b>	0.0	0.0	0.2	0.5	1.0	0.5	0.2	0.0	0.0	0.0	0.0	0.0
<b>6</b>	0.0	0.0	0.0	0.2	0.5	1.0	0.5	0.2	0.0	0.0	0.0	0.0
<b>7</b>	0.0	0.0	0.0	0.0	0.2	0.5	1.0	0.5	0.2	0.0	0.0	0.0
<b>8</b>	0.0	0.0	0.0	0.0	0.0	0.2	0.5	1.0	0.5	0.2	0.0	0.0
<b>9</b>	0.0	0.0	0.0	0.0	0.0	0.0	0.2	0.5	1.0	0.5	0.2	0.0
<b>10</b>	0.0	0.0	0.0	0.0	0.0	0.0	0.0	0.2	0.5	1.0	0.5	0.2
<b>11</b>	0.0	0.0	0.0	0.0	0.0	0.0	0.0	0.0	0.2	0.5	1.0	0.5
<b>12</b>	0.0	0.0	0.0	0.0	0.0	0.0	0.0	0.0	0.0	0.2	0.5	1.0

# **Chapter 4**

## **Results**

### **4.1 Physical models of shallow reservoirs**

#### **4.1.1 Sensitivity analysis of parameters involved**

##### **Influence of the neighborhood and halving distance**

The two main parameters involved in the consideration of fuzziness of location are the neighborhood and halving distance (see Sections 2.4.2 and 2.4.3). A sensitivity analysis of these parameters is shown in this section. Realizations of both fuzzy kappa and fuzzy numerical map comparisons are done by changing the parameters within the ranges of 2 - 8 and 1 - 4 cells. The effect of these changes on the comparison methods is assessed through the Fuzzy Kappa coefficient (for the fuzzy kappa method) and the Global Fuzzy Similarity (for the fuzzy numerical method). The simulated and observed  $\Delta_z$  of the diamond-shaped model are compared.

Table 4.1 shows the results of the sensitivity analysis of the parameters from the fuzzy numerical method. The values suggest that the halving distance and the neighborhood practically do not play a role in the evaluation of the numerical models of shallow reservoirs. This happens because the fuzzy numerical methods works to take the maximum similarity among all pairwise comparisons between the central cell and the neighbors. If a value in the central cell of the simulated map already matches the analogous cell in the observed map, the neighborhood does not affect the comparison.

## 4.1. Physical models of shallow reservoirs

---

If the neighborhood is set to zero, meaning that the comparison is performed cell-by-cell and not anymore constitutes a fuzzy map comparison, the  $S_{fuzzy}$  values show no significant change (0.9079 and 0.8956 for the diamond- and hexagon-shaped models, respectively).

Table 4.1: Global fuzzy similarities[-] from the sensitivity analysis of the neighborhood and halving distance in the evaluation of the diamond-shaped model (Resolution of 0.1, method: **Fuzzy numerical**).

		Neighborhood (Number of cells)			
		2	4	6	8
Halving distance (Number of cells)	1	0.9079	0.9079	0.9079	0.9079
	2	0.9080	0.9080	0.9080	0.9080
	3	0.9083	0.9083	0.9083	0.9083
	4	0.9088	0.9088	0.9088	0.9088

In contrast to fuzzy numerical map comparison, fuzzy kappa map comparison is moderately influenced by the halving distance. Fuzzy Kappa coefficients range from 0.4921 to 0.5561 when applying halving distances from 1 to 4 cells, respectively. For same halving distances, even if the neighborhood increases from 2 to 8 cells, the Fuzzy Kappa coefficients does not change. This result is expected because, despite the neighborhood being larger, it does not affect the comparison if their memberships are too low. By increasing the halving distance, however, the memberships of the cells surrounding the central cell are higher, and therefore, the local similarity between neighbors increases.

In fact, if one takes a closer look, the halving distance is also the limiting parameter for fuzzy numerical map comparison. There, changes in the global similarity due to wider neighborhoods are also not observed, whereas the increase of the halving distance improves the similarity between observed and simulated maps to some degree.

Table 4.2: Fuzzy Kappa coefficients[-] from the sensitivity analysis of the neighborhood and halving distance in the evaluation of the diamond-shaped model (Resolution of 0.1m, method: **Fuzzy kappa**).

		Neighborhood (Number of cells)			
		2	4	6	8
Halving distance (Number of cells)	1	0.4921	0.4921	0.4921	0.4921
	2	0.5170	0.5170	0.5170	0.5213
	3	0.5391	0.5391	0.5391	0.5391
	4	0.5561	0.5561	0.5561	0.5561

### Influence of the cell size

Table 4.3 shows the global fuzzy similarities for different cell sizes. The global similarities presented only minor changes (at the 3<sup>rd</sup> or 4<sup>th</sup> decimal digit) with the change in the cell size. Since observed and simulated data are densely available in both x and y directions, the interpolation method does not significantly interfere in the evaluation.

When performing this type of sensitivity analysis, the modeler should bear in mind that by changing the cell size, the spatial tolerance should also change, because the latter is expressed with number of cells. For instance, Table 4.3 results from a spatial tolerance of 0.4 m (4 cells of neighborhood, resolution of 0.1m), where at a distance of 0.2 m, the membership decays to the half. Therefore, using a cell size of 0.1 m, the spatial tolerance is equivalent to 4 cells of neighborhood and 2 cells of halving distance, whereas for 0.2 m resolution, the neighborhood must be 2 cells with a halving distance equal to 1 cell.

Table 4.3: Global fuzzy similarities[-] from the sensitivity analysis of the cell size in the evaluation of both shallow reservoir models (Method: **Fuzzy numerical**).

		Cell size [m]		
		0.05	0.1	0.2
Model	Diamond-shaped	0.9072	0.9080	0.9083
	Hexagon-shaped	0.8935	0.8956	0.8954

### 4.1.2 Fuzzy numerical

#### The Global Fuzzy Similarity $S_{fuzzy}$

The  $S_{fuzzy}$  values indicate that the hydro-morphodynamic models successfully predict the observed bed elevation changes. With a neighborhood of 4 cells and a halving distance of 2 cells, the similarity between observed and simulated bed elevation change was 0.9080 for the diamond-shape model, and 0.8956 for the hexagon-shaped model.

$S_{fuzzy}$  values are obtained for the baseline predictions (see Section 3.2.2) using a neighborhood of 4 cells and a halving distance of 2 cells. The baseline predictions (i.e., randomly generated rasters) present  $S_{fuzzy}$  values of 0.6600 and 0.5959 for the diamond- and hexagon-shaped model, respectively. These results confirm the ability of the numerical models to predict bed elevation change and suggest elevated model skill.

#### 4.1. Physical models of shallow reservoirs

---

It is worth mentioning that the interpolation method has little influence on the fuzzy comparison. When a cubic interpolation is used, the values of  $S_{fuzzy}$  for both models only change at the  $3_{rd}$  decimal case. This outcome confirms the low interpolation uncertainty expected from such data-rich models, where densely distributed points in both observed and simulated DEMs are available.

Although there is no framework for associating model efficiency with the Global Fuzzy Similarity, one can assume that values ranging from 0.8 to 0.9 convincingly indicate a substantial model performance, especially if the neighborhood is reasonably small (2 cells of halving distance is equivalent to 0.20 m). In addition, the  $S_{fuzzy}$  values of the numerical models are considerably higher than the  $S_{fuzzy}$  values obtained for the randomly generated maps.

It is worth to point out that the  $S_{fuzzy}$  measure is able to capture agreement where measures of collinearity, such as the coefficient of determination, fail. Table 4.4 shows the  $R^2$  obtained by (Shoarinezhad et al., 2021), and global fuzzy similarities for both models. While the global fuzzy similarities suggests that the diamond-shaped model performs better than the hexagon-shaped, the coefficient of determination indicates the opposite. As discussed in Section 2.2.5, it is crucial to perform model evaluation with additional measures besides collinearity statistics and that is where fuzzy-based measures may be substantially beneficial.

Table 4.4: Global Fuzzy Similarity versus coefficient of determination.

Measure	Diamond-shaped	Hexagon-shaped
$S_{fuzzy}$ (Linear)	0.9080	0.8956
$S_{fuzzy}$ (Cubic)	0.9079	0.8944
$R^2$ (source: Shoarinezhad et al., 2021)	0.7600	0.8500

#### Comparison maps

The maps of the comparisons (Figures 4.1b and 4.1a) show that the numerical models performed well in the majority of the area. In both shapes, the models fail only to simulate bed level change in the surroundings of the inflow and outflow areas, where local similarities reach poor performances around 0.34. The comparison maps reaffirm the findings from Shoarinezhad et al. (2021), which noticed limitations of the numerical models in reproducing bed level changes near the inflow and outflow.

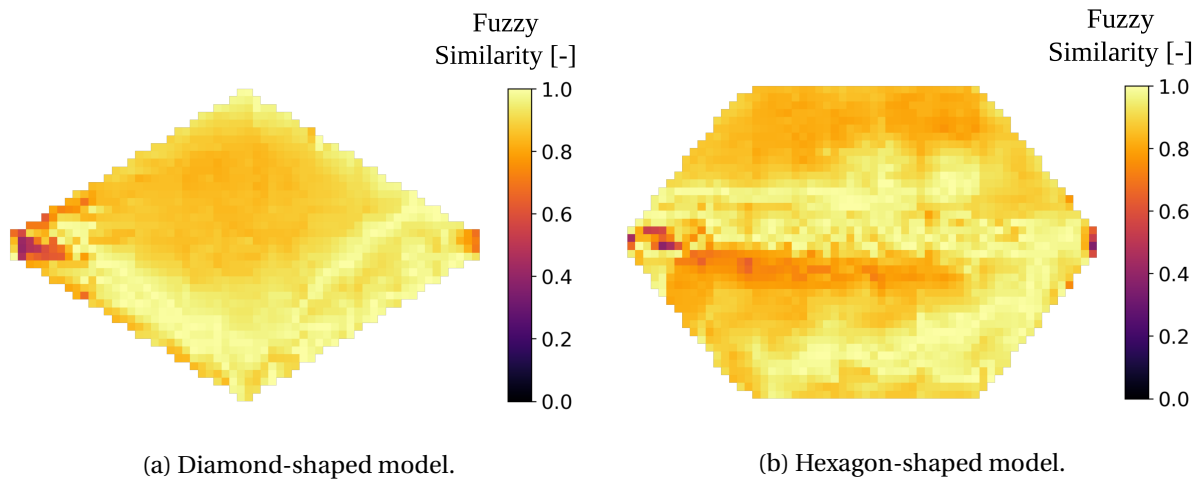


Figure 4.1: Maps of comparison between observed and simulated  $\Delta z$  (Resolution of 0.1m, method: **Fuzzy numerical**).

### Model performance analysis

A performance analysis shown in Figures 4.2a and 4.2b displays the distribution of fuzzy similarities resulting from the maps of comparison. The analysis of the numerical simulations revealed that for a considerable number of cells, the fuzzy similarity indicates very good model performance, with values above 0.8.

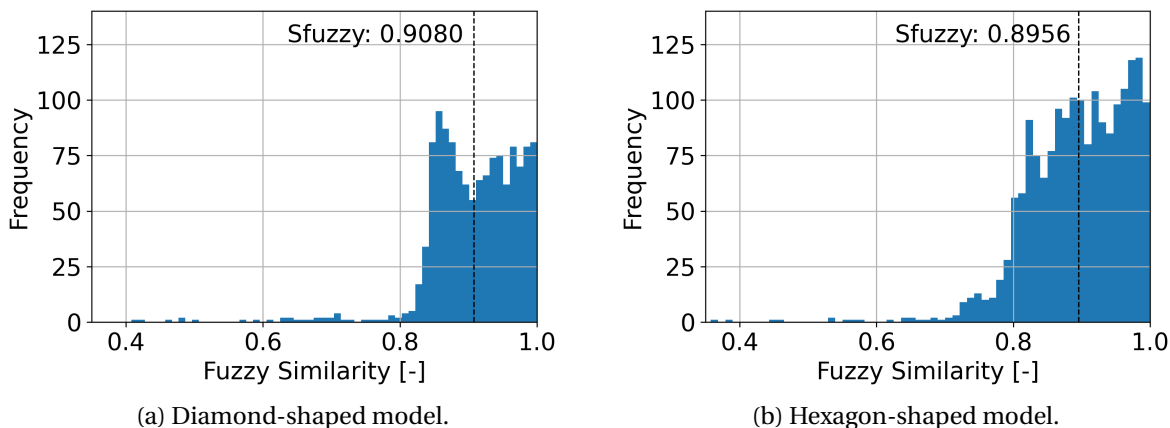


Figure 4.2: Performance analysis of the numerical models of shallow reservoirs (Method: **Fuzzy numerical**).

### 4.1.3 Fuzzy kappa

#### The Fuzzy Kappa coefficient $K_{fuzzy}$

For the hexagon-shaped model, the Fuzzy Kappa coefficient results higher ( $K_{fuzzy} = 0.6497$ ) than the value obtained for the diamond-shaped model ( $K_{fuzzy} = 0.5170$ ) using 4 cells of neighborhood and 2 cells of halving distance. These  $K_{fuzzy}$  values suggest that the numerical model of the hexagon-shaped reservoir performs better than the numerical model of the diamond-shaped reservoir. In contrast to fuzzy numerical map comparison, fuzzy kappa map comparison results in Fuzzy Kappa coefficients (Table 4.2) considerably lower than the Global Fuzzy Similarity.

The baseline predictions (i.e., randomly generated maps) present  $K_{fuzzy}$  values of 0.0022 and -0.0011 for the diamond- and hexagon-shaped models, respectively. The  $K_{fuzzy}$  values close to zero are expected as the  $K_{fuzzy}$  coefficient is a statistical measure that is corrected by the similarity expected when an observed map is compared to a randomly generated map (Wealands et al., 2005b). The  $K_{fuzzy}$  values obtained for the randomly generated rasters suggest that the numerical models perform considerably better than the baseline prediction.

Table 4.5: Fuzzy kappa coefficients [-] of the numerical models of shallow reservoirs (Resolution of 0.1m).

Model	$K_{fuzzy}$
Diamond-shaped numerical model	0.5170
Baseline prediction (Diamond-shaped)	0.0022
Hexagon-shaped numerical model	0.6497
Baseline prediction (Hexagon-shaped)	-0.0011

#### Comparison maps

The comparisons of the maps using the fuzzy kappa approach are shown in Figures 4.3a and 4.3b. It is noticeable how both the fuzzy numerical and fuzzy kappa methods are able to capture the locations where the numerical models do not perform well. The fuzzy kappa method, however, displays dissimilarities in a more pronounced way than the results from fuzzy numerical map comparison.

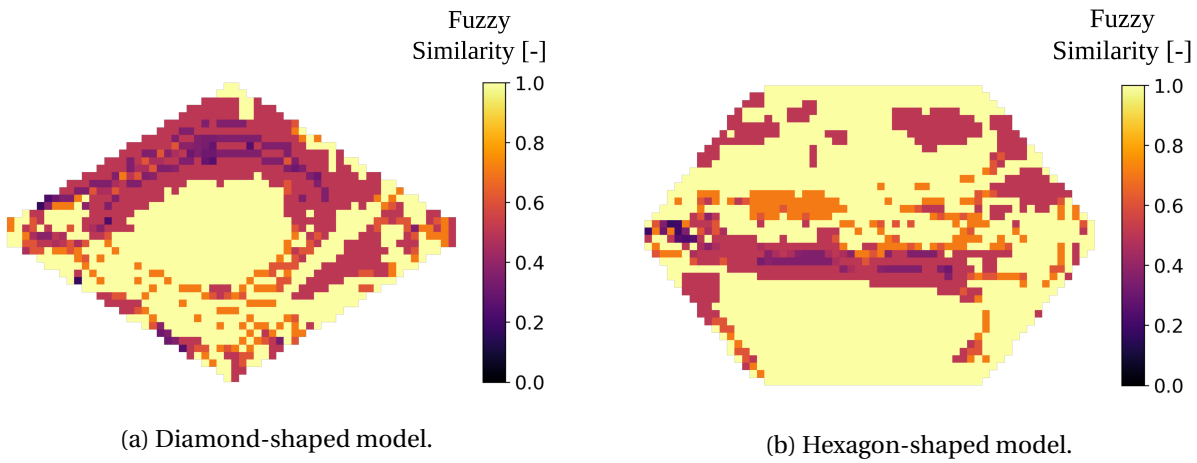


Figure 4.3: Maps of comparison between observed and simulated  $\Delta z$ . Neighborhood = 4 cells and halving distance = 2 cells (Resolution of 0.1m, method: **Fuzzy kappa**).

## 4.2 Terrain change analyses of the lower Salzach River

### 4.2.1 Optimization of the fuzzy numerical algorithm

Due to the large size of the rasters of the lower Salzach River, the code had to be optimized to reduce the computation time of the fuzzy numerical method. The optimization reduced the time to compute the fuzzy numerical algorithm by approximately 30 times. The key adaptations were:

1. Assign *nodata* values to the cells outside of the study area. Thus, when each pair of rasters are read, the computation is executed only for cells that have an entry value (non-masked cells).
2. Perform array operations with efficient Python packages (i.e., the *numpy* built-in functions), instead of working with entry-by-entry computations.

The result of the code optimization is shown in Table 4.6. The code ran on an Intel(R) Core (TM) i5-3470 CPU with a base speed of 3.20 GHz.

## 4.2. Terrain change analyses of the lower Salzach River

---

Table 4.6: Computation time [s] for fuzzy numerical map comparison after algorithm optimization.  
Note: number of cells refers to non-masked cells.

Fuzzy evaluation	Cells	Neighborhood	Running time [s]
Numerical models of the lower Salzach River	22,178	4	28.6
Diamond-shaped numerical model	1,276	4	1.9
Hexagon-shaped numerical model	1,836	4	2.7

### 4.2.2 Sensitivity analysis of parameters involved

#### Influence of the neighborhood and halving distance

In the case of the models of the lower Salzach River, a sensitivity analysis of the neighborhood and halving distance is performed. The values of  $S_{fuzzy}$  show that the Global Fuzzy Similarity significantly improves the more spatial tolerance is allowed. Both neighborhood and halving distance have influence on the comparison. Table 4.7 shows that the larger is the neighborhood, the higher is the improvement of the  $S_{fuzzy}$  values. For instance, by increasing the neighborhood when the halving distance is 1, the global similarity increases a little, whereas by increasing the neighborhood when the halving distance is 4, the global similarity considerably improves.

Table 4.7: Global fuzzy similarities [-] from the sensitivity analysis of the neighborhood and halving distance in the comparison of the aPC surrogate model with observations (Resolution of 5 m).

		Neighborhood			
		2	4	6	8
Halving distance	1	0.2368	0.2538	0.2553	0.2555
	2	0.2304	0.2805	0.2926	0.2951
	3	0.2315	0.3064	0.3320	0.3392
	4	0.2348	0.3283	0.3668	0.3793

Figure 4.4 demonstrates how the tolerance for spatial error is considered using the concept of fuzziness of location. By increasing the halving distance, the membership of cells farther from the central also increase. That results in higher local fuzzy similarities.

As obtained in the case study of the physical models, the sensitivity analysis for the Fuzzy Kappa values demonstrates that the neighborhood plays a minor role in the comparison and that the most sensitive comparison parameter is the halving distance (Table 4.8).

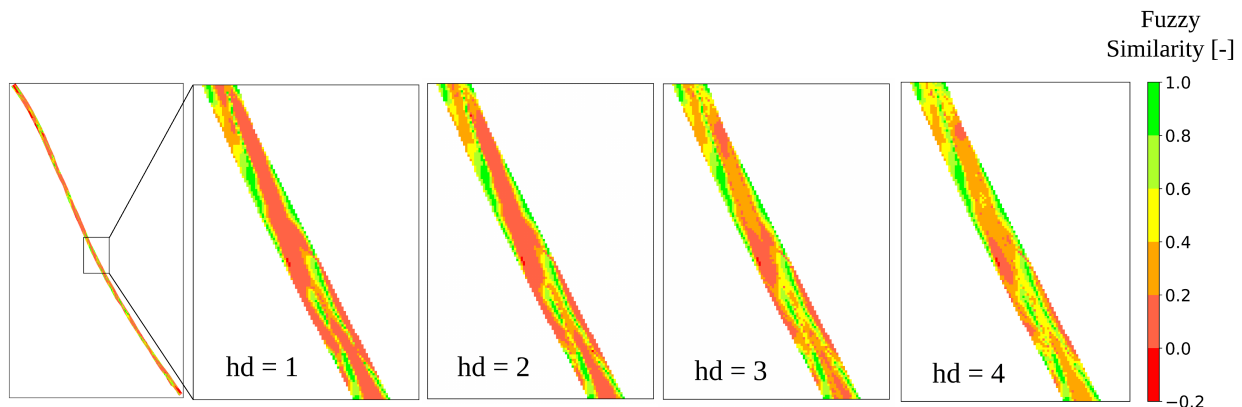


Figure 4.4: Effect of increased fuzziness in location on the evaluation of the aPC surrogate model (versus measurements) for a neighborhood of 8 cells (hd= halving distance).

Table 4.8: Fuzzy Kappa coefficients [-] from the sensitivity analysis of the neighborhood and halving distance in the evaluation of the aPC surrogate model of the lower Salzach River for the validation period 2010-2013 (Resolution of 5m, method: **Fuzzy kappa**).

		Neighborhood			
		2	4	6	8
Halving distance	1	0.0428	0.0428	0.0428	0.0428
	2	0.0563	0.0563	0.0563	0.0563
	3	0.0709	0.0709	0.0709	0.0709
	4	0.0858	0.0858	0.0858	0.0858

### Influence of the cell size

The cell size has an elevated influence on  $S_{fuzzy}$  values. For a constant neighborhood of 40m and a halving distance of 20 m, the increase in cell size significantly decreases the similarity, as it is shown in Table 4.9.

#### 4.2.3 Fuzzy numerical

##### The Global Fuzzy Similarity $S_{fuzzy}$

The aPC surrogate model has the highest similarity between simulated and observed bed elevation changes. These results are in agreement with Beckers et al. (2020). For a spatial tolerance of 20 meters of halving distance and 40 m of neighborhood, the aPC surrogate model results in a  $S_{fuzzy}$  of 0.3793. However, the models present many zones with poor fuzzy similarities, as shown in Figure 4.5, which consequently result in low  $S_{fuzzy}$  values. Table 4.10

## 4.2. Terrain change analyses of the lower Salzach River

---

Table 4.9: Global fuzzy similarities [-] from the sensitivity analysis of the cell size in the evaluation of the models of the lower Salzach River (Method: **Fuzzy numerical**).

		Model		
		Manually calibrated	Stochastically calibrated	aPC surrogate
<b>Cell size [m]</b>	<b>5</b>	0.3470	0.3541	0.3793
	<b>10</b>	0.3182	0.3183	0.3427
	<b>20</b>	0.2755	0.2791	0.2995

shows the result of the fuzzy numerical method for the validation period.

In addition, a  $S_{fuzzy}$  value of reference is obtained to assess the skill of the models relative to a baseline prediction (see Section 3.2.2). The raster of baseline predictions is compared with the raster of observations using the fuzzy numerical method with the neighborhood of 8 cells and halving distance of 4 cells. The resultant  $S_{fuzzy,baseline}$  is 0.2534 (Table 4.10).

Table 4.10: Global fuzzy similarities [-] of the lower Salzach River models and baseline prediction (compared with measurements) for a spatial tolerance of 4 cells of halving distance and 8 cells of neighborhood (Resolution of 5m, method: **Fuzzy numerical**).

Model	$S_{fuzzy}$ [-]
Manually calibrated model	0.3470
Stochastically calibrated model	0.3541
aPC surrogate model	0.3793
Baseline prediction	0.2534

It is important to note that the models were calibrated and evaluated based on the calibration nodes ( $n=204$ ), while here a whole spatial comparison is performed with a total of 22,178 cells. The raster maps reconstruct the complete river channel without white spaces nor discontinuities. That being said, it is possible that the interpolation technique has influenced the evaluation of the models.

### Comparison maps

The fuzzy numerical method is able to highlight disagreements between simulated and observed bed elevation change, as shown in Figure 4.5. The comparison maps suggest that the models predict different river dynamics as it was observed in reality. The stochastically calibrated model predicts a high erosion pattern in the left bank near the outflow boundary (Figure 3.15), while the map of observations (Figure 3.13) indicates sediment deposition. The

map of comparisons (Figure A.6) captures this mismatch.

The comparison maps reveal that in a large number of cells, negative fuzzy similarities are obtained. That happens because there are many zones where the models should predict erosion, but instead they predict deposition, and vice-versa. This is why the fuzzy numerical comparison results in negative local similarities.

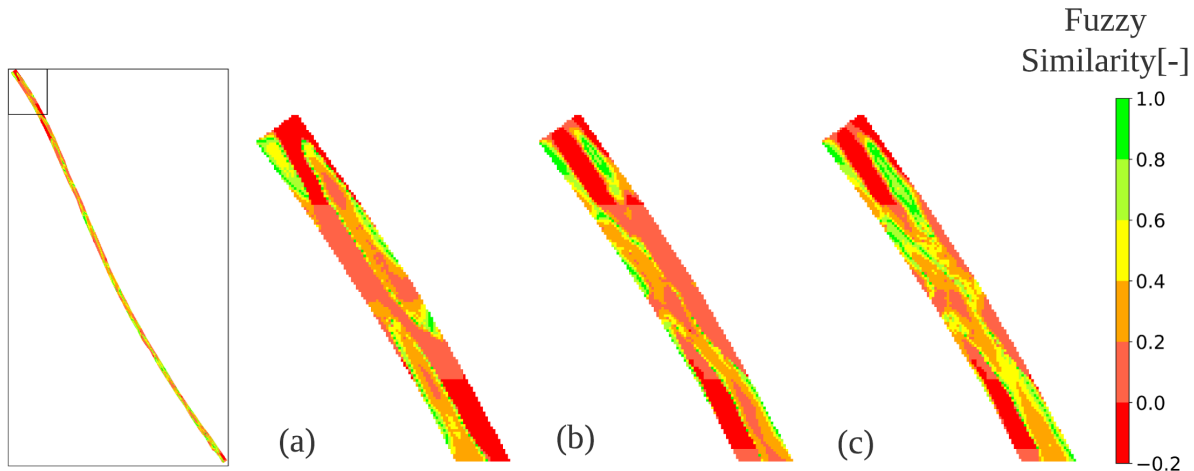


Figure 4.5: Fuzzy map comparison of the models of the lower Salzach River for the validation period 2010-2013 compared to observed  $\Delta z$ . (a) manually calibrated *HYDRO\_FT-2D* model; (b) stochastically calibrated *HYDRO\_FT-2D* model; (c) aPC surrogate model (Resolution of 5m, method: **Fuzzy numerical**).

### Model performance analysis

The comparisons of the simulated and observed bed level change result in similarity values according to the histograms in Figure 4.6b. The histograms are right-skewed and only a few cells present fuzzy similarities higher than 0.8. The map generated by the aPC surrogate model has the lowest number of cells presenting negative fuzzy similarities.

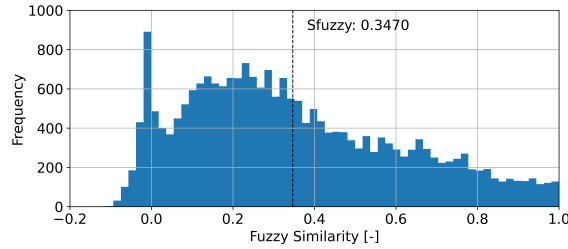
#### 4.2.4 Fuzzy kappa

##### The Fuzzy Kappa coefficient $K_{fuzzy}$

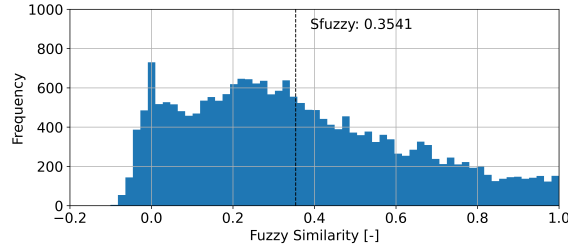
Table 4.11 shows the results of fuzzy kappa map comparison of the models. The  $K_{fuzzy}$  values are critically low. Similar to  $K_{fuzzy}$  values of baseline prediction in the physical models case

## 4.2. Terrain change analyses of the lower Salzach River

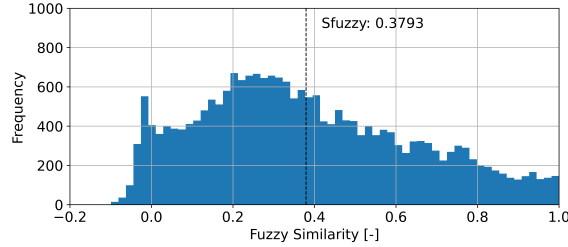
---



(a) Manually calibrated *HYDRO\_FT-2D* model.



(b) Stochastically calibrated *HYDRO\_FT-2D* model.



(c) aPC surrogate model.

Figure 4.6: Performance analysis of the models for the validation period (2010-2013).

study, the  $K_{fuzzy}$  value obtained for the baseline prediction of the lower Salzach River (i.e., randomly generated maps) is approximately zero ( $K_{fuzzy} = 0.0030$ ).

### Comparison maps

The complete comparison maps can be seen at Appendix A. Similarly to the results of the fuzzy kappa map comparison from the physical models (Section 4.1.3), the fuzzy kappa map comparisons of the lower Salzach River models express dissimilarities with more emphasis. Several zones, especially near inflow and outflow boundaries, present  $K_{fuzzy}$  values below 0.2.

Table 4.11: Fuzzy Kappa coefficients of the lower Salzach River models and baseline prediction (compared with measurements) for a spatial tolerance of 4 cells of halving distance and 8 cells of neighborhood (Resolution of 5m).

Model	$K_{fuzzy}$ [-]
Manually calibrated model	0.0544
Stochastically calibrated model	0.0659
aPC surrogate model	0.0858
Baseline prediction	0.0030

Table 4.12: Summary of the results (n = neighborhood, hd = halving distance).

		Cell size [m]	Parameters [cells]		Performance measure [-]	
			n	hd	$S_{fuzzy}$	$K_{fuzzy}$
<b>Physical models</b>	Diamond-shaped	0.1	4	2	0.9080	0.5170
	Baseline (Diamond-shaped)	0.1	4	2	0.6600	0.0022
<b>Hexagon-shaped</b>	0.1	4	2	0.8956	0.6497	
	Baseline (Hexagon-shaped)	0.1	4	2	0.5959	-0.0011
<b>Lower Salzach River</b>	Manually calibrated	5.0	8	4	0.3470	0.0544
	Stochastically calibrated	5.0	8	4	0.3541	0.0659
	aPC surrogate model	5.0	8	4	0.3793	0.0858
	Baseline	5.0	8	4	0.2534	0.0030

# Chapter 5

## Discussion

### 5.1 Limitations of the fuzzy kappa method

By classifying bed elevation change  $\Delta z$  into classes, this study aims at conveying information of terrain change in a qualitative manner. The categorization of the data is a considerable challenge, but it enables the characterization of the data by classes of erosion and deposition patterns. These classes aim at being more meaningful than continuous values. Deterministic predictions of terrain change (e.g., at a certain location, the exact depth of 0.234 m will be eroded), are inconceivable, as the probability of a particular event occurring is practically zero. Rather than that, the value of a prediction must be understood as an estimate and, therefore, it ranges within intervals (i.e., categories).

Previous works (Wealands et al., 2005a) attempted to categorize continuous spatial data in intervals to compare predicted and observed maps and obtained very low  $K_{fuzzy}$  values (-0.026 to -0.807). The study assigns the low  $K_{fuzzy}$  to problems in the consideration of fuzziness of category of fuzzy kappa map comparison.

The categorization performed in this study sought to assign classes that meaningfully characterize the sediment transport processes of the numerical models. However, the results from the comparison of continuous rasters using the fuzzy numerical method suggest a better and more "honest" comparison than those with categorized rasters using the fuzzy kappa method. Sutherland et al. (2004) argues that a model performance statistic should be "honest", in the sense that it should have a clear conceptual basis and match up with expert opinion. The fuzzy

kappa method introduces additional steps to the pre-processing of the comparison. These are the categorization and determination of the fuzziness of category. The categorization step involve additional handling of the data that may significantly alter the results of the comparison if the definition of the categories change.

While both methods yield results that consider error in a more explicit way than traditional measures (e.g., RMSE, MAE, MSE,  $R^2$  and r), the fuzzy kappa method produces values that are difficult to interpret without a baseline prediction. In the case of the shallow reservoir numerical models, the maps of simulated  $\Delta z$  are close to the observed maps, which is confirmed by the fuzzy numerical method. However, the Fuzzy Kappa coefficients were far from the optimum performance of 1.0. Also in the case study of the lower Salzach River very low values of  $K_{fuzzy}$  were observed, whereas the  $S_{fuzzy}$  values from fuzzy numerical method are more coherent (i.e., they match up with expert opinion). Problems in the consideration of the fuzziness of category, in the categorization method, or in the calculation of the expected agreement may be the cause for the low Fuzzy Kappa coefficients.

There are great challenges in the categorization and selection of the memberships for the consideration of fuzziness of category that have to be overcome to adequately apply fuzzy kappa comparison in the evaluation of hydro-morphodynamic models. In this study, the categorization of bed level change is done with the natural breaks algorithm (Section 3.3). While this method demonstrates ability to produce qualitative maps of the output data, it changes the original data and causes information loss. In addition, the results from the  $K_{fuzzy}$  did not reflect the performance of the numerical models of shallow reservoirs as it would be expected.

## 5.2 Algorithm efficiency and the Map Comparison Kit (MCK)

### 5.2.1 Computation time

An important issue in numerical modeling is the computation time. In the present study, although the code algorithm was optimized, the computation time necessary to run the algorithm of fuzzy numerical map comparison is considerably higher than with the MCK. For instance, for comparing each pair of maps of the lower Salzach River the novel algorithm of this study took in average 28 seconds (for a neighborhood of 4 cells), while the MCK takes approximately 3 seconds. This is due to the fact that Python (high-level language) is a

programming language developed from C++ (low-level language) and generally takes longer to run. As to the MCK, it is written directly in C++ language, and therefore, it runs faster.

#### 5.2.2 Limitations of the Map Comparison Kit (MCK)

Even though the MCK runs the fuzzy numerical method faster than the novel algorithm of this study, it has a critical problem. The rasters of terrain change for the lower Salzach River contain cells with negative and positive values. When performing the fuzzy comparison, the novel algorithm of this study reveals zones where the local fuzzy similarity results negative values (Figure 4.5). The reason for this is explained in Section 4.2.3. However, when using the MCK, the comparison map shows no cells with negative fuzzy similarity, which in turn results in a higher  $S_{fuzzy}$ .

This problem is not observed in the comparisons of the diamond- and hexagon-shaped simulated and observed  $\Delta z$  because the rasters contain only positive  $\Delta z$ . A possible reason for the MCK problem may be the way or datatype with which the variables are declared in its code, as it is possibly designed to compare only positive real values.

### 5.3 Uncertainty in datasets: from laboratory to nature

Computations of sediment and fluid dynamics are faced with several sources of parameter uncertainty. Winkler (1996) points out, that the uncertainty is, in general, a function of the state of knowledge (i.e., of the available information). Here, the state of knowledge (and consequentially the uncertainty) of the data of the case studies is considered.

#### 5.3.1 Uncertainty in the grain size distribution

The grain size distribution is an important boundary condition and possible source of uncertainty in hydro-morphodynamic models. The grain size distribution of the lower Salzach River was obtained from sediment samples that were taken in few locations and in different years (Beckers et al., 2020). Since the data do not have equal temporal resolution, uncertainty in the estimated grain size distribution is introduced. The uncertainties in the dataset become especially relevant, when noted that the grain size distribution is a sensitive calibration parameter of the lower Salzach River models (Beckers et al., 2018, 2020). In contrast to the lower Salzach River models, in the physical models of shallow reservoirs, the grain size distribution

### 5.3. Uncertainty in datasets: from laboratory to nature

---

of the input sediment was analyzed before the experiments were conducted. The grain size distribution was determined with a Laser-Particle-Sizer instrument (Kantoush, 2008), thus it is well known.

Table 5.1: Complexity differences between the case studies.

Feature	Physical models of shallow reservoirs	Lower Salzach River
Water Level	Controlled and constantly monitored	Measured peak water levels may contain error (Beckers et al., 2016)
Bed elevation measurements (initial and final)	Every 0.1 m (5 m in reality)	Every 200 m
Grain size distribution	Controlled and determined	Measurements were conducted at only a few places in different years
Geometry	Simple geometries	Sinuous
Georeferencing errors	Relevant	Neglectful

#### 5.3.2 Uncertainty in the observed water levels

Now, the water level data of both case studies are considered. The peak water levels used in the calibration and validation of the lower Salzach River models are prone to errors (Beckers et al., 2016). The flood water levels were inferred from traces and marks left from the flood events. As opposed to the water level data of the lower Salzach River models, the water level of the physical models of shallow reservoirs was constantly monitored by an ultrasonic probe. In addition, 3D velocity, 2D surface velocity, and the discharge were measured over time at several profiles (Kantoush, 2008).

#### 5.3.3 Uncertainty in the bed elevation data

Riverbed profiles of the lower Salzach River were available every 200 m (along the river course). The geometry of the channel was obtained by interpolating the measured profiles, which had different temporal resolutions. The transformation of the bed elevation points to an unique coordinate system was necessary, since the original profiles were available in different coordinate systems (Beckers et al., 2016). Ren et al. (2015) argue that any 3D coordinate transformation introduces uncertainty into the unified measurements. Moreover, uncertainty

related to the interpolation should be taken into consideration here. These uncertainties are not as significant in the physical models of shallow reservoirs as they are in the models of the lower River Salzach. In the first, the thickness of the deposited sediment was measured with a miniature echo sounder. The echo sounder scanned the water surfaces of the entire basin area before and after the experiment, and the difference between the two surfaces gave the  $\Delta_z$ . A high accuracy ( $\pm 1\text{ mm}$ ) in the measurements was achieved (Kantoush, 2008).

#### 5.3.4 Fuzzy map comparison and the consideration of uncertainty

It is noticeable that the uncertainty of the datasets of the lower Salzach River models is significantly higher than that of the physical models of shallow reservoirs. Uncertainty in the datasets, especially in the initial conditions such as the initial bed elevation, propagate and lead to uncertain simulated bed level changes (Refsgaard, van der Sluijs, Højberg, & Vanrolleghem, 2007). Here, the use of fuzzy numerical map comparison can address the challenge of comparing uncertain simulated and observed datasets.

The results from fuzzy numerical map comparison show that the method is able to give high fuzzy similarities for accurate and data-rich laboratory models, whereas the evaluation of the models of lower Salzach River indicates lower model performances. The low performances are expected due to the lower density and higher heterogeneity of field data, and the more challenging interpolation in the models of the lower Salzach River. However, as the comparison becomes more fuzzy (i.e., larger neighborhoods and halving distances are selected), discrepancies between simulated and observed  $\Delta z$  become less evident (see Figure 4.4). This study considers fuzzy numerical map comparison particularly beneficial to compare uncertain datasets, such as the output of lower Salzach River models, because it can handle and tolerate possible errors in a transparent manner.

### 5.4 Reasons for using fuzzy map comparison

In the last decades, numerical modeling has been a widely applied tool for investigations in environmental sciences (Ganju et al., 2016). While many techniques are available for model evaluation, more advances are necessary to improve model testing and interpretation. On the one hand, there are many statistical measures that can be applied to determine the quality of a hydro-morphodynamic model (Sutherland et al., 2004). On the other hand, human visual comparison (the so-called expert assessment) is still today frequently used for assessing model

#### 5.4. Reasons for using fuzzy map comparison

---

predictions, despite the limitations. Therefore, one concern arises: how to evaluate models using features of human comparison?

Human comparison is capable of tolerating shifts and minor errors, thus focusing on what really needs to be compared. Here, fuzzy map comparison is applied for the first time for the assessment of hydro-morphodynamic models. The results show potential of the methods in revealing zones where, even considering tolerance for spatial errors, the model is unable to perform satisfactorily.

The complexity of the physics behind sediment transport results in an elevated complexity of hydro-morphodynamic model calibration. The latter requires more tolerable and sophisticated solutions than traditional model evaluation techniques. Statistics such as the RMSE are overly sensitive to minor disagreements. Because of this, calibrated models may take longer to be achieved. Fuzzy map comparison methods tolerate minor shifts and can be a strong ally for indicating model adequacy in automatic calibrations.

Wealands et al. (2005a) mentions that observations have a major role in the rejection of parameter sets. By comparing simulated with observed data, possible acceptable model parameter sets are limited during calibration. The modeler should, therefore, come up with creative ways of using observations to find an optimum solution (i.e., a calibrated and validated model).

With the rise of remote sensing and *in situ* measurement techniques, dense geospatial data is becoming more available. Rather than comparing only profiles, comparing complete 2D maps of simulated and observed bed elevation changes makes more sense. This study confirms that fuzzy numerical map comparison is able to perform such task while tolerating possible measurement errors or model uncertainty. Furthermore, a map of comparisons (see Figure A.5) enables the modeler to achieve a more concrete evaluation of regions where the model performs well or not.

In the lower Salzach River case study, the models seem to predict alternate bed changes, as if they expected the channel to develop alternate bars. This behavior is well-known to happen in straight channels that have undergone bank fixation (Chang, 1988). However, that was not observed in reality, as sediment dynamics are poor. When the fuzzy numerical is performed, the comparison maps illustrate this hypothesis in a clear manner, as it can be seen in Figure 4.5, especially in Figure (a) comparison of the manually calibrated versus measurements.

From the results of the lower Salzach case study, a possible explanation for the obtained Global Fuzzy Similarity values can be drawn. Considering the  $S_{fuzzy,baseline}$ , the  $S_{fuzzy}$  values obtained for the lower Salzach River models suggest unsatisfactory model efficiency. There is a high chance that the comparisons do not perform poorly because of small shifts (which are tolerated in the consideration of fuzziness of location), but because the models are globally insufficient of reproducing river dynamics. That is however expected, as morphodynamic modeling of fluvial systems is extremely challenging.

Beckers et al. (2020) recognized the overestimation of river dynamics by the models and attributed this to the numerical implementation of sediment input coming from the River Saalach (tributary at the upstream boundary). Fuzzy numerical map comparison alone is not able to reveal the reasons that caused these mismatches, but provides a visualization of the zones where this problem is critical. One of these zones is located at the upstream boundary, where the Saalach River mouths into the River Salzach (see Figures A.5 to A.7). Complex erosion and deposition processes take place in river confluences, where the interaction between flow dynamics and bed morphodynamics is not yet completely understood (Guillén-Ludeña, Franca, Cardoso, & Schleiss, 2015). It is, therefore, expected that the models do not perform well there.

Beven (2006) explains that there is always a commensurability problem when comparing observed against simulated data. The latter is hardly at the same spatial and temporal resolution as the first. The results from the fuzzy map comparison techniques assessed here show that, even though interpolation and re-sampling of data carry an amount of error, comparisons can still be performed, as this commensurability error is accounted in the concepts of neighborhood and halving distance.

The ultimate goal of a numerical model is to adequately reproduce reality. How well a model performs can be measurable by means of several statistics such as those discussed in Section 2.2.5. More precisely, model performance should be evaluated according to the purpose of the model and the quality of the available data (Hunter, 2006). The results from the sensitivity analysis of the physical models of shallow reservoirs indicate that when simulated results match well observed data, a cell-by-cell comparison is possible. The consideration of fuzziness of location appears to behave as a tolerance for spatial error that is not exceeded because the models and measurements are considerably accurate. The fuzzy numerical method thus poses as a generalization that comprises crispy comparison. This finding is in line with the

#### 5.4. Reasons for using fuzzy map comparison

---

idea from Zadeh (1965), which states that fuzzy sets is a generalization of all sets.

This interpretation is confirmed by analyzing the effect of the neighborhood in both case studies. Any increase in the fuzziness of location do not reflect an improvement of the performance measure for the numerical models of shallow reservoirs. In contrast, the performances of the lower Salzach River models are significantly more sensible to changes in fuzziness of location. This result suggests that there is small practical need for applying fuzzy map comparison in accurate models, as the comparison reduces to cell-by-cell comparison, but the method works just as well. Therefore, the fuzzy numerical method can be applied regardless of the exact quantification of the data uncertainty, as the spatial tolerance is either way considered, whether necessary or not.

Finally, the map of comparison (e.g., Figure 4.1) groups all local fuzzy similarities of the same area of interest as the compared rasters. It assists in visually understanding areas that are responsible for a decline in model performance. The latter can be a tricky task when dealing with complex shaped river morphology such as braided or meandering channels, or alternate bars channels.

# **Chapter 6**

## **Conclusions**

This study provides answers to a fundamental research question: how can a realistic evaluation of hydro-morphodynamic models be achieved?

The results and discussion of this research study lead to the following conclusions that answers the research question:

1. The fuzzy numerical method behaves as a generalization that automatically converges to a simple cell-by-cell comparison if the model is accurate (i.e., the simulated dataset matches well the observed dataset). Therefore, it can be applied regardless of the quantification of data uncertainty.
2. Fuzziness of location refers to spatial tolerance. The term "tolerance" accounts for the limit to which a modeler is willing to accept spatial error. This aspect is supported by the results of the numerical models of shallow reservoirs, where an increase in fuzziness of location did not have significant effect on the overall fuzzy global similarity. The comparison was not influenced because the simulated cells and their exact counterparts in the observed cells already result in the best match even if a neighborhood is considered.
3. The generation and comparison of 2D maps offer a more thoroughly way of drawing conclusions about the modeling of bed level change as a whole and not only at sparse cross-sections.
4. The fuzzy numerical method is suitable for evaluating hydro- morphodynamic models in a realistic manner. It has potential in the validation of numerical models.

- 
5. When using the fuzzy numerical method, attention has to be payed to the interpolation and cell size, as the results show that they may significantly affect the fuzzy comparison, especially when dealing with uncertain datasets.

The use of fuzzy measures brings a delineated and transparent subjectivity to spatial comparison. The fuzzy map comparison techniques presented here can be applied in a variety of modeling applications. For categorical data, the fuzzy-kappa poses as a suitable option, whereas for continuous-valued data, the present study considers the fuzzy numerical method more appropriate. Particularly habitat and coastal modeling, where spatial data have categorical responses, would benefit from fuzzy kappa map comparison.

As a whole, the novel algorithms for map comparison developed in this study (codes for pre-processing and for fuzzy numerical map comparison), as well as the computational investigations performed, offer an additional and more realistic approach to hydro-morphodynamic model assessment in the future. The knowledge gained here will be particularly important in future research, since geospatial data will gradually become more available and hydro-morphodynamic model calibration and validation are be expected to evolve towards automated map comparison.

# **Chapter 7**

## **Recommendations and outlook**

### **7.1 Application in hydro-morphodynamic modeling**

Fuzzy numerical map comparison has the potential to aid river scientists in model validation, calibration, and in analyzes of terrain change. For these purposes, some recommendations should be noted, which are:

1. The similarity function used in the novel algorithm of this study (Equation 2.29) is not analytical. Thus, it can be difficult to handle it in calibration processes (especially the gradient-based). The equation can be modified or substituted with the open-source package (Negreiros, 2020) though.
2. The novel algorithms developed in this study are subjected to maintenance in the future. The reader is referred to future updates by Negreiros (2020).
3. If repetitive runs of the fuzzy numerical algorithm are necessary, the rasterization step should be avoided as it increases the computation time. It is though important for the method that the data to be compared is put to an overlay-able regular grid.

### **7.2 Future Research**

Rather than a measure of model accuracy, the Global Fuzzy Similarity serves as a measure of model performance. The latter can be used as a stop-index for model calibration processes. Automatic calibration is yet a very demanding task in morphodynamic modeling due to the

enormous amount of calibration parameters and computational effort. The development of innovative techniques that increase the computational efficiency is pointed out as one of the most important research needs in the field of hydro-morphodynamic modeling (Rijn, Ribberink, Werf, & Walstra, 2013). Measures of fuzzy similarity can contribute as a performance index that is less sensitive to small shifts and thus may lead to fewer model runs. Here, stochastic and gradient-free calibration may present more potential over gradient-based optimization algorithms. That is because to use gradient-based algorithms, the objective function has to be differentiable and sensitive enough to indicate the direction of steepest gradient. Due to the applied fuzzy logic operations, the fuzzy numerical method may not be sufficiently sensitive. In addition, Equation 2.29 is not differentiable in the whole domain of real numbers.

Future research is suggested to investigate an improvement in stochastic model calibration using, in early stages of calibration, the Global Fuzzy Similarity as performance indicator. As a following step, more sensitive measures (such as the RMSE) can provide a finer calibration, if required. More research has to be done until fuzzy comparison can be coupled to model calibration, but if accomplished, it could result in a more comprehensive model evaluation, which bring traits of subjectivity that resembles human comparison.

# References

- Aguirre Iñiguez, D. V., Bui, M. D., Giehl, S., Reisenbüchler, M., & Rutschmann, P. (2019). Development of a hydro-morphodynamic model for sediment management in the rosenheim reservoir. In *Proceedings of the XXVIIth TELEMAC user conference*. doi: <https://doi.org/10.5281/zenodo.3611498>
- Ahn, J., & Yen, H. (2015). Semi-two dimensional numerical prediction of non-equilibrium sediment transport in reservoir using stream tubes and theory of minimum stream power. *KSCE Journal of Civil Engineering*, 19(6), 1922–1929. doi: <https://doi.org/10.1007/s12205-014-0098-x>
- Annandale, G. W. (2006). Reservoir sedimentation. *Encyclopedia of Hydrological Sciences*. doi: <https://doi.org/10.1002/0470848944>
- Beckers, F., Heredia, A., Noack, M., Nowak, W., Wieprecht, S., & Oladyshkin, S. (2019). *Data related to the manuscript "bayesian calibration and validation of a large-scale and time-demanding sediment transport model"*. doi: <http://doi.org/10.5281/zenodo.3576395>
- Beckers, F., Heredia, A., Noack, M., Nowak, W., Wieprecht, S., & Oladyshkin, S. (2020). Bayesian calibration and validation of a large-scale and time-demanding sediment transport model. *Water Resources Research*, e2019WR026966. doi: <https://doi.org/10.1029/2019WR026966>
- Beckers, F., Noack, M., & Wieprecht, S. (2016). *Geschiebetransportmodellierung (GTM) Salzach und Saalach [Bed load transport modeling of the rivers Salzach and Saalach]* (Tech. Rep.). Stuttgart: Department of Hydraulic Engineering and Water Resources Management: Institute for Modelling Hydraulic and Environmental Systems (IWS).
- Beckers, F., Noack, M., & Wieprecht, S. (2018). Uncertainty analysis of a 2d sediment transport model: an example of the lower river salzach. *Journal of Soils and Sediments*, 18(10), 3133–3144. doi: <https://doi.org/10.1007/s11368-017-1816-z>
- Bell, P., Biester, T., Burovski, E., Caswell, T. A., Gommers, R., Molden, S., ... Virtanen, P. (2020).

- SciPy reference guide, release 1.5.2.* Retrieved from <https://docs.scipy.org/doc/scipy-1.5.2/scipy-ref-1.5.2.pdf>
- Beven, K. (2006). A manifesto for the equifinality thesis. *Journal of hydrology*, 320(1-2), 18–36. doi: <https://doi.org/10.1016/j.jhydrol.2005.07.007>
- Bloch, I. (2005). Fuzzy spatial relationships for image processing and interpretation: a review. *Image and Vision Computing*, 23(2), 89–110. doi: <https://doi.org/10.1016/j.imavis.2004.06.013>
- Boyle, D. P., Gupta, H. V., & Sorooshian, S. (2000). Toward improved calibration of hydrologic models: Combining the strengths of manual and automatic methods. *Water Resources Research*, 36(12), 3663–3674. doi: <https://doi.org/10.1029/2000WR900207>
- Brady, A., & Sutherland, J. (2001). COSMOS modelling of COAST3D egmond main experiment. *HR Wallingford Report TR, 115*.
- Burkholder, E. F. (2008). *The 3-d global spatial data model: Foundation of the spatial data infrastructure*. CRC Press.
- Carley, J. K., Pasternack, G. B., Wyrick, J. R., Barker, J. R., Bratovich, P. M., Massa, D. A., ... Johnson, T. R. (2012). Significant decadal channel change 58–67 years post-dam accounting for uncertainty in topographic change detection between contour maps and point cloud models. *Geomorphology*, 179, 71–88. doi: <https://doi.org/10.1016/j.geomorph.2012.08.001>
- Chang, H. H. (1988). *Fluvial processes in river engineering*.
- Cheng, H. D., & Chen, Y. H. (1998). Thresholding based on fuzzy partition of 2d histogram. In *Proceedings. fourteenth international conference on pattern recognition (cat. no. 98ex170)* (Vol. 2, pp. 1616–1618). doi: <https://doi.org/10.1109/ICPR.1998.712025>
- Civanlar, M. R., & Trussell, H. J. (1986). Constructing membership functions using statistical data. *Fuzzy sets and systems*, 18(1), 1–13. doi: [https://doi.org/10.1016/0165-0114\(86\)90024-2](https://doi.org/10.1016/0165-0114(86)90024-2)
- Cohen, J. (1960). A coefficient of agreement for nominal scales. *Educational and psychological measurement*, 20(1), 37–46. doi: <https://doi.org/10.1177/001316446002000104>
- Cohen, J. (1972). Weighted chi square: An extension of the kappa method. *Educational and Psychological Measurement*, 32(1), 61–74. doi: <https://doi.org/10.1177/001316447203200106>
- Doherty, J., et al. (1994). PEST: a unique computer program for model-independent parameter optimisation. *Water Down Under 94: Groundwater/Surface Hydrology Common Interest Papers; Preprints of Papers*, 551.

## References

---

- Dombi, J. (1990). Membership function as an evaluation. *Fuzzy sets and systems*, 35(1), 1–21.  
doi: [https://doi.org/10.1016/0165-0114\(90\)90014-W](https://doi.org/10.1016/0165-0114(90)90014-W)
- Dou, W., Ren, Y., Wu, Q., Ruan, S., Chen, Y., Bloyet, D., & Constans, J. M. (2007). Fuzzy kappa for the agreement measure of fuzzy classifications. *Neurocomputing*, 70(4-6), 726–734.  
doi: <https://doi.org/10.1016/j.neucom.2006.10.007>
- Dung, N. V., Merz, B., Bárdossy, A., Thang, T. D., & Apel, H. (2011). Multi-objective automatic calibration of hydrodynamic models utilizing inundation maps and gauge data. *Hydrology & Earth System Sciences*, 15(4). doi: <https://doi.org/10.5194/hess-15-1339-2011>
- Exner, F. M. (1925). Über die Wechselwirkung zwischen Wasser und Geschiebe in Flüssen [About the Interdependency of Water and Bed load in Rivers]. *Akademie der Wissenschaften in Wien, math.-naturw. Klasse, Sitzungsberichte, Abt. IIa*, 134, 165-203.
- Ferreira, C., Silva, P., Fernández-Fernández, S., Ribeiro, A., Abreu, T., Bertin, X., & Dias, J. (2017). Validation of a morphodynamic model to figureira da foz inlet. In *Proceedings of international short course and conference on applied coastal research (SCACR)* (pp. 1–12).
- Fleiss, J., Levin, B., & Paik, M. (1981). Statistical methods for rates and proportions. *New York*, 870.
- Foeckler, F., Diepolder, U., & Deichner, O. (1991). Water mollusc communities and bioindication of lower Salzach floodplain waters. *Regulated Rivers: Research & Management*, 6(4), 301–312. doi: <https://doi.org/10.1002/rrr.3450060408>
- Foody, G. M. (2007). Map comparison in GIS. *Progress in Physical Geography*, 31(4), 439–445.  
doi: <https://doi.org/10.1177/0309133307081294>
- Ganju, N. K., Brush, M. J., Rashleigh, B., Aretxabaleta, A. L., Del Barrio, P., Grear, J. S., ... others (2016). Progress and challenges in coupled hydrodynamic-ecological estuarine modeling. *Estuaries and Coasts*, 39(2), 311–332. doi: <https://doi.org/10.1007/s12237-015-0011-y>
- Garcia, M. H. (2008). Sediment transport and morphodynamics. In *Sedimentation engineering: Processes, measurements, modeling, and practice* (pp. 21–163).
- Graf, W. H., & Altinakar, M. S. (1998). *Fluvial hydraulics: Flow and transport processes in channels of simple geometry* (No. 551.483 G7).
- Guillén-Ludeña, S., Franca, M. J., Cardoso, A. H., & Schleiss, A. J. (2015). Hydro-morphodynamic evolution in a 90° movable bed discordant confluence with low discharge ratio. *Earth Surface Processes and Landforms*, 40(14), 1927–1938. doi: <https://doi.org/10.1002/esp.3770>

- Hagen, A. (2003). Fuzzy set approach to assessing similarity of categorical maps. *International Journal of Geographical Information Science*, 17(3), 235–249. doi: <https://doi.org/10.1080/13658810210157822>
- Hagen, A. (2006). *Comparing continuous valued raster data: A cross disciplinary literature scan* (Tech. Rep.). Research Institute for Knowledge Systems (RIKS), Maastricht, The Netherlands.
- Hagen, A. (2009). An improved fuzzy kappa statistic that accounts for spatial autocorrelation. *International Journal of Geographical Information Science*, 23(1), 61–73. doi: <https://doi.org/10.1080/13658810802570317>
- Hagen, A. (2018). *raster*. <https://github.com/ahhz/raster>. GitHub repository.
- Hagen, A., Straatman, B., & Uljee, I. (2005). Further developments of a fuzzy set map comparison approach. *International Journal of Geographical Information Science*, 19(7), 769–785. doi: <https://doi.org/10.1080/13658810500072137>
- Haining, R. (1991). Bivariate correlation with spatial data. *Geographical Analysis*, 23(3), 210–227. doi: <https://doi.org/10.1111/j.1538-4632.1991.tb00235.x>
- Hauer, C., Mandlburger, G., & Habersack, H. (2009). Hydraulically related hydro-morphological units: description based on a new conceptual mesohabitat evaluation model (MEM) using LiDAR data as geometric input. *River Research and Applications*, 25(1), 29–47. doi: <https://doi.org/10.1002/rra.1083>
- Hauer, C., Unfer, G., Schmutz, S., & Habersack, H. (2007). The importance of morphodynamic processes at riffles used as spawning grounds during the incubation time of nase (*chondrostoma nasus*). *Hydrobiologia*, 579(1), 15–27. doi: <https://doi.org/10.1007/s10750-006-0406-7>
- Haun, S., Dorfmann, C., Harb, G., & Olsen, N. R. B. (2012). 3D numerical modelling of the reservoir flushing of the Bodendorf reservoir, Austria. In *2nd IAHR european conference, munich, germany*.
- Hunter, N. (2006). Flood inundation modelling - phd thesis. *School of Geography, Bristol University, Bristol*.
- Jenks, G. F., & Caspall, F. C. (1971). Error on choroplethic maps: definition, measurement, reduction. *Annals of the Association of American Geographers*, 61(2), 217–244. doi: <https://doi.org/10.1111/j.1467-8306.1971.tb00779.x>
- Jørgensen, S. E., & Bendoricchio, G. (2001). *Fundamentals of ecological modelling* (Vol. 21). Elsevier.
- Kantoush, S. A. (2008). *Experimental study on the influence of the geometry of shallow reservoirs*

## References

---

- on flow patterns and sedimentation by suspended sediments* (Doctoral dissertation, ÉCOLE POLYTECHNIQUE FÉDÉRALE DE LAUSANNE). (THÈSE No. 4048) doi: 10.5075/epfl-thesis-4048
- Kantoush, S. A., Bollaert, E., & Schleiss, A. J. (2008). Experimental and numerical modelling of sedimentation in a rectangular shallow basin. *International Journal of sediment research*, 23(3), 212–232. doi: [https://doi.org/10.1016/S1001-6279\(08\)60020-7](https://doi.org/10.1016/S1001-6279(08)60020-7)
- Klir, G., & Yuan, B. (1995). *Fuzzy sets and fuzzy logic* (Vol. 4). Prentice hall New Jersey (USA).
- Kraemer, H. C. (1980). Extension of the kappa coefficient. *Biometrics*, 207–216. doi: <https://doi.org/10.2307/2529972>
- Kunz, M. (2019). *3-D Numerische Modellierung eines physikalischen Modellversuchs zur Bestimmung des Spülkegels während einer Stauraumspülung* (Unpublished master's thesis). Universität Stuttgart, Germany.
- Landis, J. R., & Koch, G. G. (1977). The measurement of observer agreement for categorical data. *biometrics*, 159–174. doi: <https://doi.org/10.2307/2529310>
- Landry, M., Malouin, J.-L., & Oral, M. (1983). Model validation in operations research. *European Journal of Operational Research*, 14(3), 207–220. doi: [https://doi.org/10.1016/0377-2217\(83\)90257-6](https://doi.org/10.1016/0377-2217(83)90257-6)
- Legates, D. R., & McCabe Jr, G. J. (1999). Evaluating the use of “goodness-of-fit” measures in hydrologic and hydroclimatic model validation. *Water resources research*, 35(1), 233–241. doi: <https://doi.org/10.1029/1998WR900018>
- Legleiter, C. J. (2012). Remote measurement of river morphology via fusion of lidar topography and spectrally based bathymetry. *Earth Surface Processes and Landforms*, 37(5), 499–518. doi: <https://doi.org/10.1002/esp.2262>
- MacIure, M., & Willett, W. C. (1987). Misinterpretation and misuse of the kappa statistic. *American journal of epidemiology*, 126(2), 161–169. doi: <https://doi.org/10.1093/aje/126.2.161>
- Marcus, W. A., & Fonstad, M. A. (2010). Remote sensing of rivers: the emergence of a subdiscipline in the river sciences. *Earth Surface Processes and Landforms*, 35(15), 1867–1872. doi: <https://doi.org/10.1002/esp.2094>
- McKibbon, J., & Mahdi, T.-F. (2010). Automatic calibration tool for river models based on the MHYSER software. *Natural hazards*, 54(3), 879–899. doi: <https://doi.org/10.1007/s11069-010-9512-y>
- Medasani, S., Kim, J., & Krishnapuram, R. (1995). Estimation of membership functions for pattern recognition and computer vision. In *Fuzzy logic and its applications to*

- engineering, information sciences, and intelligent systems* (pp. 45–54). Springer. doi: [https://doi.org/10.1007/978-94-009-0125-4\\_5](https://doi.org/10.1007/978-94-009-0125-4_5)
- Melo, W., Pinho, J., Iglesias, I., Bio, A., Avilez-Valente, P., Vieira, J., ... Veloso-Gomes, F. (2020). Hydro-and morphodynamic impacts of sea level rise: The Minho estuary case study. *Journal of Marine Science and Engineering*, 8(6), 441. doi: <https://doi.org/10.3390/jmse8060441>
- Meyer-Peter, E., & Müller, R. (1948). Formulas for Bed-Load transport. *IAHSR, appendix 2, 2nd meeting*, 39-65.
- Mohammadi, F. (2017). *Bayesian model selection for hydro-morphodynamic models* (Master's thesis, Universität Stuttgart, Germany). doi: <http://dx.doi.org/10.18419/opus-9159>
- Moriasi, D. N., Arnold, J. G., Van Liew, M. W., Bingner, R. L., Harmel, R. D., & Veith, T. L. (2007). Model evaluation guidelines for systematic quantification of accuracy in watershed simulations. *Transactions of the ASABE*, 50(3), 885–900.
- Negreiros, B. M. F. (2020, October). *fuzzycorr*. <https://github.com/beatriznegreiros/fuzzycorr>. GitHub repository. (Version 0.0.1)
- Noack, M., Ortlepp, J., & Wieprecht, S. (2015). Simulations of spawning habitats for brown trout in an Alpine river reach using a two-stage multivariate fuzzy-logical approach. *Journal on Protected Mountain Areas Research and Management*, 7, 41–49. doi: <https://doi.org/10.1553/eco.mont-7-2s41>
- Noack, M., Schneider, M., & Wieprecht, S. (2013). The habitat modelling system CASiMiR: A multivariate fuzzy-approach and its applications. *Ecohydraulics: An Integrated Approach*, 75. (Online ISBN: 9781118526576) doi: <https://doi.org/10.1002/9781118526576.ch4>
- Oladyshevkin, S., & Nowak, W. (2012). Data-driven uncertainty quantification using the arbitrary polynomial chaos expansion. *Reliability Engineering & System Safety*, 106, 179–190. doi: <https://doi.org/10.1016/j.ress.2012.05.002>
- Oliphant, T. E. (2007). Python for scientific computing. *Computing in Science Engineering*, 9(3), 10-20. doi: <https://doi.org/10.1109/MCSE.2007.58>
- Olsen, N. (2014). *A three-dimensional numerical model for simulation of sediment movements in water intakes with multiblock option: User's manual* (Tech. Rep.). Norwegian University of Science and Technology (NTNU), Trondheim, Norway.
- Olsen, N., & Haun, S. (2010). Free surface algorithms for 3D numerical modelling of reservoir flushing. In *River flow 2010* (Vol. 2010, pp. 1105–1110). (Karlsruhe: Bundesanstalt für Wasserbau. ISBN 978-3-939230-00-7)
- Oreskes, N., Shrader-Frechette, K., & Belitz, K. (1994). Verification, validation, and confir-

## References

---

- mation of numerical models in the earth sciences. *Science*, 263(5147), 641–646. doi: <https://doi.org/10.1126/science.263.5147.641>
- Pappenberger, F., Frodsham, K., Beven, K., Romanowicz, R., & Matgen, P. (2007, January). Fuzzy set approach to calibrating distributed flood inundation models using remote sensing observations. *Hydrology and Earth System Sciences Discussions*, 11(2), 739-752. Retrieved from <https://hal.archives-ouvertes.fr/hal-00305049>
- Parsapour-Moghaddam, P., Brennan, C. P., Rennie, C. D., Elvidge, C. K., & Cooke, S. J. (2019). Impacts of channel morphodynamics on fish habitat utilization. *Environmental management*, 64(3), 272–286. doi: <https://doi.org/10.1007/s00267-019-01197-0>
- Pawłowski, K., & Godzik, A. (2001). Surface map comparison: Studying function diversity of homologous proteins. *Journal of molecular biology*, 309(3), 793–806. doi: <https://doi.org/10.1006/jmbi.2001.4630>
- Pearson, E., Smith, M., Klaar, M., & Brown, L. (2017). Can high resolution 3D topographic surveys provide reliable grain size estimates in gravel bed rivers? *Geomorphology*, 293, 143–155. doi: <https://doi.org/10.1016/j.geomorph.2017.05.015>
- Power, C., Simms, A., & White, R. (2001). Hierarchical fuzzy pattern matching for the regional comparison of land use maps. *International Journal of Geographical Information Science*, 15(1), 77–100. doi: <https://doi.org/10.1080/136588100750058715>
- Refsgaard, J. C., & Henriksen, H. J. (2004). Modelling guidelines—terminology and guiding principles. *Advances in Water Resources*, 27(1), 71–82. doi: <https://doi.org/10.1016/j.advwatres.2003.08.006>
- Refsgaard, J. C., van der Sluijs, J. P., Højberg, A. L., & Vanrolleghem, P. A. (2007). Uncertainty in the environmental modelling process—a framework and guidance. *Environmental modelling & software*, 22(11), 1543–1556. doi: <https://doi.org/10.1016/j.envsoft.2007.02.004>
- Ren, Y., Lin, J., Zhu, J., Sun, B., & Ye, S. (2015). Coordinate transformation uncertainty analysis in large-scale metrology. *IEEE Transactions on Instrumentation and Measurement*, 64(9), 2380–2388. doi: <https://doi.org/10.1109/TIM.2015.2403151>
- Rijn, L. C. V., Ribberink, J. S., Werf, J. V. D., & Walstra, D. J. (2013). Coastal sediment dynamics: recent advances and future research needs. *Journal of hydraulic research*, 51(5), 475–493. doi: <https://doi.org/10.1080/00221686.2013.849297>
- Robinson, A. H., Sale, R. D., Morrison, J. L., & Muehrcke, P. C. (1985). *Elements of cartography* (5th Edition ed.). John Wiley & Sons.
- Sánchez-Arcilla Conejo, A., Gracia Garcia, V., & García León, M. (2014). Hydro morphodynamic

- modelling in mediterranean storms: errors and uncertainties under sharp gradients. *Natural hazards and earth system sciences*, 2(2), 1693–1728. doi: <https://doi.org/10.5194/nhess-14-2993-2014>
- Shoarinezhad, V., & Haun, S. (2018, April). Automated calibration for 3D morphodynamic numerical models. In *EGU general assembly conference abstracts* (p. 8238).
- Shoarinezhad, V., Weprecht, S., & Haun, S. (2020). Comparison of local and global optimization methods for calibration of a 3d morphodynamic model of a curved channel. *Water*, 12(5), 1333. doi: <https://doi.org/10.3390/w12051333>
- Shoarinezhad, V., Weprecht, S., Kantoush, S., & Haun, S. (2021). *The geometry effect of shallow reservoirs on the sedimentation pattern: numerical analysis of lozenge-and hexagon-shaped reservoirs*. IAHR. (Paper has been accepted for publication)
- Skinner, K. D. (2011). *Evaluation of LiDAR-acquired bathymetric and topographic data accuracy in various hydrogeomorphic settings in the deadwood and south fork boise rivers, west-central idaho, 2007* (U.S. Geological Survey Scientific Investigations Report 2011-5051). U.S. Geological Survey, Boise (USA): USGS.
- Stevens, S. S. (1946). On the theory of scales of measurement. *Science*, 20, 677–680.
- Stock, K., & Guesgen, H. (2016). Geospatial reasoning with open data. In *Automating open source intelligence* (pp. 171–204). Elsevier. doi: <https://doi.org/10.1016/B978-0-12-802916-9.00010-5>
- Strickler, A. (1923). Contributions to the question of velocity formula and the roughness numbers for rivers, channels and pipes. *Mitteilung* 16.
- Sun, S. (2011). Meta-analysis of Cohen's kappa. *Health Services and Outcomes Research Methodology*, 11(3-4), 145–163. doi: <https://doi.org/10.1007/s10742-011-0077-3>
- Sutherland, J., Hall, L., & Chesher, T. (2001). Evaluation of the coastal area model PISCES at Teignmouth (UK). *HR Wallingford Report TR125*.
- Sutherland, J., Peet, A., & Soulsby, R. (2004). Evaluating the performance of morphological models. *Coastal engineering*, 51(8-9), 917–939. doi: <https://doi.org/10.1016/j.coastaleng.2004.07.015>
- Sutherland, J., & Soulsby, R. (2003). Use of model performance statistics in modelling coastal morphodynamics. In *Proceedings of the international conference on coastal sediments* (pp. 1–14).
- Thompson, W. D., & Walter, S. D. (1988). A reappraisal of the kappa coefficient. *Journal of clinical epidemiology*, 41(10), 949–958. doi: [https://doi.org/10.1016/0895-4356\(88\)90031-5](https://doi.org/10.1016/0895-4356(88)90031-5)

## References

---

- Tonina, D., McKean, J. A., Benjankar, R. M., Wright, C. W., Goode, J. R., Chen, Q., ... Edmondson, M. R. (2019). Mapping river bathymetries: Evaluating topobathymetric lidar survey. *Earth Surface Processes and Landforms*, 44(2), 507–520. doi: <https://doi.org/10.1002/esp.4513>
- Toshiro, O. (2002). Classification methods for spatial data representation. *Center for Advanced Spatial Analysis. University College London. London (UK)*.
- Van Rijn, L., Walstra, D., Grasmeijer, B., Sutherland, J., Pan, S., & Sierra, J. (2003). The predictability of cross-shore bed evolution of sandy beaches at the time scale of storms and seasons using process-based profile models. *Coastal Engineering*, 47(3), 295–327. doi: [https://doi.org/10.1016/S0378-3839\(02\)00120-5](https://doi.org/10.1016/S0378-3839(02)00120-5)
- Villaret, C., Hervouet, J.-M., Kopmann, R., Merkel, U., & Davies, A. G. (2013). Morphodynamic modeling using the Telemac finite-element system. *Computers & Geosciences*, 53, 105–113. doi: <https://doi.org/10.1016/j.cageo.2011.10.004>
- Visser, H., & De Nijs, T. (2006). The map comparison kit. *Environmental Modelling & Software*, 21(3), 346–358. doi: <https://doi.org/10.1016/j.envsoft.2004.11.013>
- Wealands, S. R., Grayson, R. B., & Walker, J. P. (2005a). Quantitative comparison of spatial fields for hydrological model assessment—some promising approaches. *Advances in Water Resources*, 28(1), 15–32. doi: <https://doi.org/10.1016/j.advwatres.2004.10.001>
- Wealands, S. R., Grayson, R. B., & Walker, J. P. e. a. (2005b). Quantitative measures for the local similarity of hydrological spatial patterns. In *29th Hydrology and Water Resources Symposium: Water Capital, 20-23 February 2005, Rydges Lakeside, Canberra* (p. 760).
- White, R. (2006). Pattern based map comparisons. *Journal of Geographical Systems*, 8(2), 145–164. doi: <https://doi.org/10.1007/s10109-006-0026-9>
- Wieprecht, S., Tolossa, H. G., & Yang, C. T. (2013). A neuro-fuzzy-based modelling approach for sediment transport computation. *Hydrological sciences journal*, 58(3), 587–599. doi: <https://doi.org/10.1080/02626667.2012.755264>
- Willmott, C. J. (1981). On the validation of models. *Physical geography*, 2(2), 184–194. doi: <https://doi.org/10.1080/02723646.1981.10642213>
- Winkler, R. L. (1996). Uncertainty in probabilistic risk assessment. *Reliability Engineering & System Safety*, 54(2-3), 127–132. doi: [https://doi.org/10.1016/S0951-8320\(96\)00070-1](https://doi.org/10.1016/S0951-8320(96)00070-1)
- Winter, C. (2007). On the evaluation of sediment transport models in tidal environments. *Sedimentary Geology*, 202(3), 562–571. doi: <https://doi.org/10.1016/j.sedgeo.2007.03.019>
- Wright, N., & Crosato, A. (2011). *The hydrodynamics and morphodynamics of rivers*. Elsevier

- Science Ltd. doi: <https://doi.org/10.1016/B978-0-444-53199-5.00033-6>
- Wu, C.-Y., Mossa, J., Mao, L., & Almulla, M. (2019). Comparison of different spatial interpolation methods for historical hydrographic data of the lowermost Mississippi River. *Annals of GIS*, 25(2), 133–151. doi: <https://doi.org/10.1080/19475683.2019.1588781>
- Wyrick, J., Gonzalez, R., & Pasternack, G. (2013). *Hydraulic geometry of the Lower Yuba River: Depth-discharge relationships* (Lower Yuba River Accord Monitoring and Evaluation Program). University of California, Davis, USA.
- Zadeh, L. A. (1965). Fuzzy sets. *Information and control*, 8(3), 338–353. doi: [https://doi.org/10.1016/S0019-9958\(65\)90241-X](https://doi.org/10.1016/S0019-9958(65)90241-X)
- Zadeh, L. A. (1988). Fuzzy logic. *Computer*, 21(4), 83–93. doi: <https://doi.org/10.1109/2.53>
- Zimmermann, H.-J. (2011). *Fuzzy set theory—and its applications*. Springer Science & Business Media. doi: <https://doi.org/10.1007/978-94-015-8702-0>

# **Appendices**

## **Appendix A**

### **Complete rasters of the lower Salzach River**

The entire maps of the lower Salzach River can be better visualized in full page as follows:

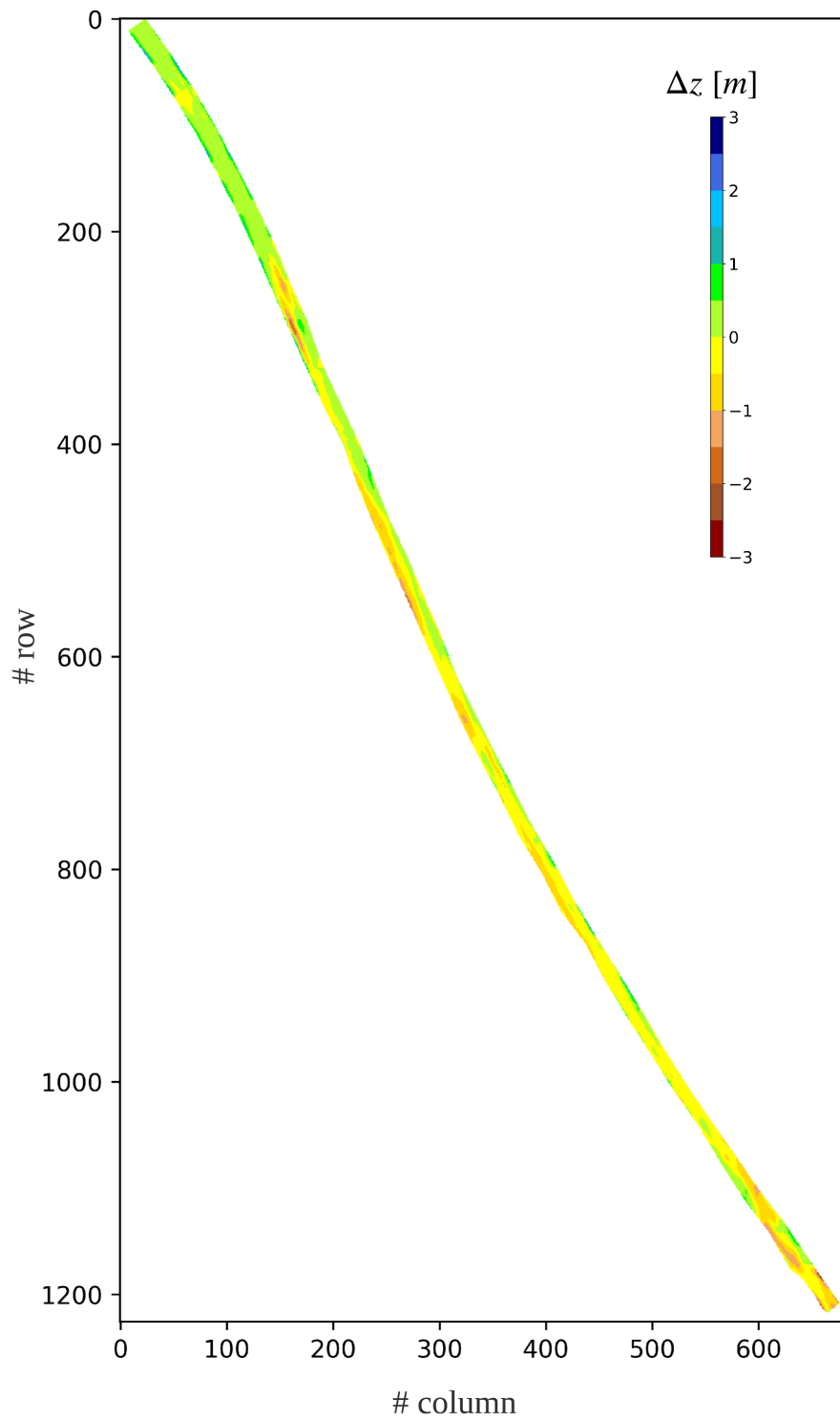


Figure A.1: Raster of observed  $\Delta z$  in the lower Salzach River for the validation period 2010-2013 (Resolution of 5m).

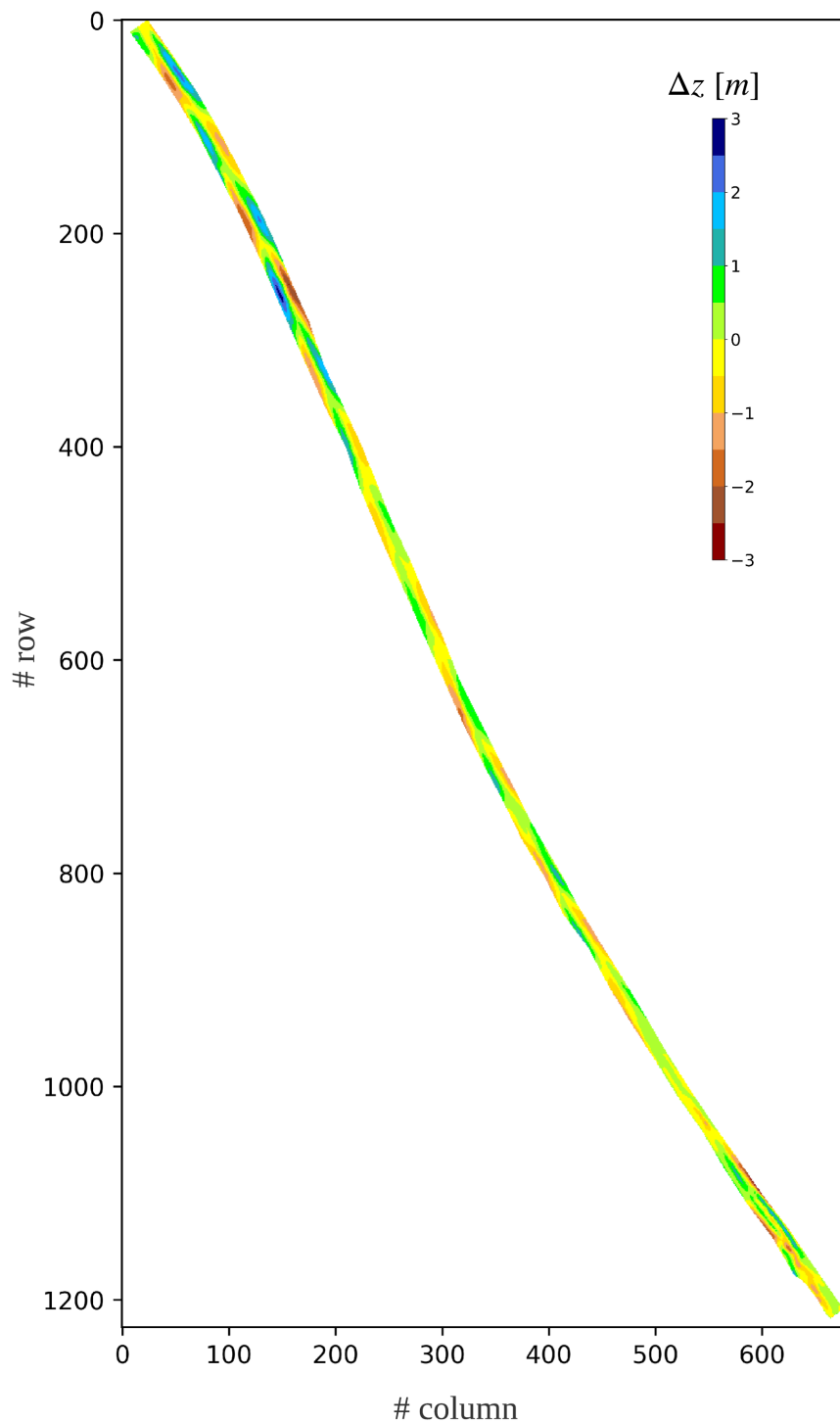


Figure A.2: Raster of simulated  $\Delta z$  in the lower Salzach River for the validation period 2010-2013 from the manually calibrated *HYDRO\_FT-2D* model (Resolution of 5m).

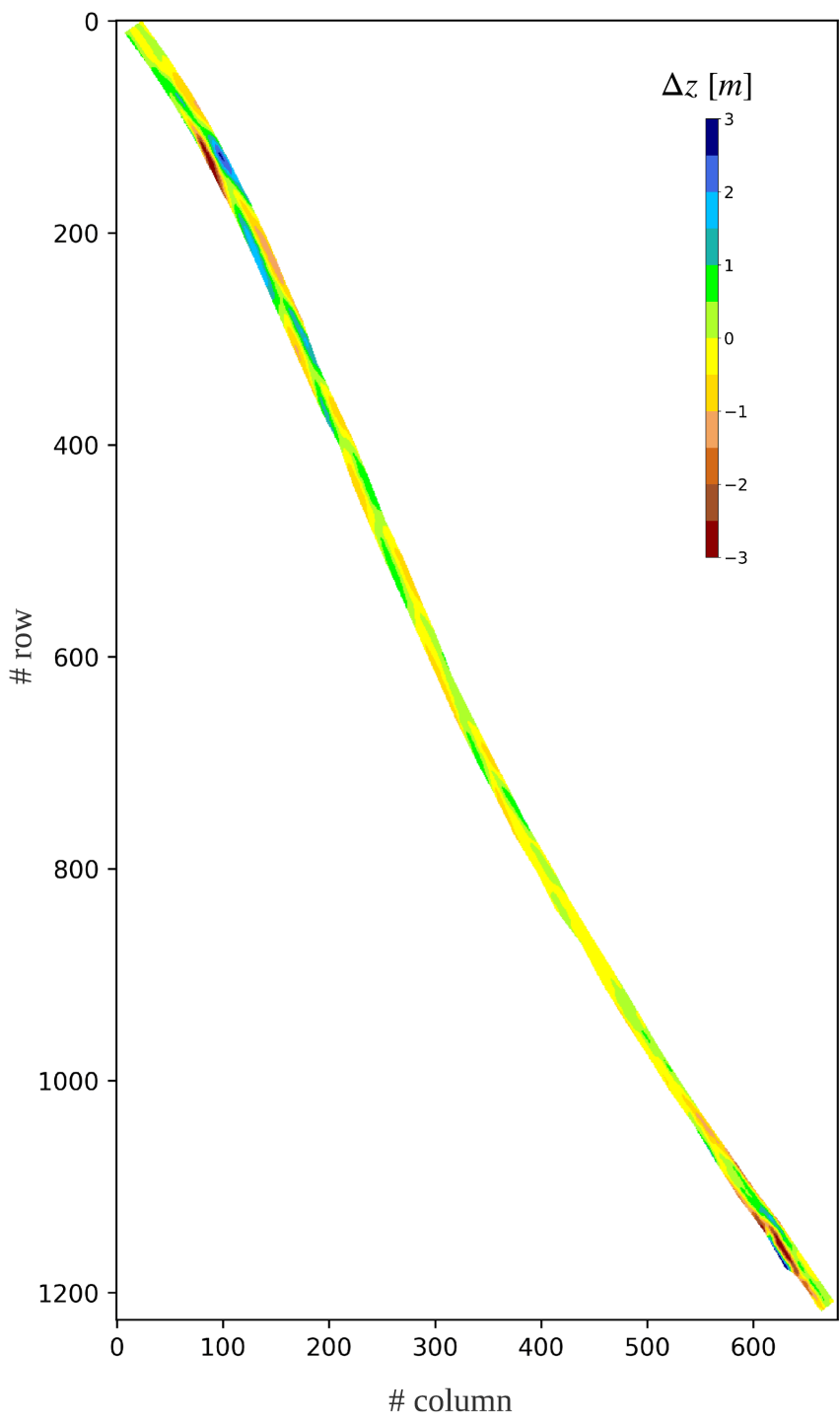


Figure A.3: Raster of simulated  $\Delta z$  in the lower Salzach River for the validation period 2010-2013 from the stochastically calibrated *HYDRO\_FT-2D* model (Resolution of 5m).

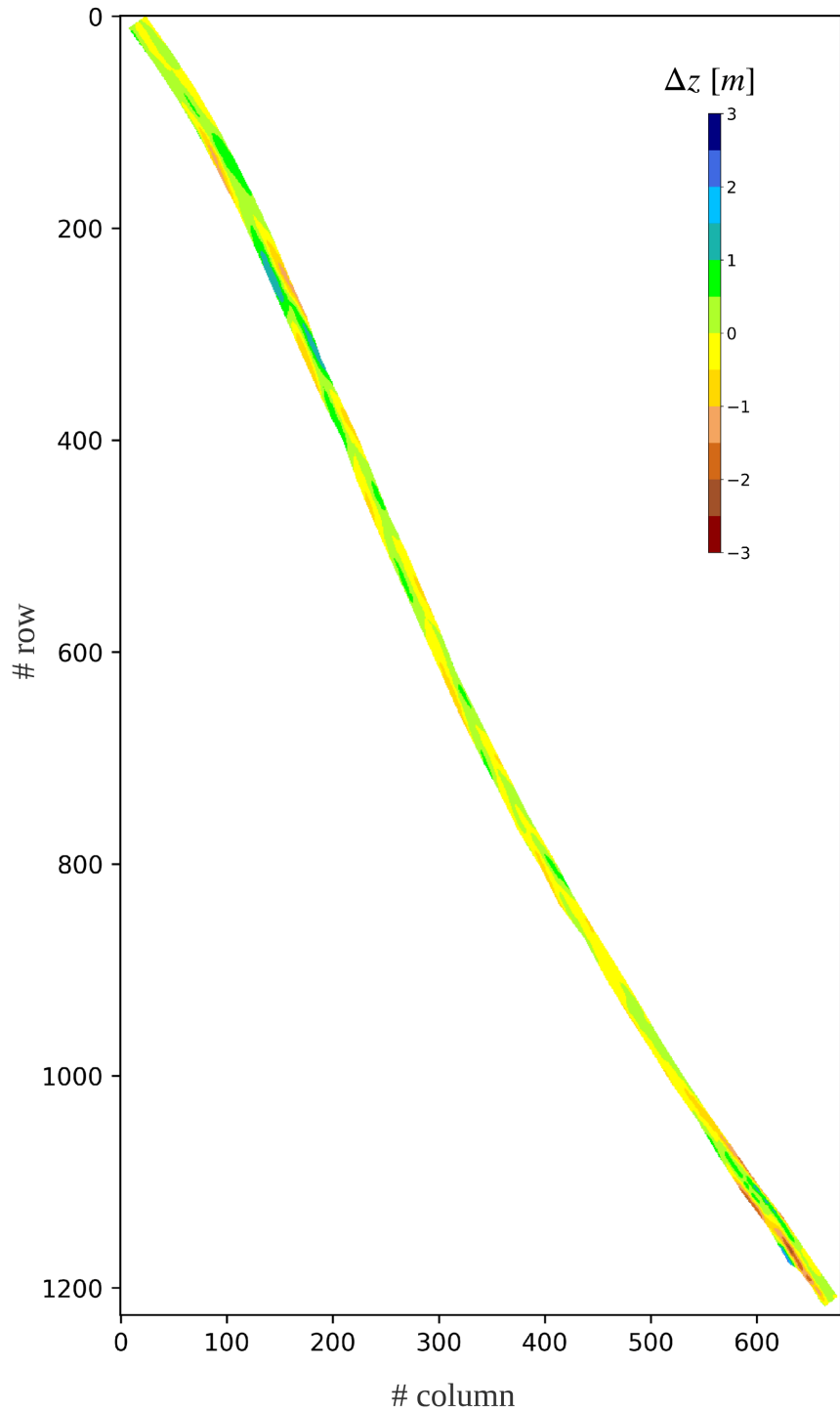


Figure A.4: Raster of simulated  $\Delta z$  in the lower Salzach River for the validation period 2010-2013 from the aPC surrogate model (Resolution of 5m).

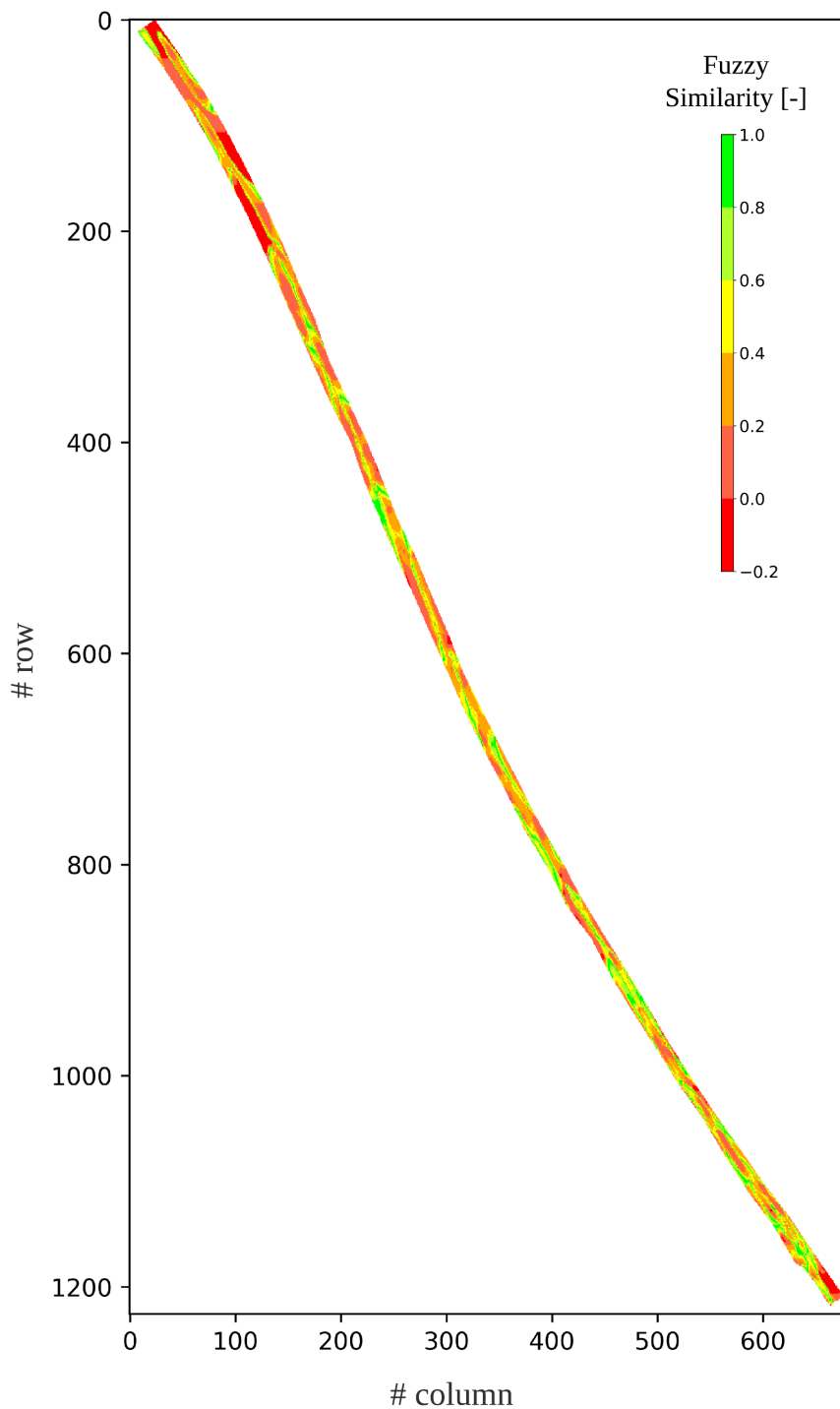


Figure A.5: Fuzzy evaluation of the manually calibrated *HYDRO\_FT-2D* model of the lower Salzach River for the validation period 2010-2013 compared to observed  $\Delta z$  (Resolution of 5m, method: **Fuzzy numerical**).

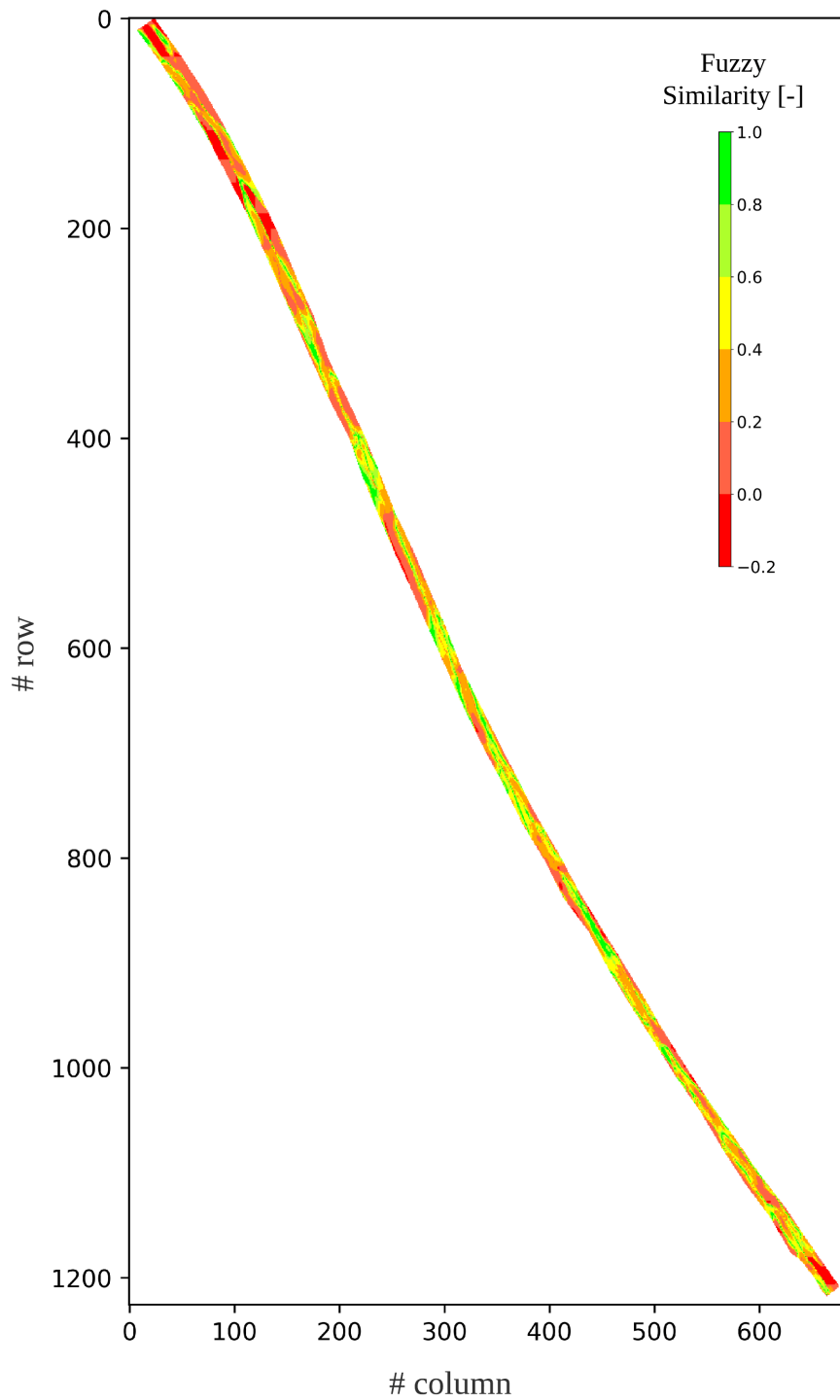


Figure A.6: Fuzzy evaluation of the stochastically calibrated *HYDRO\_FT-2D* model of the lower Salzach River for the validation period 2010-2013 compared to observed  $\Delta z$  (Resolution of 5m, method: **Fuzzy numerical**).

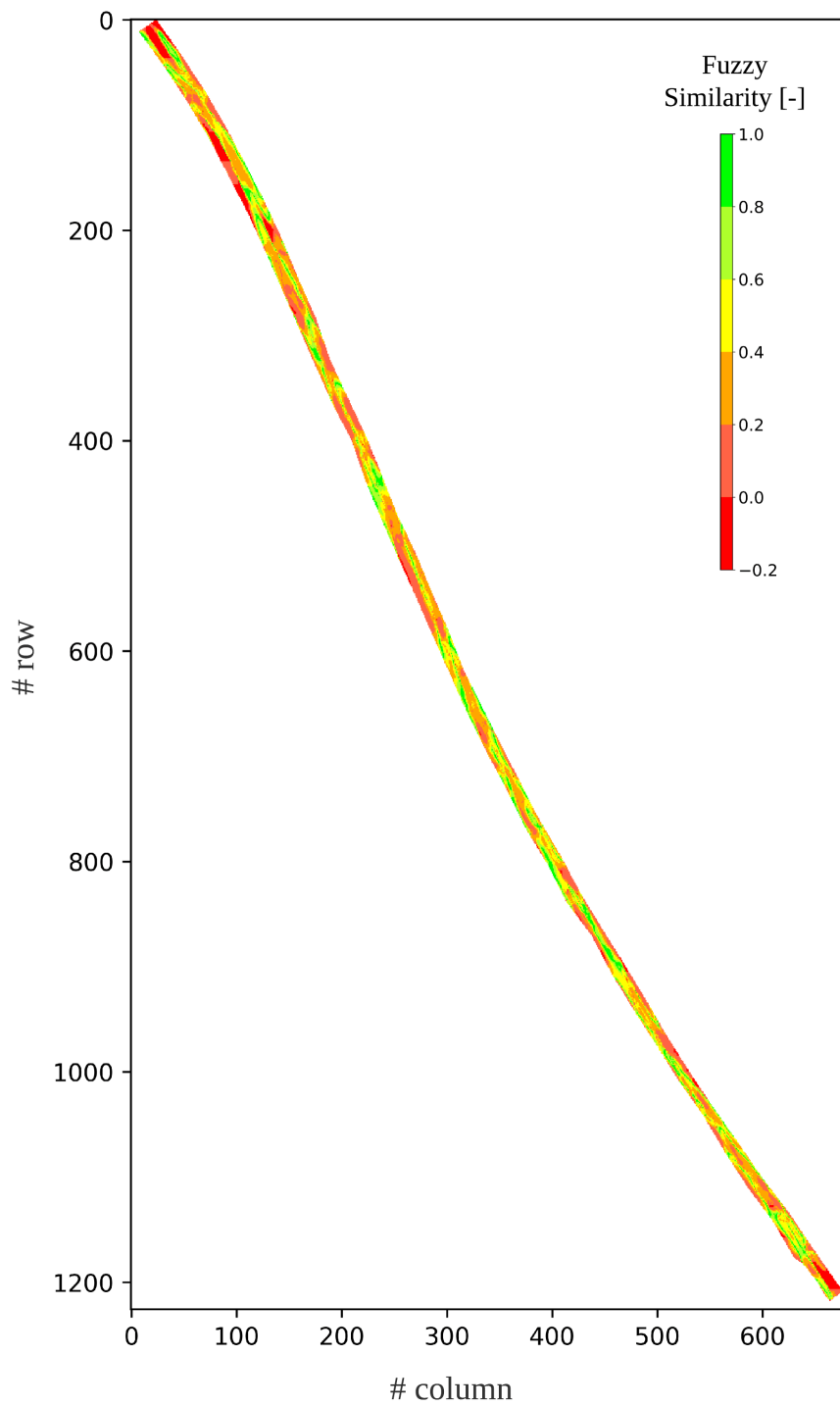


Figure A.7: Fuzzy evaluation of the aPC surrogate model of the lower Salzach River for the validation period 2010-2013 compared to observed  $\Delta z$  (Resolution of 5m, method: **Fuzzy numerical**).

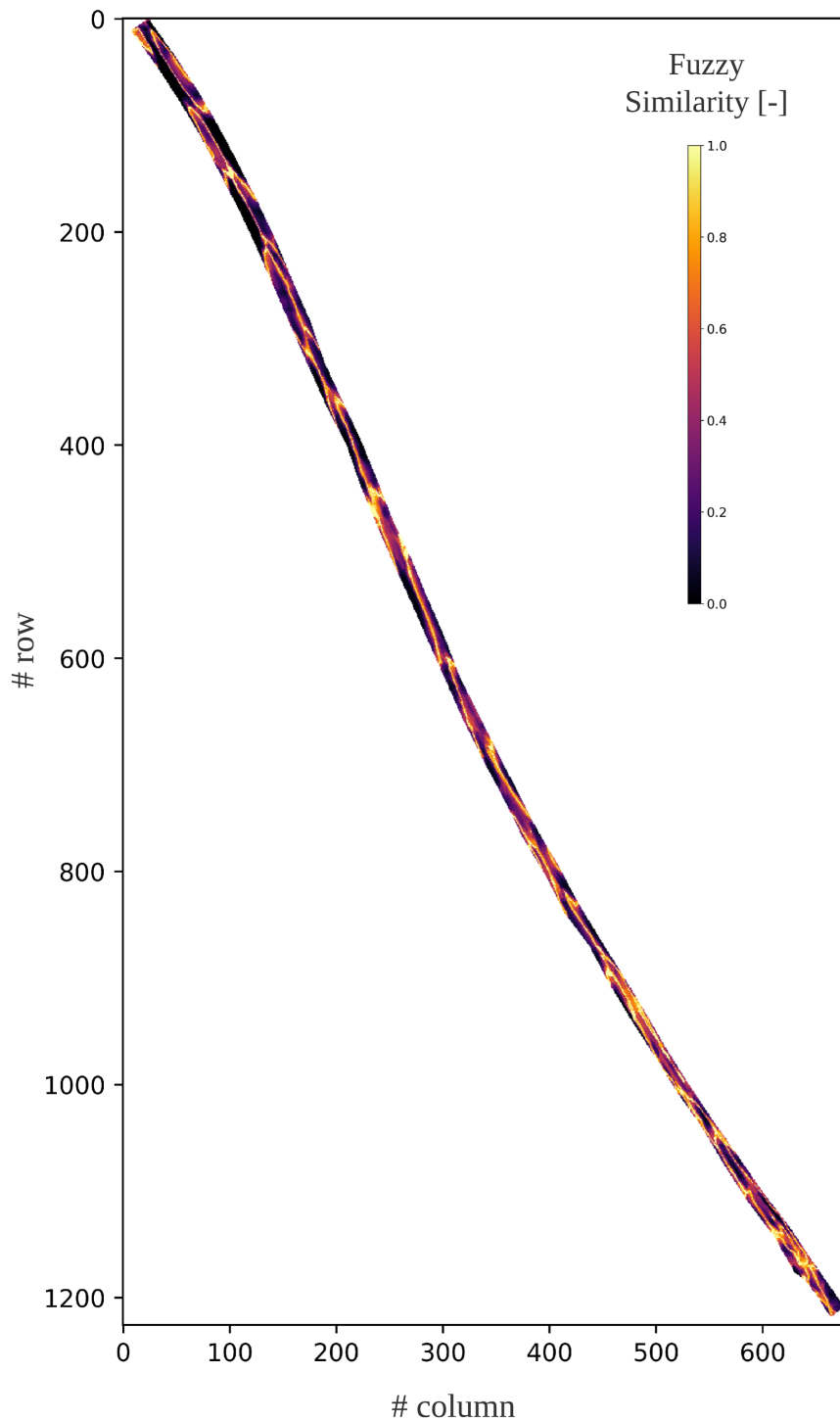


Figure A.8: Fuzzy evaluation of the manually calibrated *HYDRO\_FT-2D* model of the lower Salzach River for the validation period 2010-2013 compared to observed  $\Delta z$  (Resolution of 5m, method: **Fuzzy kappa**).

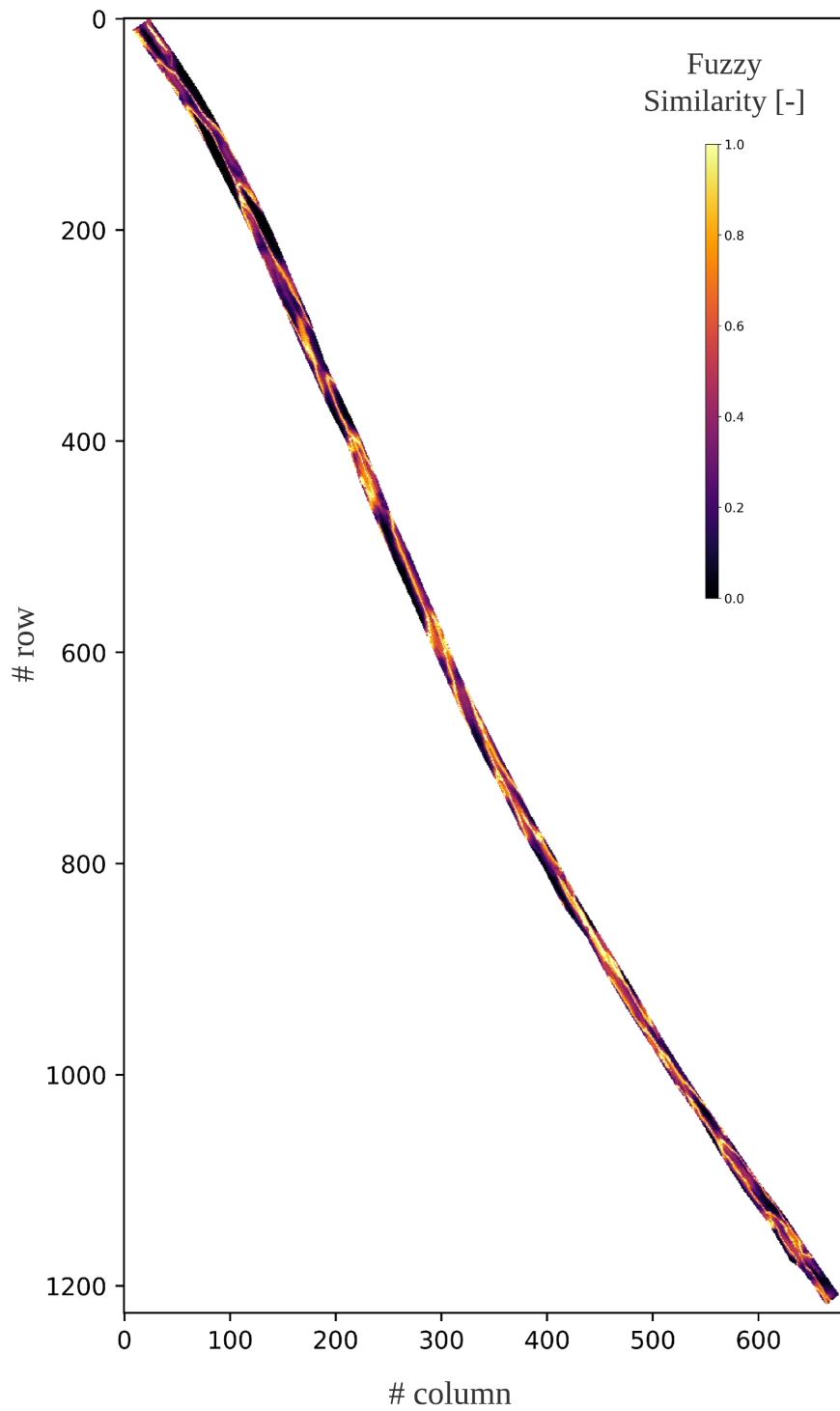


Figure A.9: Fuzzy evaluation of the stochastically calibrated *HYDRO\_FT-2D* model of the lower Salzach River for the validation period 2010-2013 compared to observed  $\Delta z$  (Resolution of 5m, method: **Fuzzy kappa**).

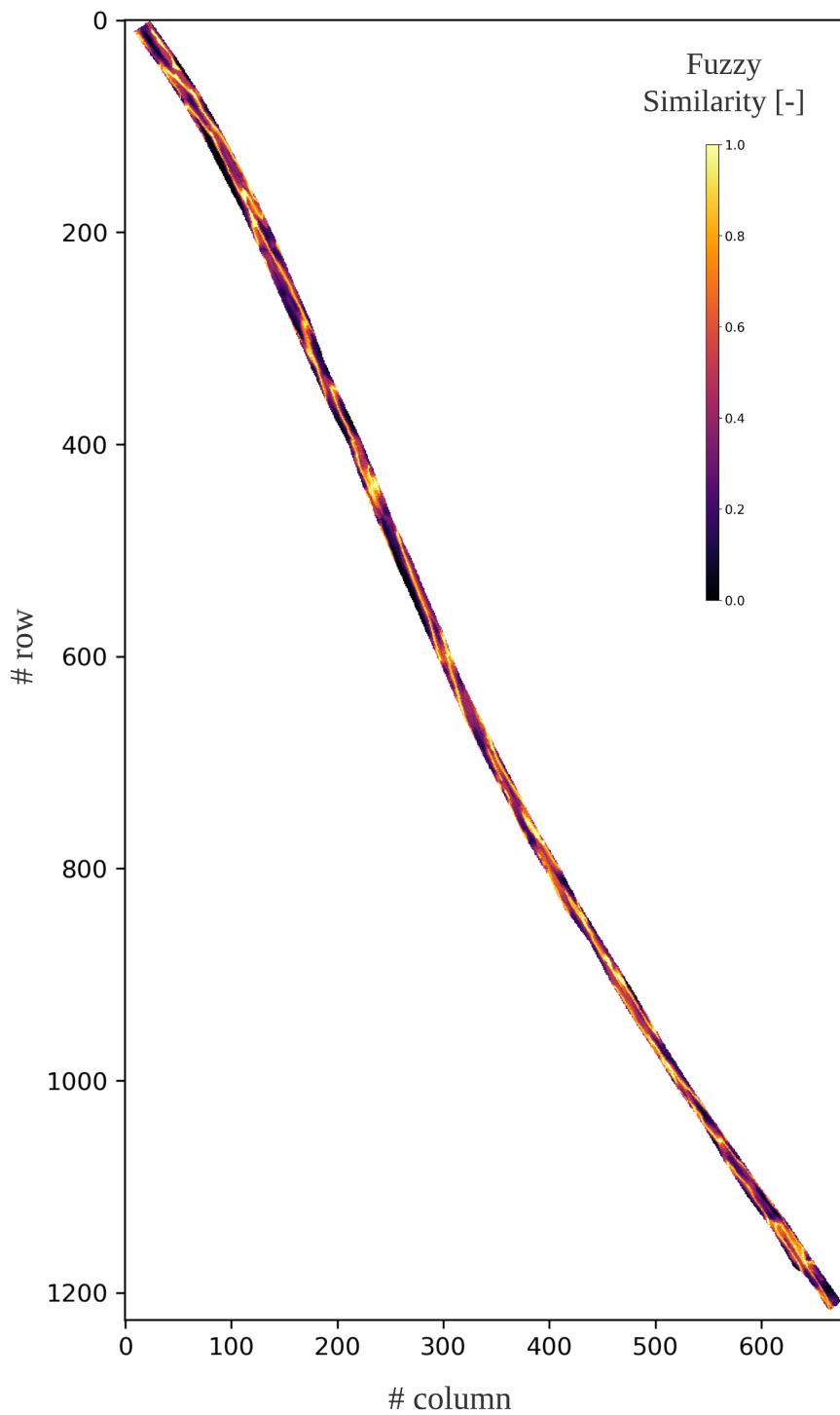


Figure A.10: Fuzzy evaluation of the aPC surrogate model of the lower Salzach River for the validation period 2010-2013 compared to observed  $\Delta z$  (Resolution of 5m, method: **Fuzzy kappa**).

## Appendix B

# Mathematical definitions of membership functions

Figure 2.2 presents some common shapes of MFs. Their mathematical definition is as follows:

(a) Triangular and

(b) trapezoidal functions;

$$\mu_A(x) = \begin{cases} 0 & x \leq a \\ w_1 \frac{x-a}{b-a} & a \leq x \leq b \\ 1 & b \leq x \leq c \\ w_2 \frac{d-x}{d-c} & c \leq x \leq d \\ 0 & x > d. \end{cases} \quad (\text{B.1})$$

(c) Gaussian membership function;

$$\mu_A(x) = f(x, \sigma, c) = e^{-\frac{(x-c)^2}{c\sigma^2}} \quad (\text{B.2})$$

(d) Sigmoid-type function;

$$\mu_A(x) = f(x, a, b) = \frac{1}{1 + e^{-a(x-c)}} \quad (\text{B.3})$$

(e) The  $\pi$ -function according to Medasani, Kim, and Krishnapuram (1995);

$$\mu_A(x) = \Pi(x; a, b, c) = \begin{cases} S\left(x ; c-b, c-\frac{b}{2}, c\right) & x \leq c \\ 1 - \left(x ; c, c+\frac{b}{2}, c+b\right) & x > c \end{cases} \quad (\text{B.4})$$

(f) S-function, as proposed from Cheng and Chen (1998);

$$\mu_A(x) = S(x; a, b, c) = \begin{cases} 0 & x \leq a \\ \frac{(x-a)^2}{(b-a)(c-a)} & a \leq x \leq b \\ 1 - \frac{(x-c)^2}{(c-b)(c-a)} & b \leq x \leq c \\ 1 & c \leq x \end{cases} \quad (\text{B.5})$$

Where  $a, b, c, d, w_1$  and  $w_2$  are parameters of the shape of the functions.